This is to certify that the

thesis entitled

THE SIGNIFICANCE OF THE DISTRIBUTION OF CLASTIC LENSES WITHIN THE NEGAUNEE IRON FORMATION AT THE EASTERN END OF THE PALMER BASIN, MARQUETTE SYNCLINORIUM, NORTHERN MICHIGAN

presented by

Mark S. Breithart

has been accepted towards fulfillment of the requirements for

Masters **degree in** Geology

C. H. Lamborn

Major professor

Date February 25, 1983

THE SIGNIFICANCE OF THE DISTRIBUTION OF CLASTIC LENSES WITHIN THE NEGAUNEE IRON FORMATION AT THE EASTERN END OF THE PALMER BASIN, MARQUETTE SYNCLINORIUM, NORTHERN MICHIGAN

by

Mark S. Breithart

A THESIS

Submitted to
Michigan State University
in partial fulfillment of the requirements
for the degree of

MASTER OF SCIENCE

Department of Geology

1983

ABSTRACT

THE SIGNIFICANCE OF THE DISTRIBUTION OF CLASTIC LENSES WITHIN THE NEGAUNEE IRON FORMATION AT THE EASTERN END OF THE PALMER BASIN, MARQUETTE SYNCLINORIUM, NORTHERN MICHIGAN

by

Mark S. Breithart

The Palmer Basin is a fault-bounded, wedge-shaped basin on the south margin of the Marquette Synclinorium in the Upper Peninsula of Michigan. The principal stratigraphic unit contained within the basin is the Negaunee Iron Formation. It contains numerous lenses of graywacke-type sediments interbedded with the iron formation.

Previous geologists have inferred that the Palmer Basin is a relict sedimentary basin of early Proterozoic age. This study attempts to quantify their early observations by detailed analysis of the clastic sediments. The vertical, horizontal and textural relationships of the clastics supports the previous models that the Palmer Basin is a relict sedimentary basin.

It is hypothesized that the Palmer Basin was a rift related basin receiving immature sediments from the south. A mass flow environment is the most consistent sedimentary facies which fits the data. The periodic influxes of clastics could have been controlled by faulting associated with rifting.

ACKNOWLEDGEMENTS

The author wishes to acknowledge some of the many people who gave their time and effort toward this study. Professors F. W. Cambray, J. W. Trow and J. T. Wilband, who formed the committee, provided invaluable assistance. Professor D. F. Sibley critically reviewed the sedimentation model section.

Nancy S. Breithart and Kirsten K. Cummings provided moral support and encouragement toward the completion of this study.

Fellow graduate students Rudi Meyer, Bill Monaghan and Steve Mattson helped the author through useful ideas and discussions.

Loretta Knutson typed the final draft and her aid is gratefully acknowledged.

TABLE OF CONTENTS

TABLE OF CONTENTS

LIST OF FIGURES

LIST OF FIGURES (Continued)

LIST OF TABLES

INTRODUCTION

Early Proterozoic (Precambrian X age) rocks of the Marquette Range Supergroup (first called the Huronian Group, then later the Animikie Group) outcrop in the Upper Peninsula of Michigan. The first detailed description of the area was published by Van Hise and Bayley in 1897. The stratigraphy and origin of these metasediments has been discussed by many geologists (Van Hise, 1892; Van Hise and Bayley, 1897; Van Hise and Leith, 1911; Tyler and Twenhofel, 1952; James, 1958). Recent work on the Marquette Range Supergroup and similar strata in Ontario, Minnesota and Wisconsin has been mainly concerned with the tectonics of the area during the early Proterozoic sedimentation period and subsequent deformation during the Penokean orogeny (1.8 to 1.9 Ga, Van Schmus, 1976). Recently, considerable discussion has centered upon the origin of the deformation of the sediments (Cambray, 1977, 1978; Cannon, 1973; Klasner, 1978; Larue, 1979, 1981; Larue and Sloss, 1980; Morey, 1978; Sims, 1976, Sims et al., 1980; Van Schmus, 1976).

The Marquette Range Supergroup was originally named the Huronian Group by Van Hise (1892). The rock sequence retained this name until James (1958) raised serious questions regarding the correlation between the rocks in the Upper Peninsula of Michigan with the true Huronian sequence found on the north shore of Lake Huron. He argued that the rocks in the Upper Peninsula (U.P.) of Michigan share more similarities with the Animikie Group found in Minnesota and Ontario and thus the name Animikie Group is applicable to the sequence of rocks in the U.P. of Michigan (James, 1958, p. 34). Later work by Cannon and Gair (1970) questioned this correlation made by James (1958) and suggested a

new term, the Marquette Range Supergroup would be more appropriate (Cannon and Gair, 1970, p. 2845).

The Marquette Range Supergroup sediments of early Proterozoic age (Precambrian X) rest unconformably on a basement of older Archean age (Precambrian W) rocks consisting of greenstones, granites and gneisses (Van Hise and Bayley, 1897). The general character of the Marquette Range Supergroup is of a fining-upward sequence indicative of a subsiding basin showing increasing water depth with time (Cannon, 1973). The original thickness has been estimated to have been 8,000 meters or more (Boyum, 1975). The present maximum thickness is estimated to be 2,500 meters (Klasner and Cannon, 1976).

The metasediments comprising the Marquette Range Supergroup are found today in somewhat isolated structural troughs separated by the Archean (Precambrian W) age gneisses, granites and greenstones (Morey, 1978). The trend of these structural troughs varies from east-west to northwest-southeast to northeast-southwest (James, 1958, Figure 2).

Three models for the sedimentation and subsequent deformation of the Marquette Range Supergroup sediments have emerged. These models can be grouped into two general schools of thought depending upon whether or not plate tectonic forces played an important role during the time interval from 2.1 to 1.8 Ga.

Cannon (1973), Klasner (1978), Morey (1978), Sims (1976) and Sims et al. (1980) have advocated that vertical tectonic forces were dominant during the early Proterozoic and hence a plate tectonic theory is not needed. Cambray (1977, 1978), Larue (1979, 1981), Larue and Sloss (1980) and Van Schmus (1976), on the other hand, have argued that the events recorded in the early Proterozoic sequence of rocks that comprise the Marquette Range Supergroup are more

simply explained with a plate tectonic theory for their origin (horizontal tectonic forces dominate).

Cannon (1973) proposed that Marquette Range Supergroup sedimentation took place in a large east-west striking basin which deepened to the south. Provenance was from the north and a northern miogeosynclinal facies and a southern eugeosynclinal facies developed. James (1954) earlier proposed a similar model for the area to explain the sedimentation of the iron formations.

According to Cannon (1973), deformation associated with the Penokean orogeny began midway through Marquette Range Supergroup sedimentation with mild crustal warping and erosion. Toward the close of sedimentation, regional tilting occurred along an east-west axis which caused large scale gravity sliding of the sediments. This event was followed by vertical block faulting which created the present structural troughs into which the sediments were passively draped. His model is based upon the observations that 1) the Precambrian W basement rocks do not appear to have undergone any of the significant shortening which affected the overlying Precambrian X age sediments, 2) the non-parallelism of small scale folds with the larger scale folds which are parallel to the axes of the troughs, and 3) the apparent random orientation of the present axes of the structural troughs. Klasner (1978) performed a structural study in the western Marquette Trough area and concurred with Cannon's (1973) results.

Sims (1976) and Morey (1978) have proposed a model which is slightly different than Cannon's (1973) for the early Proterozoic events in the Upper Peninsula of Michigan. They postulate that sedimentation and deformation were controlled by the differences in stability between two contrasting lithologies of a northern complex and a southern complex of Archean rocks. The granite-greenstone terrain, which outrcops north of the Marquette Range Supergroup

sediments, was much more stable than the granite-gneiss terrain which outrcrops south of the early Proterozoic sediments.

Sedimentation during the early Proterozoic occurred in an intracratonic basin centered approximately over the boundary between these two Precambrian W terrains. The sediment source was dominantly from the north, although some areas had a locally derived southern source (Sims, 1976). A miogeosynclinal assemblage of sediments developed in the north on the stable cratonic rocks, while an eugeosynclinal assemblage was deposited in the south on the unstable granite-gneiss terrain. The Penokean orogeny was the result of vertical movement of basement fault blocks. The differences in behavior between the two basement terrains resulted in complex structural patterns in the overlying Precambrian X age sediments. The northern terrain, which was not very active during the orogeny, was only mildly deformed and metamorphosed (greenschist facies). In contrast, the southern terrain was highly active and the overlying sediments show complex structural patterns and amphibolite grade metamorphism. The U.P. of Michigan lies dominantly over the granite-gneiss terrain (Sims, 1976).

Cambray (1977, 1978), Larue (1979, 1981), Larue and Sloss (1980) and Van Schmus (1976) have presented a plate tectonic model for the early Proterozoic that explains the sedimentation and deformation in terms of horizontal forces. Van Schmus (1976) first postulated the plate tectonic theory based upon the division of the early Proterozoic rocks into two suites: a northern belt of sediments typical of a miogeosynclinal and transitional assemblage facies (the Animikie and Marquette Range Supergroups) and a southern volcanic-plutonic complex (Northern and Central Wisconsin). Van Schmus (1976) proposes that an inactive continental margin controlled sedimentation during the early phases resulting in the miogeosynclinal

assemblage. Later an active collisional plate margin developed with the volcanic-plutonic arc to the south and a back-arc basin between the active arc and the northern craton resulting in the eugeosynclinal facies. The Marquette Range Supergroup sediments record the transition from the miogeosynclinal environment to the deeper water eugeosynclinal environment. Van Schmus (1976) finds little evidence for northward transport of sediment and agrees with Cannon's (1973) model for events during the Penokean orogeny (e.g., gravity sliding and vertical block faulting).

Cambray (1977, 1978), Larue (1979, 1981) and Larue and Sloss (1980) have further defined the plate tectonic model advanced by Van Schmus (1976) by postulating an early rifting environment created a major basin of sedimentation which also contained the structural troughs in which the Marquette Range Supergroup and related sediments are today preserved. This was followed by collision-type closure of the basin which resulted in the Penokean orogeny. Sedimentation, controlled by rifting, evolved from an early epicontinental sea, through subsiding restricted basins (structural troughs of today) to a period of regional subsidence prior to closure and deformation (Cambray, 1978). The structural troughs were closed by high angle reverse faults and were the centers of high strain. The intervening platform areas, between troughs, which did not receive as great a sedimentary pile as the troughs were the centers of low strain (Cambray, 1978; Larue, 1979; Larue and Sloss, 1980). Strain in the basement rocks was taken up by ductile shearing along diabase dikes and in discrete shear zones (Cambray, 1978).

Larue (1979, 1981) and Larue and Sloss (1980) have documented the existence of the structural troughs at the time of sedimentation (as opposed to their later formation in Cannon's, 1973; Morey's, 1978; Sim's, 1976 models) by careful analysis of paleocurrent flow indicators (flute casts and crossbedding)

and the location of basal conglomerates. Their work has shown that currents were flowing parallel to the present axes of the structural troughs and when combined with the restriction of basal conglomerates to the present structural troughs this indicates that the troughs were in existence at the time of sedimentation. They concluded that sediments were derived from both the north and the south.

This study is designed to show the existence, during sedimentation, of one of these proposed rift related troughs which is located on the south edge of the Marquette Trough in the vicinity of Palmer, Michigan and to delimit the direction of the sediment source for the trough.

The Palmer Basin is filled with approximately one kilometer of Menominee Group sediments (Gair, 1975). The principal formation contained within the Palmer Basin is the Negaunee Iron Formation which is anomalous because it contains numerous lenses of graywacke type sediments within the normally clastic-starved, chemically precipitated iron formation (Gair, 1975).

Previous workers (Tyler and Twenhofel, 1952; Mengel, 1956; Davis, 1965; Gair, 1975; Larue, 1979; Larue and Sloss, 1980) have suggested that the Palmer Basin is a relict south margin of a sedimentary basin based upon the presence and texture of these clastic lenses found within the Negaunee Iron Formation. This study attempts to quantify their observations using extensive drill core data to plot the distribution and texture of these clastics in the subsurface. If the present distribution and texture of these clastic lenses can be fitted into a sedimentary facies model, then the present distribution can be related to the past distribution and hence inferences about the existence and the shape of the basin can be made.

The results of this study indicate that the south margin of the Palmer Basin resembles a relict sedimentary basin margin. A sedimentary facies model

involving slumping of sediments along a steep slope and the possible development of a submarine fan environment which best fit the models of Walker (1978) and Normark (1978). Sediment transport was from the south to the north with limited distance of transport because of the immature nature of the clastics. This study helps to support the rifting aspect of the plate tectonic models of Cambray (1977, 1978), Larue (1979, 1981), Larue and Sloss (1980) and Van Schmus (1976) by showing that the pattern of sedimentation, within the Palmer Basin during Negaunee time, is more consistent with their models than the vertical tectonic and post-deposition origin of the basins models of Cannon (1973), Sims (1976) and Morey (1978). The existence of a relict sedimentary basin and the south-to-north direction of sediment transport is not consistent with the vertical tectonic model of a southward sediment transport direction and creation of sediment filled troughs by passively draping the sediments into them during deformation. Also, the immature nature of the clastics indicates a short distance of transport and deposition in relatively deep water below normal wave base. This implies that an eroding landmass must be close by to the south and that the basin drops off steeply. The close proximity of this southern landmass is contrary to the sedimentation models of Cannon (1973), Morey (1978) and Sims (1976) whereby the northward derived sediments are visualized as filling an intracratonic basin with the negligible contribution of a southern landmass.

REGIONAL GEOLOGY

The Marquette Synclinorium located in the Upper Peninsula of Michigan was first described by Van Hise and Bayley (1897). It is a westward plunging syncline containing Precambrian X age sediments of the Marquette Range Supergroup. Sedimentation took place between 2.1 and 1.9 Ga (Morey, 1978). The Penokean orogeny deformed and metamorphosed the Marquette Range area around 1.9 to 1.8 Ga (K-Ar and Rb-Sr, Van Schmus, 1976). Rocks of a similar age and geologic setting occur in Minnesota and Wisconsin where they are termed the Animikie Group (Sims et al., 1980). A similar, although older, sequence (2.1 to 2.3 Ga) is present on the north shore of Lake Huron in Ontario and the eastern part of Michigan's Upper Peninsula (Van Schmus, 1976; Sims, 1976 and Morey, 1978).

The Marquette Synclinorium approximately overlies the boundary between two Archean (Precambrian W) terrains (Sims et al., 1980). To the north greenstones and granites of the Superior Province outcrop (approximately 2.7 Ga) while older (3.5 to 2.8 Ga) granites and gneisses of the Southern Complex outcrop to the south (Sims et al., 1980). The Marquette Range Supergroup sediments (Precambrian X age) were deposited unconformably upon this older terrain (Van Hise and Bayley, 1897).

The Marquette Range Supergroup, in Marquette County, has been divided into three groups (James, 1958) (Figure 1). In stratigraphic order they are the Chocolay, the Menominee and the Baraga groups. Each is separated from the other by an unconformity (James, 1958) but the Chocolay-Menominee boundary has also been interpreted as a facies change associated with transgression (Tyler and Twenhofel, 1952).

Stratigraphic Column of the Eastern Marquette Range				
Proterozoic	0.57 Ga Precambrian Y	Keweenawan		Intrusives, Volcanics Sediments
	0.8 Ga Precambrian X	Marquette Range Supergroup	Baraga Group	Goodrich Quartzite
			Menominee Group	Negaunee Iron Fm. Siamo Slate Ajibik Quartzite
			Chocolay Group	Wewe Slate Kona Dolomite Mesnard Quartzite
	2.5 Ga Precambrian W (Archean)	Bell Creek and Compeau Creek Gneisses		Gneisses, Granites Greenstones

Figure 1. Stratigraphic column of the Eastern Marquette Range around the Palmer Basin. Upper Peninsula of Michigan.

Because detailed descriptions of the lithologies of the three groups and their respective formations have been done previously (Van Hise and Bayley, 1897; Tyler and Twenhofel, 1952; James, 1958; Cannon and Klasner, 1975; Gair, 1975; Cambray, 1977; Larue, 1979, 1981 and Larue and Sloss, 1980) and only a brief review will be presented here.

The lowermost group, the Chocolay, is interpreted to be a shallow, stable shelf assemblage representative of a miogeosynclinal facies (Cannon, 1973) or a shallow epicontinental sea (Cambray, 1978). Clean sands, followed by carbonates and finally some muds were deposited during this stage (the Mesnard, Kona and Wewe formations, respectively). Sedimentation was considered to equal the subsidence rate during this time (Larue, 1979, 1981). The Menominee Group is the next stratigraphically higher group. This sequence has deeper water affinities (Larue, 1979) as evidenced by the sediments which, in stratigraphic order, are composed of "dirty" to clean sands (the Ajibik Formation), shales and graywackes (the Siamo Formation) and lastly a thick, economic banded iron formation (the Negaunee Iron Formation). During this period subsidence was occurring at a faster rate than sedimentation (Larue, 1979). The uppermost major stratigraphic unit is the Baraga Group. These are clearly of a deep water depositional environment since the sediments (the Michigamme Formation) are composed almost entirely of graywackes, shales, volcanics and some minor iron formation. A minor basal quartzite, the Goodrich Formation, is present at the bottom of the formation. Intrusion of diabase dikes and sills occurred either during or after Baraga Group sedimentation, but before the Penokean orogeny (Van Hise and Bayley, 1897).

The Marquette Range Supergroup sediments were deformed during the Penokean orogeny, a complex series of events which culminated at about 1.8 to 1.9 Ga ago in the Upper Peninsula of Michigan (Van Schmus, 1976). Compression

was dominantly from a north-south direction and resulted in a near vertical axial plane cleavage which strikes N70 to N80W in the Marquette Synclinorium (Klasner, 1978). The exact timing of the Penokean orogeny is debatable. Gair (1967) and Cannon (1973) place the beginning in Menominee Group time while Cambray (1977) considers the orogeny to have commenced at the end of Baraga Group sedimentation time. The resulting geology today is a series of variably oriented troughs which contain thick sequences of Marquette Range Supergroup sediments separated by uplifts of older Archean rocks (Cannon, 1973). Metamorphism attained the sillmanite grade in some areas (nodes) but the chlorite grade of the lower greenschist facies is the most prevalent (James, 1955). Faults which cut the early-Proterozoic (Precambrian X) aged rocks are late events related to the Penokean orogeny according to Sims (1973). However, this observation is equivocal since sedimentation patterns born out by this study suggest faulting was active during sedimentation and before the commencement of orogenic events.

During Keweenawan time (Precambrian Y) essentially vertical diabase dikes cut through the area. These trend in a dominantly east-west direction and are associated with rifting of the Mid-Continent Rift formation. Deposition of clastic sediments, the Jacobsville Formation, marks the close of Precambrian activity in the Marquette Range area. Paleozoic sediments have either been completely eroded away or were not deposited. Pleistocene glaciation has deposited variable amounts of outwash and till over the area.

LOCAL GEOLOGY

The Palmer Basin is an east-west trending fault bounded basin located on the south limb of the Marquette Synclinorium encompassing parts of sections 26 through 34, T47N-R26W. The area of this study centers at the eastern end of the Palmer Basin and includes parts of sections 26, 27, 28, 33 and 34. The Palmer Basin has been downfaulted along its northern boundary by the east-west trending Palmer Fault relative to the Marquette Synclinorium proper. Gair (1975) has estimated the throw on the Palmer Fault to be about 3,500 feet (1,070 meters). The area was metamorphosed to the chlorite grade of the lower greenschist facies (James, 1955).

The Palmer Basin is filled with Precambrian X age sediments of the Menominee Group. The Negaunee Iron Formation is the most voluminous, but thin horizons of the Ajibik and Siamo Formations are present below the Negaunee (Gair, 1975) (see Figure 2). The Archean (Precambrian W) gneisses and granites of the Southern Complex, the Palmer and Compeau Creek Gneisses, are exposed south of the Palmer Basin. To the north of the Palmer Fault, Archean gneisses (the Compeau Creek) and strata of the Chocolay Group and lowest Meniminee Group outcrop (Tyler and Twenhofel, 1952) (see geologic map, Figure 3).

Precambrian X age sediment thickness in the Palmer Basin ranges from over 2,300 feet (700 meters) next to the Palmer Fault to zero along the south margin of the basin. In effect the sediments form an east-west striking wedge shaped complex, thickening to the north and thinning to the south.

According to Gair (1975) the Ajibik Formation in the vicinity of the Palmer Basin ranges from a rather pure vitreous quartzite along the east margin to a

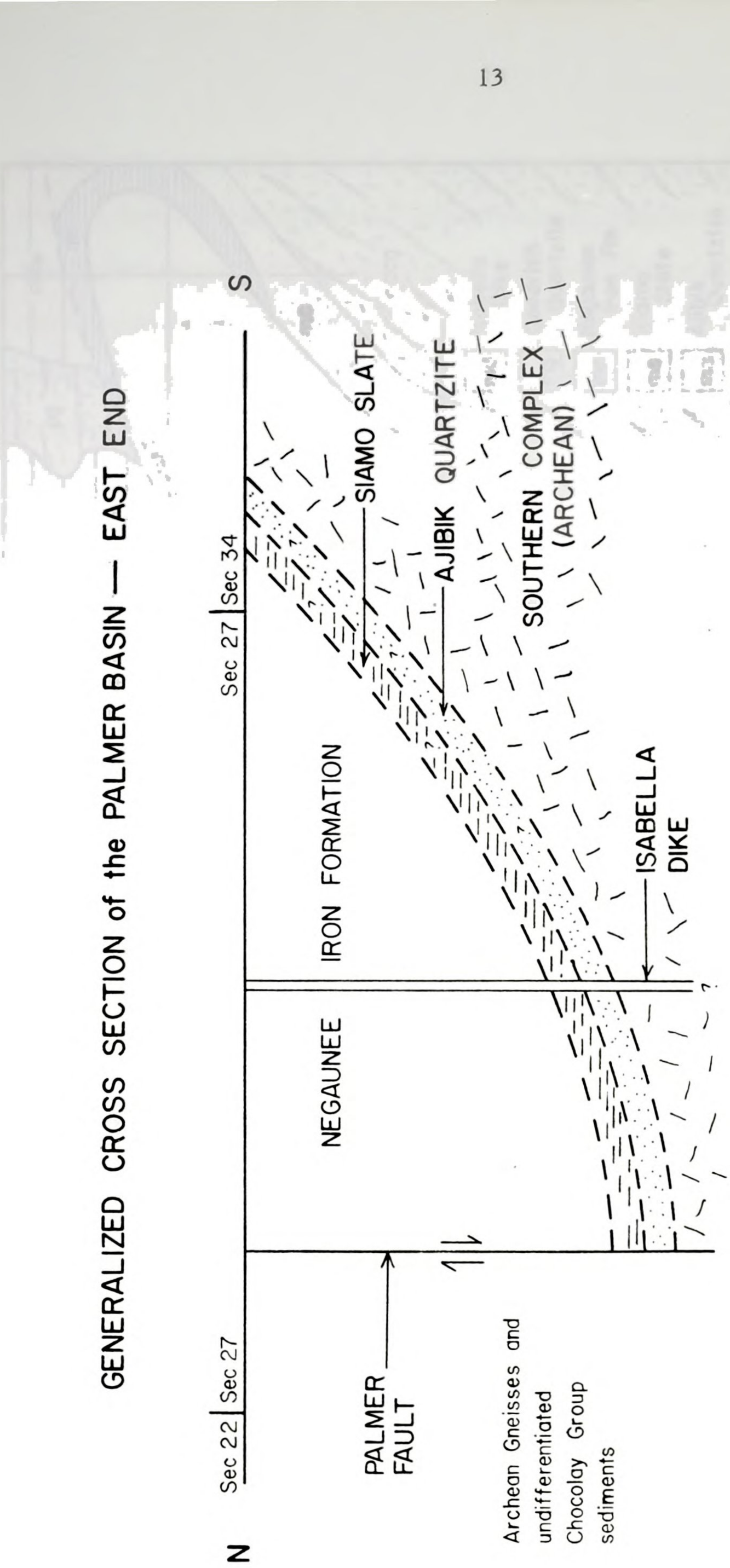

Figure 2. Generalized cross section. No vertical exaggeration.

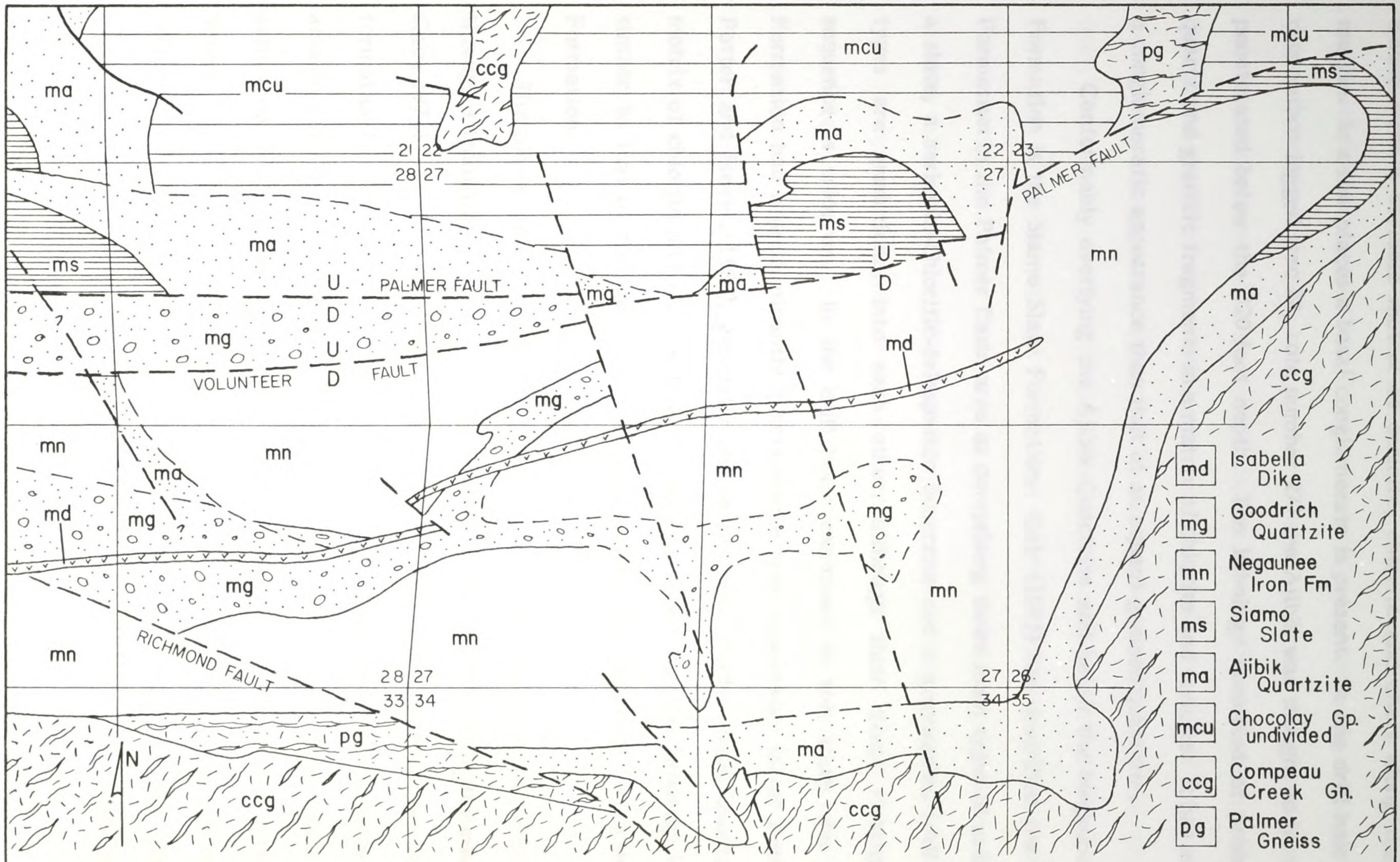

Figure 3. Generalized geologic map of the Eastern Palmer Basin (after Gair, 1975). T47N-R26W Marquette County.

wacke with a variable matrix of sericite, chlorite and chert along the south margin. In a few places a basal conglomerate is present. In one drill hole which this author logged (sec 28, hole number 27) the Ajibik was thought to have been peneterated below the 320 foot depth. The lithology consisted of pebbles of quartz and granitic fragments in a matrix of chlorite and sericite. It has more of a conglomeratic appearance than that of an equant-grained quartzite.

Conformably overlying the Ajibik Quartzite and below the Negaunee Iron Formation is the Siamo Slate Formation. Gair (1975) has described the Siamo Formation in the Palmer Basin area as comprising three main types of sediment: a slate, a sericitic-chloritic-feldspathic quartzite and a graywacke. All three types are gradational into each other, although their exact stratigraphic sequence is unknown. In the drill holes examined in this study the Siamo Formation had a predominantly quartz-wacke type appearance (after Pettijohn, Potter and Siever, 1973), generally coarse grained, poorly sorted quartz in a matrix of chlorite and iron oxides. It should be noted that this lithology is very similar to that of the clastic lenses found within the overlying Negaunee Iron Formation.

The Siamo grades conformably upward into the Negaunee Iron Formation through a transition zone (Tyler and Twenhofel, 1952; Snider, 1972; Boyum, 1975; Gair, 1975). As one nears the top of the Siamo Formation, layers of banded iron formation (iron minerals and chert) start appearing and increase in thickness and amount until the iron formation makes up 80% or so of the drill hole. Gair (1975) estimated that this transition zone was up to 100 feet (31 meters) in thickness. Snider (1972) studied the transition zone and concluded that the Siamo is predominantly a graywacke at the bottom which changes into a slate near the top. While he made no absolute thickness measurements, he did conclude that the transition zone could range from 20 to over 180 feet in thickness (6 to 55

meters). Termination of the drill holes used in his study before the interbedding of graywackes and banded iron formation ceased was given as the reason for the thickness estimate problem.

The Negaunee Iron Formation has been classified as a typical, Lake Superior type, Precambrian Banded Iron Formation (Van Hise and Bayley, 1897; Van Hise and Leith, 1911; James, 1954; Bayley and James, 1973; Boyum, 1975; Gair, 1975; Gross, 1980). The iron formation is composed of thin (0.5 mm) to thick (10 cm) lamina of iron oxide, iron carbonate and iron silicate minerals interbedded with thin to thick lamina of cryptocrystalline quartz (chert). The bedding contacts are very sharp and vary from irregular to perfectly flat.

The question of primary vs. secondary minerals is outside the scope of this investigation and only present day observed mineral assemblages will be mentioned.

The most abundant facies in the Palmer Basin is the oxide facies (Gair, 1975) of which the most important iron minerals are magnetite, hematite, martite (a hematite pseudomorph of magnetite) and geothite (James, 1955). The carbonate facies is the next most abundant facies after the oxide (Gair, 1975) and is composed of the iron mineral siderite (James, 1955). Only minor iron silicate minerals are present in the Palmer Basin and these are in the form of stilpnomelane and minnesotaite (Gair, 1975).

The lenses of clastic material which occur within the chemically precipitated iron formation serve as the focus of this study. In the present discussion they can be roughly classified as graywackes and are used in this study to deduce the existence and shape of the basin at the time of deposition of the Negaunee Iron Formation.

Following deposition of the Negaunee Iron Formation an erosional event occurred which produced the unconformity between it and the overlying

Goodrich Quartzite, the lowest formation of the Baraga Group (Van Hise and Bayley, 1897 and Gair, 1975). The unconformity is a very low angle one and the contact between the Negaunee Iron Formation and the Goodrich appears conformable in places (Gair, 1975). Based upon the observations of Gair (1975) the Goodrich can be classified as a pebbly to cobbly conglomerate to a coarse-grained impure quartzite. In the Palmer Basin area only the basal conglomerate part of the Goodrich is exposed. It contains pebbles and cobbles of iron formation along with vein quartz, chert, granite, quartzite and greenstone. The matrix commonly consists of detrital quartz, feldspar, sericite and hematite (Gair, 1975). The Goodrich is the youngest sedimentary rock unit of the Marquette Range Supergroup present in the study area (Gair, 1975).

Precambrian X age diabase dikes and sills penetrated the previously deposited sediments in the Palmer Basin prior to the Penokean orogeny. In drill core these commonly appear as gray-black or green-gray units with signs of shearing and intense secondary leaching and alteration (vuggyness). The orientation of the units relative to the iron formation varies from parallel to perpendicular to bedding. Apparently the diabases were dikes and sills which have since been highly deformed and altered (Gair, 1975). A thin section of a moderately altered diabase dike revealed a lithology of original plagioclase and pyroxene which has been mostly altered to sericite, chlorite and carbonate.

During the Penokean orogeny the rocks were metamorphosed to the chlorite grade of the lower greenschist facies and numerous small scale folds were formed which are most visible in the Negaunee Iron Formation.

Gair (1975) has identified an E-W fold trend within the Palmer Basin which he believes represents a doubly plunging syncline. This is based upon the distribution of the Goodrich Quartzite which he believes must occupy the center of the syncline. The only other major structural features identified are a series

of faults which break the Palmer Basin into a set of wedge-shaped blocks (Gair, 1975). The faults are the Palmer, the Volunteer, and the Richmond Fault (see Diagram 3). No estimates of the amount of displacement on the faults other than the Palmer Fault have been made.

A large Precambrian Y age (Keweenawan age) diabase dike, the Isabella Dike, cuts through the center of the Palmer Basin in an east-northeasterly to west-southwesterly direction (see Diagram 3). This dike is very close to vertical and has a very fresh appearance when compared with the Precambrian X age diabase dikes. It has a maximum width of about 50 feet (Gair, 1975).

Pleistocene glacial till and outwash blanket the area in variable amounts. The average thickness is on the order of 10 to 15 feet (3 to 5 meters).

PREVIOUS WORK

The first mention of the presence of clastic material within the Negaunee Iron Formation in the Palmer Basin was by Tyler and Twenhofel (1952). They used the presence of the clastic lenses incorrectly to correlate the Negaunee Iron Formation in the Palmer Basin with the Goose Lake iron member of the Siamo Formation which is found outside of the Palmer Basin (northward). They envisioned a basin with strong currents that had deltas flowing in from the east and southeast to explain the sedimentation pattern. Also normal iron formation was continually being deposited without interrupting the clastic sedimentation pattern.

Since the publication of Tyler and Twenhofel's (1952) report three other geologists have studied the clastic lenses in the Palmer Basin in detail (Mengel, 1956; Davis, 1965; and Gair, 1975). All three suggest that the Palmer Basin was situated near a paleo-shoreline during Negaunee time and that there was periodic influxes of clastic sediment from the south. They disagree on the distribution of the clastics throughout the basin and on the depositional mechanism operating to produce the form and texture of the clastic lenses.

Mengel (1956) divided the clastic occurrences in the Negaunee Iron Formation into three types of lithologies and into three distinct zones. The three lithologies are: 1) a coarse conglomerate which represents discordant channel fillings generated by storms and confined to the Moore Mine area only, 2) impure quartzites (close to graywacke in composition) which occur throughout the iron formation and represent offshore and along-shore current action, and 3) cherty quartzites which occur throughout the iron formation also, but represent a continual input of clastic quartz grains into the basin. Mengel (1956)

concluded that the Negaunee Iron Formation in the Palmer Basin could be divided into three subunits based upon stratigraphic position: an upper quartzite, a middle iron formation and a lower quartzite. The lower quartzite was extrapolated eastward across the basin from the Warner Creek Falls at the west end of the basin. It has a lithology very close to that of a graywacke and represents shallow channel fill deposits. The middle iron formation makes up the bulk of the Negaunee Iron Formation and contains lenses of the impure quartzite (graywacke) and the cherty quartzites. The upper quartzite was extrapolated westward across the basin from the New Richmond Mine and represents the same environment as the lower quartzite. From his study Mengel (1956) concluded that the iron formation in the Palmer Basin is normal Negaunee Iron Formation but has had a significant clastic input from streams during its deposition. A shallow water environment was envisioned to explain the quartzite lenses and scattered grains of quartz.

Davis (1965) divided the Negaunee Iron Formation in the Palmer Basin into three units: an upper graywacke, the middle iron formation and a lower graywacke. The middle iron formation contains two types of clastic sediment: 1) scattered graywacke lenses similar in lithology to the upper and lower graywacke units, and 2) clastic quartz lenses with an iron mineral matrix (hematite, magnetite or siderite). Davis (1965) was the first to note the general absence of graded bedding in the graywacke units and determined that the presence of clastics is independent of the facies or lithology of the iron formation (e.g., oxide or carbonate). He concluded that the graywacke units and the graywacke lenses in the middle iron formation represent turbidity current deposits or mud flows while the clastics with an iron mineral matrix represent continual basinward movement of sand and silt by currents (tide and wave generated). Davis (1965) also noted an absence of feldspars in the clastic

sediments and attributed it to extensive subaerial weathering in the source region of the sediments (Precambrian W age gneisses and granites of the Southern Complex).

The most recent report on the clastic lenses within the Negaunee Iron Formation was by Gair (1975). He reinforced the previous works of Mengel (1956) and Davis (1965) in stating that the clastic beds or lenses were more common near the top and bottom of the iron formation. He also included the western half and the southeastern corner of the Palmer Basin as areas of high percentage of clastics. Pebbles, cobbles and boulders are more common along the south margin than in the center of the basin and the main depositional mechanism for the clastics was turbidity currents. Gair (1975) attributed the periodic influx of clastics to fault movements along the south margin of the basin and called for rapid sediment transport and deposition with little differential settling to explain the general lack of graded bedding. Finally, Gair (1975) hypothesized that the Palmer Basin was an embayment off the main depositional center for the Marquette Range Supergroup and that its present shape was due to deformation during the Penokean Orogeny.

In summary then, all three geologists (Mengel, 1956; Davis, 1965; Gair, 1975) agreed that quartz is the dominant mineral in the clastic lenses, that the source area for the clastics was to the south and that the Palmer Basin was situated near a paleo-shoreline during Negaunee depositional time. Both Davis (1965) and Gair (1975) concluded that: 1) graywacke is the most common type of lithology of the clastic lenses, 2) the clastic lenses are most common near the top and the bottom of the Negaunee Iron Formation, 3) clastic occurrence is independent of iron formation lithology or facies, 4) there is a general lack of graded bedding or associated sedimentary structures, and 5) they both called for turbidity currents to act as the main depositional mechanism for the graywacke

type sediments in a deep water environment. Mengel (1956) was the only geologist to conclude that the most common lithology of the clastic lenses was of a cherty-quartzite nature, that the depositional environment was shallow water and that the main depositional mechanisms were streams and a long shore drift system. Furthermore, Mengel (1956) was the only geologist to agree with Tyler and Twenhofel's (1952) interpretation that deltas formed along the east and southeast margins fed by streams flowing in from these direction.

METHODS OF STUDY

The intent of this study is quantitively to analyze the distribution of clastic lenses in the Palmer Basin and to see if such an analysis would elucidate information concerning the development and shape of the basin during deposition of the Negaunee Iron Formation. To achieve this goal, contour maps were prepared from the diamond drill hole data to show the horizontal and vertical distribution of the clastic lenses. Parameters such as the grain size variation (coarse or fine), type matrix (chloritic or iron mineral), bed or lense thickness and number and percent clastics in specific intervals within a drill hole were used. The resulting contour maps are presented in Figures 5 to 30. It is felt that by using these methods and parameters any subsurface relationship between the clastic lense distribution and texture, as related to the basin existence and shape, could be tested.

To date the Cleveland-Cliffs Iron Company has drilled 171 diamond drill core holes in sections 26, 27, 28, 33, and 34 in the Palmer Basin. The core from most of these holes, along with the geologic records, as compiled by company geologists, was made available to the author during the summers of 1978 and 1979. This author personally logged 50 of the 171 drill holes for this study with footage totaling 37,940 feet (11,522 meters). In addition, company records were used to acquire an additional 46,323 feet (14,130 meters) of core data. After excluding some drill hole data because: 1) the holes were too shallow (50 feet or less), or 2) the company supplied drill core logs contained incomplete data, 80 holes were left to use in this study totaling 71,591 feet (21,835 meters). Of this, 33,651 feet (10,264 meters) were taken from company logs (see Figure 4 for locations).

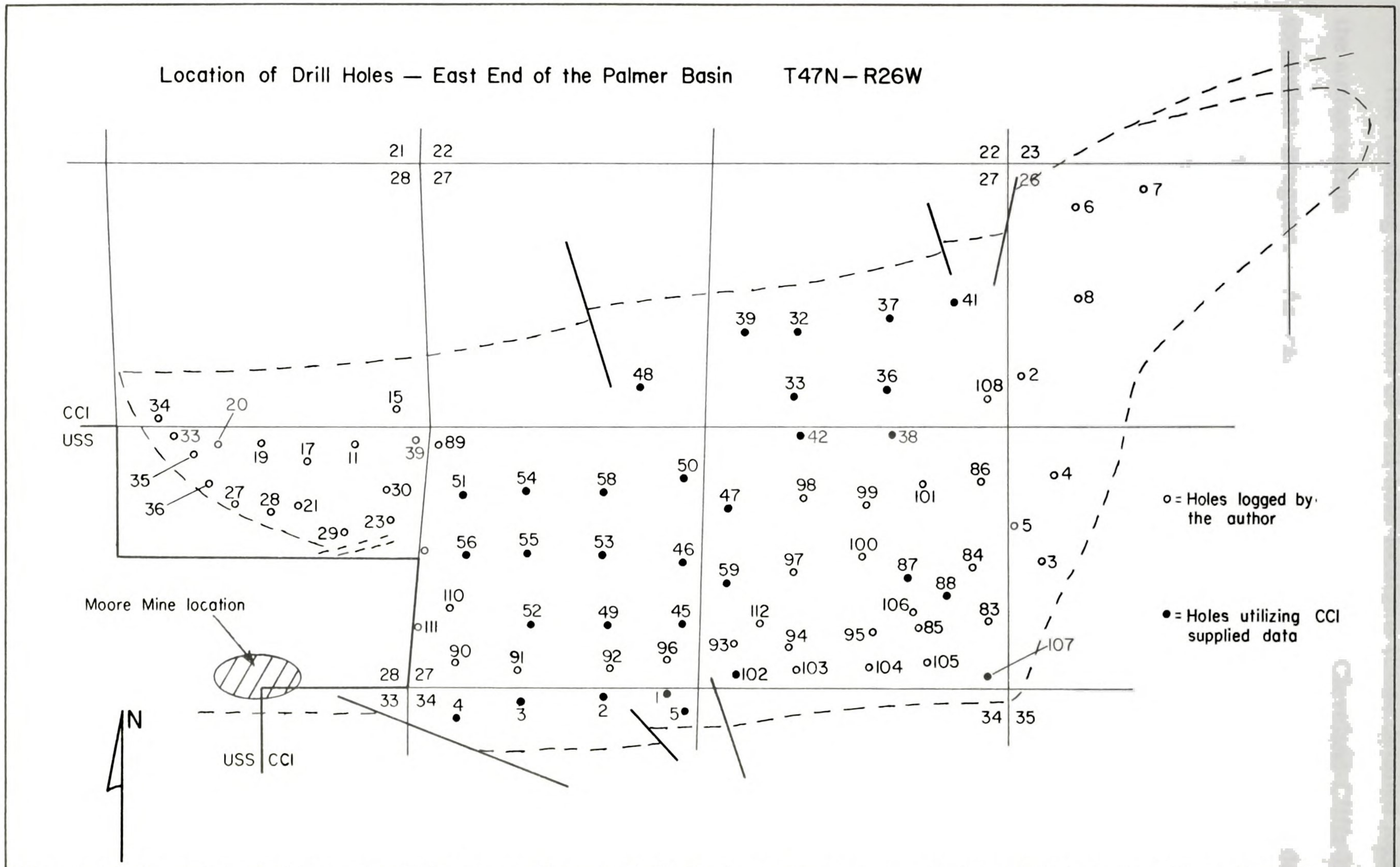

Figure 4. Location of diamond drill holes on Cleveland Cliffs Iron Company property. Note location of section corners used for scale on following contour maps.

The resulting distribution of drill hole locations (those detailed logged by the author versus drill holes whose data was taken from Cleveland-Cliffs logs) is somewhat irregular. As can be seen from Figure 4, the authors' data is concentrated in sections 26, 28 and along the south border of section 27 while the center and northern area of section 27 relies heavily upon information taken from Cleveland-Cliffs logs. This anomalous distribution of drill hole locations will be discussed in more detail after a description of the measurements made on the drill core is presented.

The logging of core done by the author for this study included the following data on each clastic lense occurrence: depth in the drill hole, thickness, grain size estimate (coarse-medium-fine), sorting estimate where visible, matrix composition (chlorite, iron oxide, iron carbonate or chert), textures (graded, upgraded, massive, sheared, etc.) and any other unusualy features (leached and vuggy, diffuse contacts with adjacent iron formation layers versus the usual sharp contacts, etc.). Also, in some holes and intervals, the following data was recorded: the lithology of the iron formation beds, occurrence of intrusive dikes and sills, breccia zones, fractures, presence of secondary gypsum, replacement textures, leached zones, type of bedding (thin lamina, massive, disrupted, etc.) or any other noticeable features. This aspect of the detailed logging was abandoned during the second summer of field work to conserve time and to place maximum concentration upon the clastic lense occurrences and lithologies.

For drill holes not personally logged by the author, the core logs supplied by the Cleveland-Cliffs Iron Company yielded the following information about clastic lense occurrence: depth in the drill hole, thickness and lithology. Textural descriptions such as grain size and sorting were very rarely present. For all drill holes used in this study the following information was needed from the Cleveland-Cliffs logs in order to interpret accurately the clastic lense data:

elevation above sea level of the drill collar, the angle of dip of the drill hole and the amount of glacial overburden the drill hole passed through. The elevation of the drill collar above the land surface was from 2 to 3 feet, the angle of the drill holes varied from vertical (90^{o}) to 45^{o} and the amount of glacial overburden ranged from 0 to 50 feet (15 meters).

All clastic intervals were corrected for the angle of the drill hole [cos (90-angle) x thickness = true thickness or depth] so that only the true depth below land surface and the true thickness of the clastic intervals were used. The drill collar elevations were used to normalize all depth and thickness data to a sea level datum (elevation of collar - subsurface depth = elevation above sea level, corrected for dip as stated above) so that clastics of one elevation could be compared with those of other elevations.

A little less than half of the drill core data were taken from Cleveland-Cliffs Iron Company logs. This was due to two factors: 1) this author did not have the time to log all the drill holes available, and 2) Cleveland-Cliffs had destroyed the core from the earliest drill holes because they believed an open pit mine would not be worked at depths below 300 feet below the land surface. The earliest holes drilled were in the deepest part of the basin (center of section 27) and this core has been destroyed. Luckily for this study the company geologists who logged these holes noted the occurrence and thickness of the more prominant clastic lenses. Generally, the clastic occurrences were described as a graywacke or an arenaceous iron formation. These terms were interpreted to indicate clastics with a chloritic and an iron mineral matrix, respectively. No clastic lense occurrences of less than one inch in thickness were recorded in the Cleveland-Cliffs supplied core logs and this was interpreted as the smallest interval noted by these geologists. Subsequently, in plotting the variation in the number of individual clastic lenses per drill hole, one inch had to be taken as the

lower thickness limit. In computing the grain size variation between drill holes, the absolute grain size in a specific interval could not be used because after inspection of the Cleveland-Cliffs Iron Company's logs it was felt that the company geologists would only note the grain size of the coarse grained lenses of clastics and not the variation from fine through coarse. Consequently, all graywacke lenses were interpreted to be fine grained unless otherwise noted as coarse grained by the company geologist. A ratio of % coarse/% fine was chosen for plotting the grain size variation across the basin because it is hoped that this effect of rationing will enhance differences between areas and thus make these differences more visible to the reader. The ratios were contoured into four broad divisions and are presented in Figure 28.

The resulting contour maps can be divided into two groups based on the degree of confidence in the data taken from the company logs and used to generate the contour maps. The high confidence diagrams are classified as such because they are based solely on the presence or absence of clastic lenses within an interval and on the thickness of the clastic lense occurrence. While the company geologist doing the core logging might not be interested in the lithology or grain size variation of the clastic lenses, they would definitely be concerned with their presence or absence and in their thickness for economic reserve calculations and for planning of mining strategies. The low confidence diagrams are such because they partly rely upon data derived from the Cleveland-Cliffs Iron Company logs which company geologists would be more likely to overlook or disregard as unimportant; namely, the lithologic descriptions of the clastic lenses including matrix type and the grain size estimate. While these parameters were mentioned frequently in the drill logs used by the author, the descriptions usually did not include enough detail to give th impression that the company geologist performing the logging was concerned about the lithology of the clastic lenses.

Also, it would be very easy to overlook fine grained clastics with an iron oxide or iron carbonate matrix unless one was truely looking for this type of clastic lense occurrence.

Diagrams with high confidence are Figures 5 to 27 and Figure 29. These are the percent clastics in specific 100 foot intervals (500 to 1199 feet above sea level), the number of beds of chloritic clastics greater than one inch in thickness per drill hole, and the thickest continuous clastic bed. Low confidence diagrams would be Figure 28, the ratio of % coarse divided by % fine and Figure 30 the % clastics in a drill hole with a chloritic matrix.

Over 150 samples of drill core containing clastics, intrusives, and some of the iron formation lithologies were taken during the logging of the core in Ishpeming, Michigan. From these, approximately 120 thin sections were prepared for petrographic analysis. The petrography determined the lithology and texture of the clastics as well as the grain size of the clastics. All petrography was performed using a standard petrographic microscope; no reflected light analyses were performed. The lithology and texture will be discussed elsewhere while a brief discussion of the grain sizes will be made here. Appendix I presents the method used to calculate the grain sizes.

The grain sizes of the clastic lenses, as recorded by the author, were recorded in the field as either coarse, medium or fine grained. Since this is a subjective measurement, the reliability of the author's measurements was tested using quantitative methods in the lab after Middleton (1962). The method utilizes the ratio between the maximum and minimum axes of grains, as measured in thin section, and relates them to the size distribution which would have been obtained by sieving the sediment. This method allows the size distribution (in phi units, ϕ) of consolidated or lithified sediments to be calculated.

At the 95% confidence interval the authors subjective grain size estimates can be divided into mean grain sizes of coarse (1.05 ± .15ϕ), medium (1.82 ± .28ϕ) and fine (2.80 ± .46ϕ). These results can be interpreted to mean that at the 95% confidence level the author correctly classified the clastic lenses into coarse, medium and fine grained based upon the grain size visible to the unaided eye. Thus there is a real variation in grain size between different clastic lenses in the Palmer Basin.

CORE APPEARANCE

Besides the presence or absence of clastic layers in the drill core many other features of interest should be noted. These bear either directly or indirectly upon an interpretation about the nature and distribution of the clastic layers that can be made. Bedding dips, faulting, brecciation and oxidation effects need to be considered.

Primarily because of the Penokean Orogeny, bedding in the Negaunee Iron Formation was deformed into folds (Gair, 1975). In drill core bedding dips vary from horizontal to vertial with a common range of 20-40°. While most of this folding can be attributed to the Penokean Orogeny, Gross (1972) noted that in many iron formation deposits small folds formed by syn-sedimentary slumping of beds are common and difficult to distinguish from larger scale folds formed by tectonic processes. Since most drill holes used in this study have a spacing no closer than 200 feet, and the drill core is only a two inch diameter sample at a given point, it is quite difficult to distinguish syn-sedimentary deformation from tectonic deformation in this study. It can only be noted that the beds are generally subhorizontal but that a wide variation in dips is noted.

The possibility of large scale folding presents a problem in that the whole sedimentary package within the Palmer Basin could be tilted toward some direction or repetition of bedding could have occurred by recumbent folding. This is a problem that at this time is unsolvable due to the relative wide drill hole spacing (compared to what is needed for structural mapping) and the unoriented nature of the drill core (no azimuth and no upward direction indicators).

Even though the problem of bed repetition by folding is unsolvable at this time, it should be noted that no recumbent folding has been found by the many geologists that have worked in the Upper Peninsula of Michigan to date. While the lack of reported recumbent folding is not proof that this type of folding did not occur, the effects of recumbent folding will not be considered further in this study.

Faulting is visible in the core as small offsets in bedding generally ranging from one-half inch to two inches, with the fault plane recemented with iron oxide and chert. Larger faults might be present as evidenced by extensive oxidized and leached zones and by brecciated core, but their presence cannot be unequivocally proven at this time. Also visible in the core are breccia zones which consist of small (one-half inch) to large (two inch), angular pieces of iron formation in a matrix of iron formation (chert and iron minerals). It is possible that these represent coarse fault gouges related to Penokean orogenic activity which were recemented with remobilized iron and chert. However a more plausible explanation is that these breccia zones represent syn-sedimentary slumps with a matrix of primary iron formation which was recrystallized during metamorphism (Gair, 1975). Gross (1972) noted similar features in Canadian iron deposits and attributed them to syn-sedimentary slumping. This explanation is preferred here due to the coarse and angular nature of the breccias and the complete cementation with iron formation lithologies similar to the breccia clasts themselves.

Many features visible in the core can be attributed to the effects of metamorphism and later secondary oxidization and leaching by meteoric and/or hydrothermal waters (Grunner, 1937; Mann, 1953; Mancuso, 1966; Gair, 1975; Cannon, 1976). Sheared diabase dikes, the presence of euhedral pyrite cubes and changes in the iron formation mineralogy are attributed to faulting and

recrystallization during metamorphism (Gair, 1975). Other features probably arise from leaching (vuggyness), dissolution and oxidization of the iron formation (hematite-goethite assemblages and presence of clays) (Mann, 1953; Mancuso, 1966; Cannon, 1976) and precipitation of secondary minerals from either meteoric or hydrothermal fluids (e.g., gypsum, clays and hematite-goethite) (Gruner, 1937; Mann, 1953).

Finally, because the pieces of drill core are handled by numerous people from the time of drilling to final storge, no true upward direction could be found for any individual piece. It cannot be assumed that all the people who handled the core preserved its original orientation. What is preserved is the relative depth in the drill hole from where the core came from.

DESCRIPTION OF CLASTICS

The clastics which make up the clastic lenses in the Negaunee Iron Formation within the Palmer Basin are immature sediments and can be classified as quartz-wackes to lithic quartz-wackes after Potter, Pettijohn and Seiver (1972). These lenses contain a high percent quartz clasts and matrix, locally a high percent lithic clasts and a low percent of feldspar which distinguishes them from typical graywackes (high percent quartz, matrix and feldspar). The clastics almost always show matrix support of predominantly quartz grains. The quartz grains themselves are generally subangular to angular although subrounded grains can constitute a few percent. Pressure solution and authigenetic overgrowths are usually visible in thin section due either to diagenesis or metamorphism. In drill core and thin section, sedimentary structures such as graded bedding, soft sediment deformation, tool marks and such are rarely visible. The thickness of individual clastic units varies from 1/4 inch to 30 feet or more and contacts with adjoining iron formation layers are usually sharp although gradational ones are present.

The matrix of the clastics can be divided into four main types: 1) chlorite, 2) iron oxide, 3) carbonate, and 4) cryptocrystalline quartz or chert. Any given clastic occurrence can have a matrix consisting of solely one type or mixtures can exist. Chlorite and iron oxide are by far the most abundant types present. The chlorite (once clays) appears as small laths generally less than 0.005 mm long. The color is predominantly light green although some darker green varieties are visible. Generally iron oxides such as hematite and geothite have a reddish hue around their rims while magnetite and martite could be distinguished by their crystal form. Most chert is fine grained, less than 0.025 mm, and

occurres as a massive filling surrounding the quartz grains. Carbonate is locally a major constituent of the matrix and is inferred to be siderite by its light brown to yellow-brown color and infrequently visible rhombohedral cleavage. Most crystals are anhedral and between 0.012 and 0.05 mm in diameter. While chlorite and iron oxide usually occurred as sole constituents of the matrix, all chert and carbonate have a significant amount of chlorite and/or iron oxide occurring with them. Point counting of 11 thin sections indicates a range of matrix percent from 43 to 58% with a mean of 49%. It can safely be stated that in all samples the matrix percent is over 40%.

The clastics generally did not possess a fabric or a preferred orientation of the quartz grains, lithic clasts and/or the matrix minerals easily visible in hand specimen or under the microscope. In a few thin sections an apparent parallelism of overgrowths or long axes of grains was visible but these instances are a minority. As discussed in Appendix I, cutting thin sections at 90^{o} angles to each other showed the possibility of preferred orientations; it cannot be unequivocally stated that a preferred orientation exists. In the sedimentation model proposed, preferred orientations of grains can develop during deposition of the sediment although the lack of it is not contrary to the model.

Quartz is the other major constituent of the clastics and point counting indicated a range from 30 to 56% with a mean of 46% (n = 11). The size ranges from 0.025 up to 5.0 mm in diameter. While diameters smaller than 0.025 mm are possible it is extremely difficult to distinguish these from isolated chert grains of metamorphic origin. A subangular to angular shape of the quartz grains is the most common although more rounded grains are visible. Authigenic overgrowths and pressure solution shadows are widespread, but by use of dust rings the original grain and its overgrowth can be detected. As revealed in thin section, authigenetic overgrowths are more common in the clastics with a

chlorite matrix while pressure solution shadows are more visible (abundant?) in clastics with an iron oxide matrix. The pressure solution shadows have a "wispy" appearance and are aligned in a single direction in a given sample (normal to λ_3 or the minimum principal strain direction, see Hobbs, Means and Williams, 1976). Embayment of authigenetic overgrowths are the original grains is locally visible. This implies that there must have been an earlier stage of authigenetic overgrowth development. At present it is unknown whether this occurred in situ or if some quartz grains were eroded from a previously consolidated sediment (Mesnard Quartzite?) where the overgrowths could have formed. Regardless of where the overgrowths formed, it is plausible that dissolution of quartz during embayment formation supplied silica to form the pressure solution shadows.

The quartz occurs as both monocrystalline and polycrystalline grains. Polycrystalline grains with up to 10 subgrains are visible. These polycrystalline grains generally show metamorphic textures (e.g., triple junctions, subequigranular size and undulatory extinction). Monocrystalline grains commonly show strong undulatory extinction patterns although grains showing uniform extinction patterns are present.

Other minerals which are thought to be detrital in origin were observed only rarely when compared with quartz abundance. These include feldspar (plagioclase), muscovite and minor biotite. The plagioclase was subhedral to anhedral in shape. Good twinning was visible in a few fresher looking grains but most of the plagioclase was highly altered to sericite and only faint twinning was visible. The size was usually comparable to a medium size quartz grain (0.2 to 0.6 mm long axis) although some smaller fragments of what was thought to be plagioclase were seen. Generally only 1 or 2 grains of plagioclase per slide or its altered equivalent were visible in only a few thin sections (4 or 5).

Muscovite and biotite were more common than plagioclase grains but still at percentages of less than one. Both muscovite and biotite were similar in nature and form of occurrence. They were primarily visible within the clastics that possess a chloritic type matrix as bent and deformed, anhedral grains averaging 0.2 mm in length.

The plagioclase, muscovite and biotite grains observed within the clastics are thought to be of a detrital origin being brought into the basin along with the quartz and clay (now fine-grained chlorite) which compose the bulk of the clastic lenses. It is doubtful that the observed muscovite and biotite grains were formed insitu by metamorphism because: 1) they are much larger than the chlorite which composes the matrix of the clastics (0.2 vs. 0.005 mm), 2) biotite and muscovite generally form at higher metamorphic grades than does chlorite (James, 1955 and Turner, 1981), and 3) their bent and deformed appearance (tectonic deformation). The fine-grained chlorite which composes the matrix of the chloritic clastic lenses probably formed from the metamorphism (chlorite grade) of what was originally clays deposited contemporaneously with the other detrital minerals. The mechanism of deposition will be discussed later.

Lithic clasts were observed in almost all thin sections studied. These were of two types: chert and chlorite. Both are believed to be "rip-up" clasts deposited during deposition of the clastic sediments and later altered by metamorphism. The origin and exact method of deposition will be discussed later. Chert is observed as rounded and deformed masses mixed with quartz grains in clastics of all matrix types. point counting indicated a range from 0 to 25% with a mean of 5.4%. The size ranges from 0.3 to 25 mm diameter. Large chlorite clasts are present, although subordinate to chert in abundance. The size of the chlorite clasts ranges from approximately 0.75 mm down to grains close to the matrix size (0.005 mm). The chlorite grains generally have a bent and

deformed appearance. Because chlorite clasts are not very common no attempt at point counting was made.

Contacts between the clastic lenses and the chemically precipitated iron formation were of two types: sharp and gradational. No estimate was made comparing the relative abundances of these two types. Both types of contacts are visible in thin section and in the core itself. Sharp contacts mark abrupt transitions from iron formation to clastics or vice-versa. Characteristically, a pencil thin line could be drawn along the contact. Layers on either side of the contact do not appear affected by the transition. It appears that normal iron formation precipitation was abruptly interrupted by an influx of clastic material which lasted only a short period of time after which normal precipitation of iron formation continued.

Sharp contacts, while extremely abrupt, generally had a wavy or undulatory contact plane as viewed in the core. While flat and planar contacts were observed it is estimated that undulatory contacts are more common. The most probable explanation for the undulatory contacts is sediment loading and differential compaction rates during diagenesis (Gross, 1972).

Gradational contacts on the other hand record a transition from dominantly chemical to dominantly clastic sedimentation (or vice-versa) over an interval ranging from one-half inch to two feet. For example, a chlorite-rich clastic layer grades upward into pure chemical iron formation by the continuous enrichment in iron oxides and decrease in clastic quartz components. In some cases this is accompanied by a decrease in grain size of the clastic quartz grains with the addition of the iron oxide component. Because of the unoriented nature of the core with regard to an upward or downward direction, it is not know if this occurs solely in an upward direction or whether it can occur in either the upward or downward direction.

The sedimentation model which will be proposed in the next section is that of a submarine fan environment depositing deep-water turbidites. Submarine fans which are exposed in outcrop may show many sedimentary structures, these are either hard to identify in drill core or are not present in the study area. The author feels the former reason to be more accurate as will be explained below.

Graded bedding, when present, is the only sedimentary structure visible, either within a clastic bed or across a gradational contact. It is estimated that graded bedding was visible only 10 to 15% of the time within any clastic interval or across gradational contacts. Other sedimentary structures such as sole marks, clastic dikes, flame structures, visible imbrication of quartz grains or complete Bouma sequences were not seen. James (1955) noted, that in meta-graywackes in the Upper Peninsula of Michigan of Early Proterozoic age, that preservation of original clastic textures was largely a function of the grain size of the sediment. Coarser grained sediments tended to preserve sedimentary textures and structures better than fine grained ones. For example, because the B to E portions of Bouma sequences are developed in the finer grained portions of wackes, these will have a high tendency to be destroyed by metamorphism. When this is combined with the probability of a two inch drill hole intersecting a sole mark or clastic dike it is not surprising that these structures are not visible.

Bed thickness of clastic layers ranges from 1/4 inch up to 30 feet or more in thickness. Most of the thinner clastic layers, less than 2 inches in thickness, show sharp contacts while thicker layers of clastics exhibit both sharp and gradational contacts. Usually the thin clastic layers have a chloritic matrix and thicker layers show any of the four main types mentioned previously. The possibility exists that thin lenses of clastic material with an iron oxide, carbonate or chert matrix were overlooked during logging because they were not as visible as the lenses with the chloritic matrix. Also the thinner lenses tended

to be solely fine grained in size while thicker lenses could have grain sizes from coarse to fine. Interlayering of clastic layers and iron formation layers varies from regular to sporadic. Many thin, fine-grained layers were regularly interbedded with the chemical iron formation every two to five inches. This would be repeated over 20 to 50 feet of core. While thicker layers (greater than two inches) tended to be sporadic in vertical distribution thin layers were observed to be sporadic. Infrequent, single thin layers of clastics could be seen in the drill hole. While these occurrences were not common their presence was noted during logging.

The clastic lenses were generally planar in appearance with straight and wavy contacts where the contacts were sharp. However lensoid shaped were present. This was visible as non-parallel contacts which converged to either one side of the core or both. Because the drill hole intersection with a clastic bed is only a small sample of the bed and lateral continuity cannot be seen, it is difficult to evaluate what the non-parallel contacts do outside the drill hole sample area. It is quite possible that these contacts are soft sediment deformation structures as described by Gross (1972) in many Canadian iron formation deposits.

SEDIMENTATION MODEL

Any sedimentation model proposed for the clastics within the Palmer Basin must explain the following observations about the sediments themselves reviewed here: the immature textural nature of the sediments including such properties as matrix support of the clastic grains (e.g., 43 to 58 percent matrix), the angular to subangular shape, the variation in grain size of the quartz grains (Figures 31 and 32, following Appendix) and the generally poorly sorted nature of the sediments.

Because these sediments are of a highly indurated nature conventional sorting measures such as sieving cannot be used. Figures 33 and 34 (following Appendix) are attempts to quantify sorting observations using thin section data. These figures are plots of the mean phi value versus the coefficient of variation and the standard deviation, respectively. They illustrate that as the coarseness of the clastic sediments increases (lower ϕ values) the sorting becomes poorer by the increases in the coefficient of variation and the standard deviation values.

Some additional observations that have to be taken into account are: 1) the interbedding of chemically precipitated iron formation (Gross, 1972) with terriginous clastics, 2) the variable matrix compositions from chlorite, to iron oxides and carbonates and chert, 3) the presence of "rip-up" clasts composed of chlorite and chert in the clastics, 4) the low feldspar content of the clastics along with the presence of muscovite and biotite, 5) both the sharp and gradational contacts between the clastics and the banded iron formation, 6) the variation in clastic distribution in both the vertical and horizontal directions within the Palmer Basin, 7) the presence of occasional graded bedding in the

clastics, and 8) the thickness variations of the individual clastic lenses (e.g., ¼ inch to 30 feet).

Subaerial clastic sedimentation models such as a fluvial or alluvial environment can unequivocally be ruled out because banded iron formations require a universally agreed upon subaqueous environment (Huber and Garrels, 1953; James, 1954; Lepp and Goldich, 1964; Govett, 1966; Cloud, 1973; Eugster and Chou, 1973; Holland, 1973; Dimroth, 1976; Eichler, 1976). Because, 1) the clastics in the Palmer Basin are intimately associated and interbedded with the Negaunee Iron Formation on a scale as small as ¼ inch, 2) there is a lack of any erosional surfaces and 3) the lateral continuity of the iron formation bands any sedimentation model for the clastics must be a subaqueous one to agree with the models for banded iron formation deposition.

In the subaqueous environment, four main areas of clastic sedimentation are possible: 1) high energy, shallow water, shoreline dominated environments (e.g., beach, offshore bar and proximal deltaic), 2) low energy, shallow water, sheltered lagoons, 3) intermediate energy and water depths characterized by distal deltaic and continental shelf environments, and 4) low energy, deeper water environments such as the continental slope and deep ocean basin (Pettijohn, Potter and Seiver, 1973). Previous workers in the Palmer Basin have discussed the possibility of a high energy, shoreline dominated environment (Tyler and Twenhofel, 1952; Mengel, 1956; Davis, 1965; Gair, 1975). All but Mengel (1956) have discarded this environment and the arguments presented by Davis (1965) and Gair (1975) against Mengel are very persuasive. The high energy, shoreline dominated environment will not be discussed any further.

A low energy, shallow water, sheltered, lagoonal environment is a possible near shore, paleo-environment for the Palmer Basin. The possibility of depositing chemically precipitated iron formation in this environment has been

discussed by Hough (1958), Drever (1974), Dimroth (1976), Eichler (1976), Dimroth (1979), and Kimberley (1979) and it appears to present no problem from a geochemical aspect. However, in proposing this environment for the eastern Palmer Basin, several problems arise.

First, the depositional environment for the Siamo Slate formation has been shown to have been a deep water, turbidite environment by Larue (1979, 1980, 1981), Gair (1975), and Tyler and Twenhofel (1952). If the Palmer Basin was a shallow water lagoonal area there should be a facies of sediment between the Siamo and the Negaunee which records the transition from deep to shallow water (e.g., low to high energy, James, 1979). This facies should be a higher energy deposit of some sort over the low energy Siamo Slate. Not only is this facies not present but the transition from the Siamo to the Negaunee is very indistinct and gradational, marked only by the apparent addition of chemically precipitated iron formation to the deep water Siamo deposits (Snider, 1972; Gair, 1975).

Second, tidal flats and protective barriers are commonly associated with lagoons (James 1979). The tidal flats will commonly show subaerial desiccation features such as mud cracks and stromatolites along with gypsum crystals or their pseudomorphs. While these features have been found associated with other iron formation basins (e.g. Sokoman Iron Formation, Dimroth, 1979) they are absent in the Palmer Basin area (Gair, 1975). The presence of an offshore protective barrier was inferred by James (1955) to explain the facies transitions of iron formations (i.e., oxide to carbonate to sulfide) yet no such barrier has been found (Tyler and Twenhofel, 1952; James, 1955; Gair, 1975).

Finally, James (1979) notes that while lagoons are protected from waves and swells they are still susceptable to storms and tides. Storms are not inconsistent with a lagoonal Palmer Basin model in that they could provide a means of washing sediment from a continental source area into the lagoon

periodically. Tides are inconsistent with a lagoonal model for the Palmer Basin in that previously deposited sediments are commonly winnowed by the actions of tides (Goldring and Bridges, 1973; Pettijohn, Potter, and Seiver, 1973; James, 1979). Because lagoons are near shore and shallower than open shelfs, the tidal forces would winnow the matrix and finer grained portions of clastic sediments away. The clastics in the Palmer Basin show no indications of winnowing by the presence of a high percent of a fine-grained matrix.

Thus, while the lagoonal environment can be applied to some banded iron formation deposits it appears not applicable to the Palmer Basin area.

While the textures of the clastic sediments within the Negaunee Iron Formation in the Palmer Basin preclude a high energy, shoreline dominated or a lagoonal environment, they are consistent with clastic textures associated with intermediate to low-energy environments, specifically areas below non-storm wave base (Davis, 1965; Gair, 1975; and this study). The submarine areas associated with these lower-energy environments are distal areas of river fed deltas (Aalto and Dott, 1970; Nelson and Kulm, 1973; Pettijohn, Potter, and Seiver, 1973; Walker and Mutti, 1973) and the continental slope to deep ocean plain areas where gravity flows (e.g., turbidites and debris flows) and gravity sliding (e.g., slumps and slides) are the primary methods of clastic sediment transport and deposition (Aalto and Dott, 1970; Mutti and Ricci Lucchi, 1978; Nelson and Kulm, 1973; Normark, 1978; Pettijohn, Potter, and Seiver, 1973; Ricci Lucchi and Valmari, 1980; Stow and Shanmugan, 1980; Walker, 1970, 1975, 1976, 1978, 1979; Walker and Mutti, 1973).

Davis (1965) and Gair (1975) have already attributed the clastic sediments to turbiditic gravity flows originating along the south margin of the Palmer Basin. They do not address, however, specific parts of the gravity flow environment which are involved in the Palmer Basin. The data generated in this

study now allows a tentative interpretation of what sub-environments were involved in the deposition of the clastics within the iron formation (e.g., slope channels, suprafan lobes, proximal to distal fan, and distal deltaic environments).

A review of gravity flow and gravity sliding environments and sub-environments is warranted and is derived from the voluminous literature available. Gravity flow transport of sediments differs from gravity sliding transport of sediments in that the former involves turbulent flow of clastics within a finer-grained fluidized matrix, while sliding or slumping involves slippage along discrete planes involving blocks of material (Middleton and Hampton, 1973). Naylor (1981) notes that to some authors, slumping implies a mass of sediment with a curved glide or failure surface, while sliding implies a planar failure surface. Obliteration of pre-transport sedimentary structures (e.g., bedding) is complete for gravity flows, whereas it can range from slight to moderate for slides and moderate to extreme for slumps (Middleton and Hampton, 1973). It should be noted that because of this possibility for extreme internal deformation in slumps, they may be indistinguishable from tectonic folds (Helwig, 1970; Woodcock, 1976).

Gravity flows are classified into four main categories by Middleton and Hampton (1973) based upon the dominant sediment-support mechanism: 1) turbidity currents, in which grains (clasts) are supported by an upward component of fluid turbulence, 2) fluidized sediment flows, in which grains are supported by the upward escape of contained fluids, 3) grain flows, where direct grain to grain collision or contact provides the support, and 4) debris flows, where larger clasts are supported or rafted by a "fluidized" matrix of sediment and water which has a finite yield strength. These four sediment-support and transport mechanism produce three main types of deposits: a) turbidites and

fluxoturbidites (1, 2, and 3), b) resedimented conglomerates and massive sandstones (2 and 3), and c) pebbly mudstones (4) (Middleton and Hampton, 1973).

The observed textures of the clastics within the Palmer Basin are roughly consistent with the a, b, and c types mentioned above and with slump features. For the three types of deposits individual bed thicknesses can range from centimeters to a few tens of meters and can be laterally continuous (turbidites) or discontinuous (pebbly mudstones) (Walker, 1978). The turbidites and fluxoturbidites generally create the most abundant original sedimentary features, such as grading, toolmarks and stratification, while the pebbly mudstones will usually lack these features. Also, turbidites will be more repetitious in a horizontal section, while pebbly mudstones and massive sandstones occur as more unique events (Middleton and Hampton, 1973; Walker, 1978).

Ancient and more recent submarine basins and their contained submarine fans can fit into a facies model which contains the features attributable to gravity flow and gravity sliding transport (Walker, 1978). In brief, the major subfacies of this model occur at a shelf-slope break or in the distal areas of deltas (sediment accumulation), on a slope (sediment transport with minor accumulation) and on a deeper water plain (sediment accumulation). According to Walker and Mutti (1973) basins which have these criteria include lakes (Lake Mead and Lake Superior), cratonic basins (prodeltaic sequences, Mississippian Borden Siltstone), block faulted continental borderlands (California coast), elongate exogeosynclinal basins (Ordovician Martinsburg Formation-Appalachians) and major ocean basins (the Atlantic and Pacific).

The primary sediment accumulation site is either along the outer margin of a delta or along the shelf-slope break where a transition from relatively shallow water to deeper water (below wave base) occurs. For the delta, sediment is

supplied by an active river system (Pettijohn, Potter, and Seiver, 1973). Transport of the sediment across a shelf, with or without a delta present, is accomplished by tidal and wave action along with storms (Goldring and Bridges, 1973). Local slumping and sliding along the shelf-slope break and at the outer delta margins is to be expected resulting in pebbly mudstones and gravity slump deposits (Walker, 1978). These events can be initiated by gravitational instabilities or seismic events (Middleton and Hampton, 1973).

The slope to the basin is used to transport sediment from the primary accumulation sites to deeper water depositional areas. Transport generally occurs in discrete channels although occasional flows outside of channel areas can occur (Normark, 1978). Channels are of three main types: 1) depositional, 2) depositional-erosional, and 3) erosional (Nelson and Kulm, 1973). Which type that is present for any given area probably depends upon numerous factors including the rate of sediment supply, the slope angle, the density of the current, the speed of the density current, the grain size variation and the percent matrix versus clasts. In the erosional and erosional-depositional channels, currents can pick up previously deposited sediments and incorporate them into their mixtures while deposition of sediment alone happens in the depositional channels (Middleton and Hampton, 1973; Nelson and Kulm, 1973). Overbank or levee deposits commonly occur alongside channels due to the sediment gravity flow overflowing its banks (Walker, 1978). These are commonly fine grained, thin bedded turbidite deposits which are not particularly laterally continuous (Normark, 1978; Walker, 1978). Within the channels themselves, turbidites and fluxoturbidites can be deposited by the waning portions of a sediment flow (commonly Bouma T_b-T_e). Resedimented conglomerates, massive sandstones and pebbly mudstones can be deposited in the channels by "freezing" of a flow

due to energy loss from the system (Walker, 1978). In addition, slumping and sliding can occur on the slope(s) outside channel areas (Walker, 1978).

Once the transported sediment reaches the basin floor, submarine fans commonly develop (Mutti, 1973; Mutti and Ricci Lucchi, 1978; Nelson and Kulm, 1973; Normark, 1978; Walker, 1976, 1978, 1979; Walker and Mutti, 1973). As reviewed by Walker (1978), the main features of submarine fans are an upper-fan to mid-fan to lower-fan basinward gradation with suprafan lobes superimposed upon the mid- to lower-fan areas.

The upper-fan area occurs at the base of the slope and generally contains the coarsest material transported into the basin (conglomerates and massive sandstones) along with finer-grained overbank levee deposits. As the slope decreases the mid-fan area is formed. The suprafan lobes are usually found in this area although they can protrude into the more distal lower-fan area. The suprafan lobes are roughly analogous to the lobes in the near-shore deltaic environment in that they possess a semi-circular shape and can migrate to different areas by breaching their channels (lobe switching and abandonment). Within the suprafan lobes, massive, medium to coarse grained sandstones and proximal turbidites (Bouma T_a-T_b or T_c) are found. Channels of all three previously mentioned types can form on the lobes although the lobes are primarily depositional sites (types 1 and 2). Outside of the suprafan lobes deposits of the mid-fan area are primarily overbank levee deposits, medium to fine massive sandstones and turbidites (Bouma T_a-T_e). The lower-fan area receives the medium- to fine-grained fraction of the sediment gravity flows and is generally characterized by turbidites showing the complete Bouma sequence (e.g., T_a-T_e). Deposits in this environment are usually laterally continuous since the flows are not confined to channels. Basinward from the lower-fan is the

basin plain where only fine grained turbidic sediments (Bouma T_c-T_e) and "normal" hemipelagic sediments accumulate.

The sediments within the Negaunee Iron Formation differ in some respects from the ancient and more recent submarine fan environments as described by Aalto and Dott (1970), Mutti and Ricci Lucci (1978), Nelson and Kulm (1973), Normark (1978), Ricci Lucchi and Valmari (1980), Walker (1970, 1975, 1976, 1978) and Walker and Mutti (1973). First, the clastics in the Palmer Basin are finer grained (coarse to fine sand) than most of the ancient and modern submarine fans described in the literature. There is no significant conglomeratic fraction (except at the Moore Mine mentioned earlier) and no textures indicative of massive sandstones. The grain sizes are similar to Bouma T_a-T_c sequences. Stow and Shanmugan (1980) have described fine grained turbidites from both ancient and recent sedimentary sequences, and except for certain sedimentary structures (e.g., graded bedding, casts, etc.), these share many similarities with the clastics in the Palmer Basin. Perhaps it is the lack of documented and published descriptions of ancient fine-grained turbidites which is anomalous and not their absence.

Second, the presence in some areas, of large numbers of individual beds of coarse to fine sand grain size, with thicknesses from centimeters to many meters which are anomalously matrix supported. The turbidite environments described in the literature generally have a grain supported matrix for the medium to coarse sand fraction of individual layer thicknesses found in the Palmer Basin. Pebbly mudstones and Bouma T_c-T_e sequences both have a high muddy-matrix percent. Those described in the literature have either larger clast size (pebbly mudstones) or finer clast size (Bouma T_c-T_e) than the ones found in the Palmer Basin. The possibility exists that the high matrix percent might be due, in part, to authigenic development of the matrix. Authigenic development of matrix

material in graywackes has been documented by many workers (see Pettijohn, Potter and Seiver, 1973, for overview) and it cannot be disregarded for the sediments in the Palmer Basin. A discussion of authigenic matrix development is beyond the scope of this paper but it should be noted that this phenomena could explain the observed high matrix percent.

Third, in the Palmer Basin, graded bedding is the exception not the rule for the clastic sediments. It is estimated that only 10 to 15 percent of the beds viewed in core possessed any textures indicative of graded bedding. The turbidite environments described in the literature have common occurrences of graded bedding. Only in the conglomerates, massive sandstones and pebbly mudstones, is grading absent. As noted previously, the first two of these three types of deposits have not been found in the area of the Palmer Basin.

Other workers have identified submarine fan environments in Precambrian age rocks, some interbedded with banded iron formations. These deposits share many similarities with the deposits in the Palmer Basin. Condie et al. (1970) and Eriksson (1980) have described a submarine, mid-fan environment in the Archean Fig Tree Group in South Africa which is interbedded with banded iron formation. The grain size of quartz ranges from less than 0.1 mm to 5 mm in diameter (fine sand to granule size) and is poorly sorted. There is a high matrix percent of the clastics which is composed of chlorite with minor muscovite. Chert is commonly found in the matrix and bed thicknesses range from 10 cm to 1 meter. Condie et al. (1970) proposed a graywacke environment with short distances of sediment transport (i.e., less than 100 km), while Eriksson (1980) went further and identified a prograding mid-fan environment with channel fill deposits and matrix supported congolmerates.

Pickering (1981) identified a suprafan lobe to fan-fringe sequence in the late Precambrian Kongsfjord Formation in Northern Norway. While there is no

banded iron formation associated with this formation, it shares similarities with the Palmer Basin deposits in bed thicknesses and turbidite facies. In the **Kongsfjord formation the suprafan lobe** deposits are composed of very coarse to medium sandstone, average greater than 80% sandstone and less than 20 percent shale and have bed thicknesses ranging from 2 to 15 meters. The lobe-fringe deposits are composed of fine sandstone, averaging 80 to 40 percent sandstone and have bed thicknesses of 10 to 50 cm. The fan-fringe deposits are composed of very fine sandstone, contain less than 40 percent sandstone and have bed thicknesses from 20 to 70 cm. The suprafan lobe is composed of Bouma T_a to T_b or T_c, the lobe-fringe has Bouma T_b to T_d or T_e while the fan-fringe area has Bouma T_c to T_e.

Meyn and Palonen (1980) working in the Archean, Superior Province in Ontario have identified a 500 meter thick sequence of graywacke turbidites, shales, siltstones, sandstones and conglomerates interbedded with banded iron formation. Many similar lithologies with the clastics in the Palmer Basin exist including a high matrix percent, graywacke and iron formation interbedded on a scale of centimeters with sharp bedding contacts and "rip-up" clasts within the clastic layers. They have identified slump folds within both the turbidites and iron formation and hypothesize that the Bouma T_e layer is represented by magnetite-carbonate-chert iron formation. They prefer the submarine fan model of Walker (1978) as a paleo-environmental interpretation.

As mentioned previously there are a few problems with fitting the clastics within the Palmer Basin exactly into the submarine fan environments proposed by workers on modern and Paleozoic aged deposits. However, these problems are common to other Precambrian age deposits which share more similarities with the submarine fan environment than with any other environment (e.g., open shelf, shallow-water near shore, lagoonal or fluvial). Condie et al. (1970),

Eriksson (1980), Meyn and Palonen (1980), and Pickering (1981) did not hypothesize why these differences exist nor have any of the workers who have developed the facies models for the submarine fan environment (Aalto and Dott, 1970; Mutti and Ricci Lucci, 1978; Middleton and Hampton, 1973; Nelson and Kulm, 1973; Normark, 1978; Ricci Lucchi and Valmari, 1980; Walker, 1970, 1975, 1976, 1978; Walker and Mutti, 1973). The grain size differences between the known Precambrian deposits and the Paleozoic to modern deposits can be accounted for in three ways: 1) finer grained source areas and/or more efficient breakdown of quartz by weathering and transportation in rivers and across shelves, 2) the Precambrian submarine deposits are of a more distal nature, and 3) that the sediments comprising the clastics in the Negaunee Iron Formation are fine-grained turbidites of the type described by Stow and Shanmugan (1980) which are not expected to have a significant coarse-grained fraction. The author feels that a combination of the above three possibilities would be most probable.

The percent matrix difference in Precambrian deposits can be attributed to five possibilities: 1) more clay (e.g., fines) in the primary accumulation site along the shelf-slope break, 2) the possible development of an authigenic matrix as described previously, 3) a portion of the observed matrix is composed of now unrecognizable, squashed lithic fragments and/or "ripped-up" matrix material acquired during transportation from the accumulation site to the depositional site, 4) some of the deposits in the geologic literature classified as turbidites are really fine-grained pebbly mudstones which are expected to have a high matrix percent, and 5) if the deposits in the literature are turbidites, they are of the Bouma T_c-T_e sequence instead of T_a-T_b. The fourth and fifth possibilities are probably unlikely due to the described graded bedding and horizontal stratification in the Precambrian deposits which are common to the Bouma T_a-T_b portions of turbidites.

The clastics in the Palmer Basin possess another unique feature not common to other Precambrian deposits; that is the lack of widespread graded bedding. This could be due to points 4 and 5 of the preceeding paragraph or as noted previously by James (1955), that finer grained sediments tend to lose sedimentary structures and textures during metamorphism faster than coarser grained sediments.

The paleo-environment of the Palmer Basin is here tentatively hypothesized to be that of a mid-fan to outer-fan area of the submarine fan environment. This interpretation is the most consistent with the observed textures of the clastics. Since, in this environment, channels in lobes can exist along with the more laterally extensive and vertically repetitious non-channel lobe and outer-fan deposits. The channels will be the sites of thicker individual beds and will have low bed numbers in the vertical section. Also, the percent total clastics will be high. Outside of channel areas the individual bed thicknesses will be less, the bed number in vertical section will be higher, and the percent total clastics will be lower.

Because of the use of drill holes and the possibility of both tectonic and slump folding, lateral continuity cannot be estimated. Likewise, a drill hole can have penetrated anywhere from the center of a channel to areas on the outer-fan. This can lead to a bias in sampling of specific environments within the basin (e.g., non-channel areas are larger in area than the channels). At best only rough and tentative interpretations of the data can be made at this point.

It is envisioned that chemical precipitation of the banded iron formation was a continuous process. The clastic influxes were discrete, short-lived events which periodically entered the basin from the south. Because gravity flow currents can be erosive events, they could pick up previously deposited iron formation and clastics and incorporate them into the flow. This would account

for the "rip-up" clasts of chert and chlorite found in the clastics, the variable matrix compositions of the clastics found, and the anomalous matrix percent. The sharp contacts between iron formation and clastics are due to the quick nature of deposition of gravity flow and gravity slump deposits. The gradational contacts are probably due to either the slow settling of suspended fines from the waining portions of flows mixing with continually precipitating iron formation or they represent flows which have incorporated a significant portion of iron formation facies into their matrixes prior to deposition. The Bouma T_e layers are represented by banded iron formation accumulations which can be thought of as replacing the hemipelagic fallout found on modern basin floors in agreement with Meyn and Palonen (1980).

In order to account for the low feldspar content of the clastics found in the Palmer Basin the source area could have had a low feldspar content or weathering was very efficient in destroying feldspar grains prior to transportation to the basin for deposition. While the mechanical destruction of feldspar grains is consistent with the fine grained nature of the more resistent quartz grains found in the basin the efficient chemical weathering of a granitic gneiss will release quartz grains into the environment while destroying feldspar grains in situ. Finally, the source rocks for the clastics must have had muscovite and biotite grains within them in order for these minerals to be present within the clastics in the Palmer Basin. These minerals only form at a higher metamorphic grade than that experienced by the Palmer Basin during the Penokean Orogeny (Turner, 1981; James, 1955).

Thus the submarine fan environment adequately accounts for the observed features mentioned at the beginning of this section and does so in the simplest possible way. Also this model is consistent with other published graywacke-banded iron formation occurrences in the Precambrian.

CONTOUR MAPS

All contour maps that will be discussed in this section are based on the 80 drill holes whose locations were previously presented in Figure 4. A number of different parameters were chosen to contour in the hope that they would convey the maximum amount of information without being redundant. The contour maps are grouped into three intervals: 1) specific 100 foot thick intervals from 500 to 1199 feet above sea level (ASL), 2) composites of the 100 foot thick intervals, and 3) total length of drill hole available. Because of limits on the data base discussed previously, only gross trends in clastic sediment thicknesses, the numbers of beds, the lithologies and textures can be inferred. To make the contour maps more presentable and to aid in the identification of gross trends, only selected contour lines have been drawn in. For all maps, mean sea level was used as a reference datum.

Figures 5 to 25 are contour maps of the parameters chosen for specific 100 foot thick intervals. For each 100 foot thick section three maps are presented: 1) the percent total clastics in that interval, 2) the thickest continuous clastic bed of any lithology, and 3) the number of clastic beds greater than or equal to one inch thick, incorporating all matrix lithologies. Figures 26 and 27 are composite maps from the 100 foot thick intervals (500 to 1199 feet ASL). Figure 27 is from the 7 intervals utilizing the number of clastic beds greater than or equal to one inch thick, incorporating all matrix lithologies while Figure 26 is of the same 7 intervals but using only those clastics with a chloritic matrix (the 7 individual interval maps are not included with this report). By comparing the two maps, differences appear which show areas which have received dominantly chloritic matrix type clastics versus areas which have received either

a mixture of iron oxide and chloritic matrix clastics or solely iron oxide matrix dominated clastics. Proximal areas along with channels will be dominantly chloritic while more distal areas will contain more iron oxides in the matrix due to dilution of the flow and the continual precipitation of banded iron formation.

The 500 to 599 foot ASL interval was selected as the lower limit because: 1) in this interval only 47 of the original 80 drill holes penetrate this interval (38 percent utilizing CCI data) and this number drops to 31 drill holes (58 percent utilizing CCI data) in the 400 to 499 foot interval, and 2) it is felt that below 500 feet ASL the influence of the Siamo-Negaunee contact-gradational zone might bias the clastic lense distribution. Because this contact cannot be accurately located (Gair, 1975; Snider, 1972) it is best to stay above its probable level of influence. The 1199 foot ASL upper limit was selected because in the 1200 to 1299 foot interval present day land surface, the Goodrich quartzite and glacial deposits are encountered.

Figures 28 to 30 are contour maps utilizing the total hole lengths available for all drill holes. Total hole lengths were utilized for the percent coarse divided by the percent fine map, Figure 28, and the map showing the percent clastics with a chloritic matrix, Figure 30. This is due to the fact that some of the data necessary to make these maps was not logged very accurately by CCI geologists for some of the 100 foot thick intervals discussed previously. It is hoped that by incorporating all the data available for the total hole lengths, some gross trends might become apparent, albeit susceptable to a somewhat higher degree of error than other maps might possess.

Figure 29, the number of discrete, chloritic clastic beds greater than or equal to one inch thick, for the total hole length is an attempt to illustrate two points: 1) the distribution of chloritic clastic beds below the 500 foot and above the 1199 foot ASL levels, and 2) to show the effect of how including estimated

numbers of chloritic clastic beds for intervals alters the distribution of chloritic clastic beds derived where only discrete beds are used. Estimated intervals are those where there were so many clastic beds that logging of the interval inch by inch would have been too time consuming. Instead, generalizations were used such as: "90 feet of core, approximately 30% clastic lenses, generally one to two inches thick" or "90 feet of core, one inch clastic lense every two inches". While generalizations such as these are easy to work with in computing percent total clastics, difficulties arise when the total number of beds is computed. Because the above statements are generalizations, and are susceptable to error, a bit of subjective interpretation is needed to derive the numbers of beds present. While it is hoped that consistency was used to keep the error low the intervals were nevertheless designated as estimated intervals to distinguish them from unequivocal clastic lense occurrences which were noted as: "419.3 feet, 2 inch chloritic clastic lense" and thus called discrete beds.

The sedimentation environment deduced from the textures of the clastics is that of a submarine fan environment. Specifically, the mid-fan to outer-fan area as described by Walker (1978). If this is a viable hypothesis of a paleo-environment, the distributions and positions of bed numbers, thicknesses and types should be consistent with this idea. Gross trends should be visible, which show the differences between channel and non-channel areas and which show a gradation from a relatively proximal mid-fan area near the south to a more distal outer-fan area to the north.

Channel versus non-channel areas should show contrasts in the percent total clastics (higher in channels), the thickest continuous clastic bed (thickest within channels, the numbers of clastic beds (higher outside of channels) and the percent coarse divided by the percent fine clastics ratio (higher ratio in channel areas). The reasons for these differences were discussed in the sedimentation

model section. A transition from a southern proximal to a northern distal environment should be evidenced by a trend in parameters from south to north. Because contrasts between channel and non-channel areas can locally overprint this trend (positions of inferred suprafan lobes) only crude generalizations of a trend can be expected to be visible. A south to north trend should be evidenced by the following change in parameters: 1) a decrease in the percent coarse divided by the percent fine clastics, 2) an increase in the number of beds with an iron oxide matrix when compared with the total number of beds present, 3) a decrease in the percent clastics with a chloritic matrix versus an iron oxide matrix, 4) a decrease in the number of discrete, chloritic clastic beds, and 5) a decrease in the percent total clastics. Point 1 is due to deposition of the coarsest material in the more proximal environment while points 2 through 5 are due to dilution of the flow by incorporated iron formation and previous deposition of clastics. Finally the thickest continuous clastic bed should not only occur within channels but in the proximal environment as well.

In Figures 26 to 30 a rough trend can be detected from south to north indicating what is interpreted as a gradation from a more proximal to a more distal environment. While this trend may not be obvious on any given diagram it does become visible when the diagrams are compared to one another. For instance, compare Figures 26, 27 and 30 (500 to 1199 foot composits of the number of chloritic clastic beds and the number of clastic beds of all lithologies and the percent clastics with a chloritic matrix). The number of clastic beds with an iron oxide matrix increases to the north (more distal), high numbers of iron oxide matrix dominated clastics generally occur outside or away from areas with a high chloritic matrix content (near channel to away from channel areas) and lastly, the percent clastics with a chloritic type matrix decreases from south to north (proximal to distal progression). While a regression of the environment

cannot unequivocally be ruled out, comparison of sediment distribution between high intervals (e.g., 1100 to 1199) and low intervals (e.g., 500 to 599) shows no trend toward a southward migration of the depositional environment.

Figure 28 (the grouped ratios of percent coarse divided by percent fine) also shows a rough trend from relatively more coarse grained in the south to more fine grained in the north. Superimposed upon this trend are what are interpreted to be local channel and depositional/erosional areas (e.g., north part center section 27). While these cause some "noise" in the proximal to distal trend, the south to north gradation from coarse to fine is still evident.

Differences between channel and non-channel areas are seen most easily on the contour maps of specific 100 foot thick intervals. Channels on modern fans are linear features which snake or meander from the slope to the outer areas of suprafan lobes (Normark, 1978). Because this study utilizes drill core the linear nature of channels cannot be expected to be visible due to the fact that only one drill hole may pass through the channel in any area. Consequently, the presence of channels will usually be visible in isolated areas and at best by the alignment from 2 or 3 adjacent drill holes.

In the 500 to 599 foot ASL interval (Figures 5 to 7) channel areas are visible in the center of section 27 and along the boundary between sections 26 and 27. The channel is delineated by thick continuous beds (30 feet or greater) and low numbers of individual beds (1 to 5, maybe 10). Adjacent to these areas the bed thicknesses decrease while the number of beds increases, indicating the surface of the suprafan lobe or the mid-fan area where deposition of overbank deposits and turbiditic sediments, which have previously emerged from channels, occurs. Because the suprafan lobes receive large amounts of sediment the percent total clastics will be high for the channel areas as seen on Figure 5.

Analyses such as this can be done for the other 100 foot thick sections with similar results. Change does occur in the inferred positions of the channel areas which in the submarine fan environment is due to lobe switching and channel abandonment as channels breach their banks and form new lobes.

It is interesting to note that two areas of sediment accumulation seem to consistently stand out in the area of the Palmer Basin with which this study is concerned. These areas are linear in an east-west direction, and are parallel to each other. One is visible along the very southern most edge of the Palmer Basin along the section 27-34 boundary line while the other occurs in about the center of section 27, about ½ mile north of the first. These two linear areas show consistently high percent total clastics, numbers of clastic beds greater than one inch thick and thickest continuous clastic bed. It is interesting to speculate on other reasons for these occurrences besides the previously discussed sedimentation model. Because the interpretation of the clastic textures supports rapid sedimentation with immature sediments and a fault-bounded trough is one mechanism to accomplish this, perhaps these two linear sediment accumulation zones are expressions of the southern trough boundary fault(s). Sediment accumulation would be expected to be greatest on the down-thrown side of these faults since they might act as sediment "traps" as the sediment makes its way down slope to deeper water. Figure 35 contains two possible methods by which the clastics can accumulate due to fault activity which would lead to the distribution visible on the contour diagrams.

If both zones are anomalous areas of sediment accumulation a pair of faults is necessary to explain the sediment pattern. The upper part of Figure 35 would be a possible model involving two parallel faults. If, however, only the southernmost sediment accumulation zone is anomalous (along the section 27-34 border) a single fault model most simply explains the occurrence. The lower part

of Figure 35 (following Appendix) shows this model where a thick accumulation of sediment occurs adjacent to the fault. In this model the zone of sediment accumulation in the center of section 27 is due to sedimentation of the type proposed for the basin as a whole (i.e., deep water turbidites with the possible development of a submarine fan environment).

Thus the contour maps support the interpretation that the clastics in the Palmer Basin were deposited in a submarine fan environment. A mid-fan to possibly outer-fan area with suprafan lobes is proposed as the sub-environment within the main submarine fan environment.

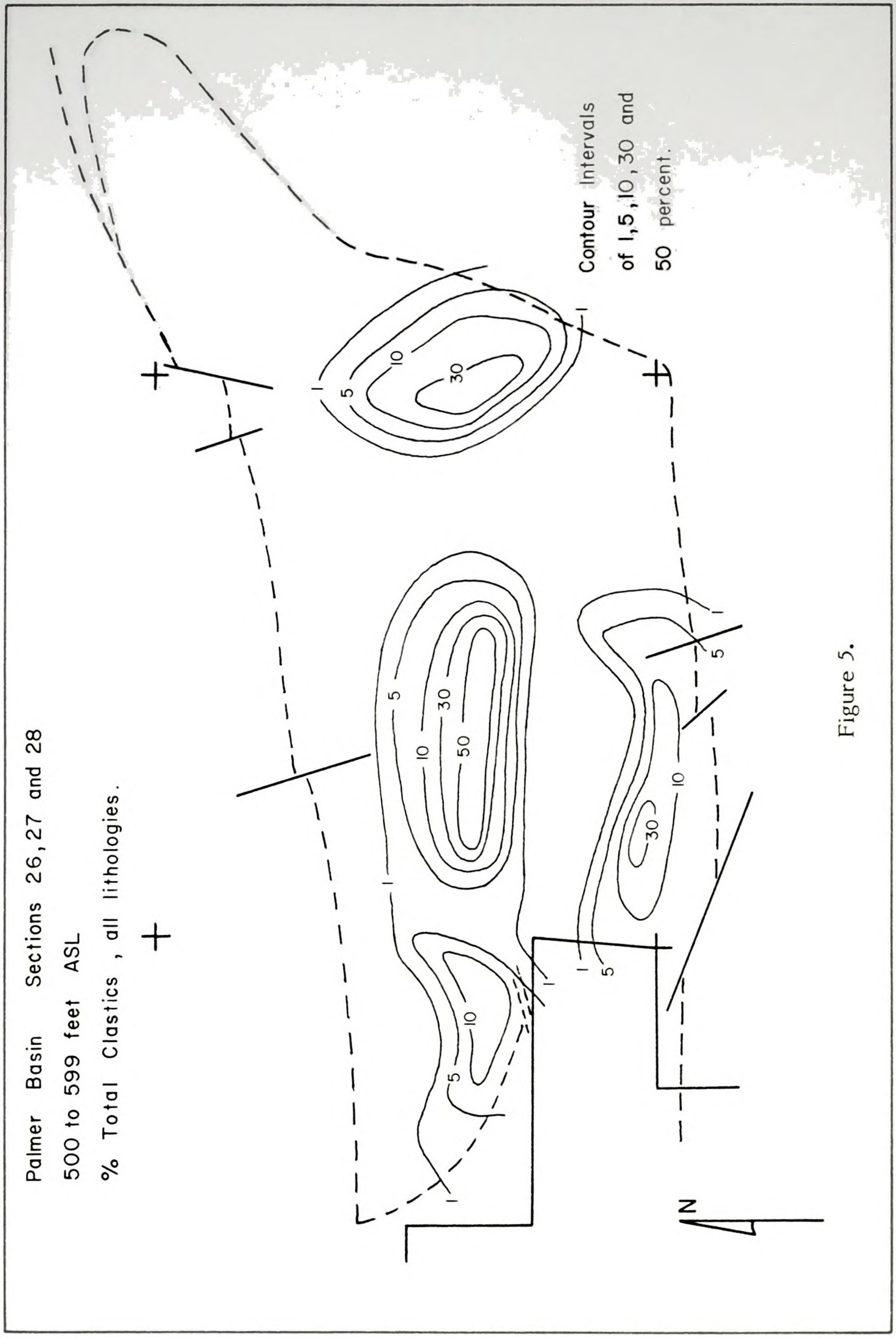
Palmer Basin Sections 26, 27 and 28
500 to 599 feet ASL
% Total Clastics, all lithologies.
Contour Intervals
of 1, 5, 10, 30 and
50 percent.
N

Figure 5.

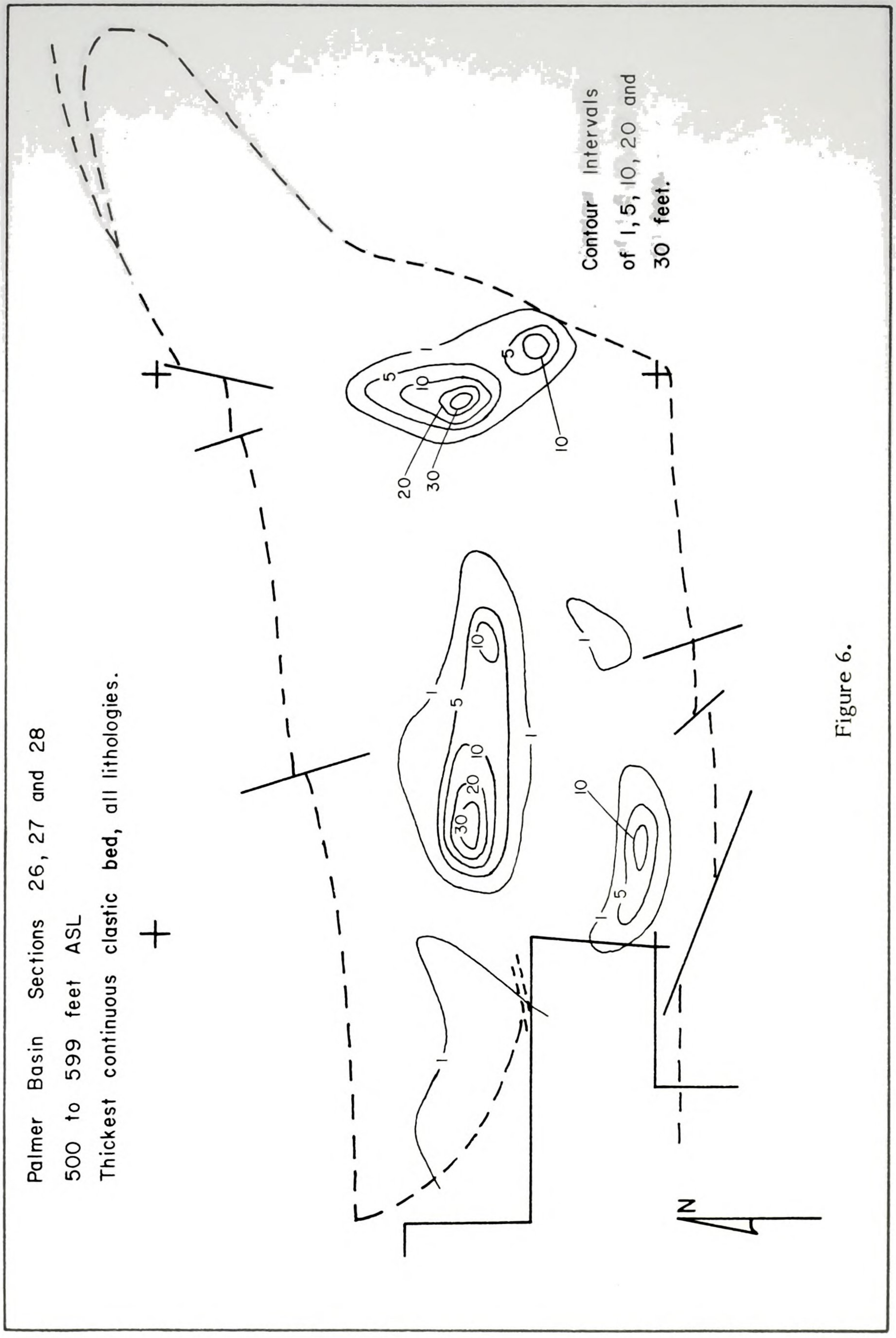
Palmer Basin Sections 26, 27 and 28
500 to 599 feet ASL
Thickest continuous clastic bed, all lithologies.
Contour Intervals
of 1, 5, 10, 20 and
30 feet.
N

Figure 6.

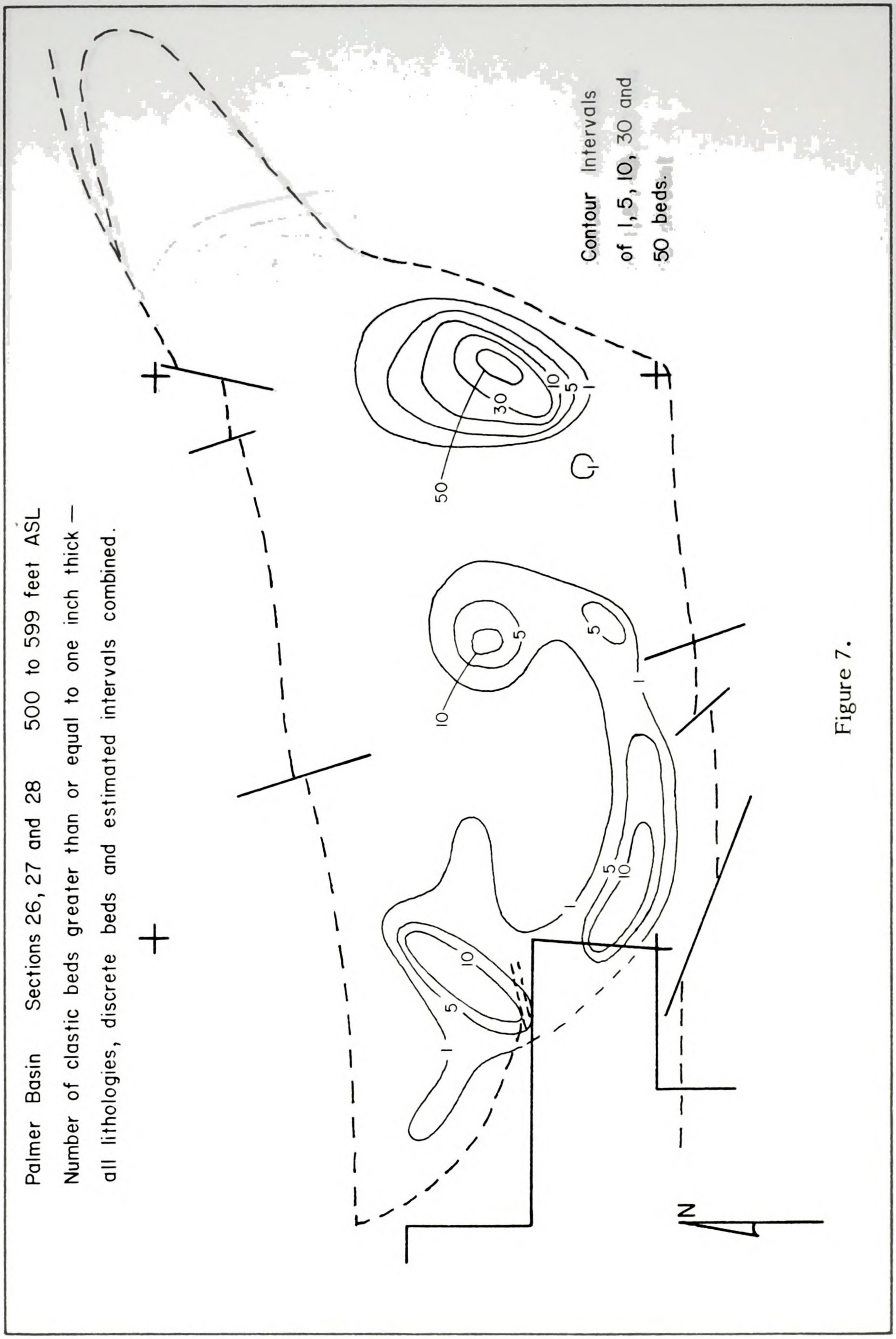

Palmer Basin Sections 26, 27 and 28 500 to 599 feet ASL
Number of clastic beds greater than or equal to one inch thick —
all lithologies, discrete beds and estimated intervals combined.

Figure 7.

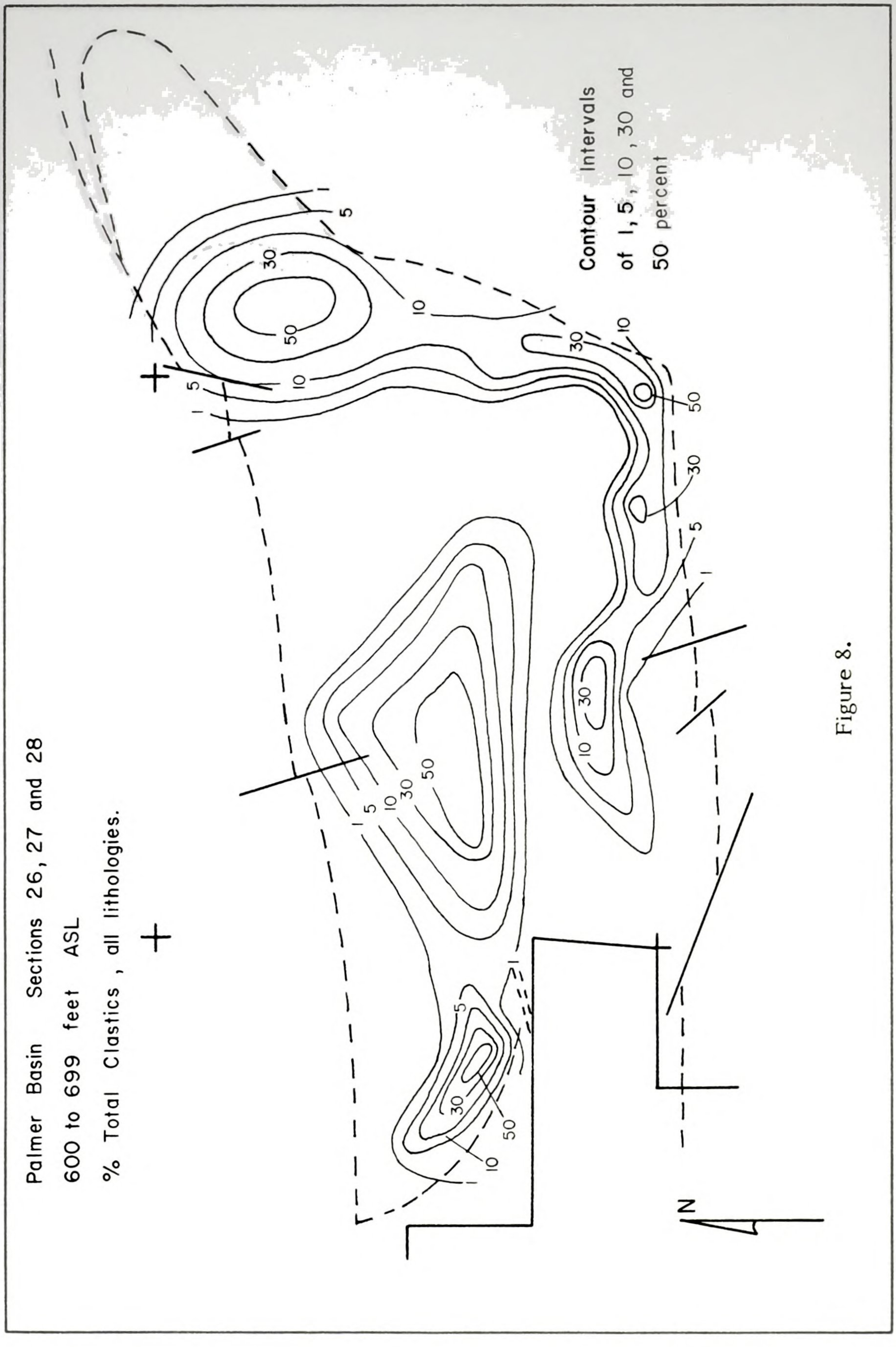
Contour Intervals
of 1, 5, 10, 30 and
50 percent
Palmer Basin Sections 26, 27 and 28
600 to 699 feet ASL
% Total Clastics, all lithologies.
N

Figure 8.

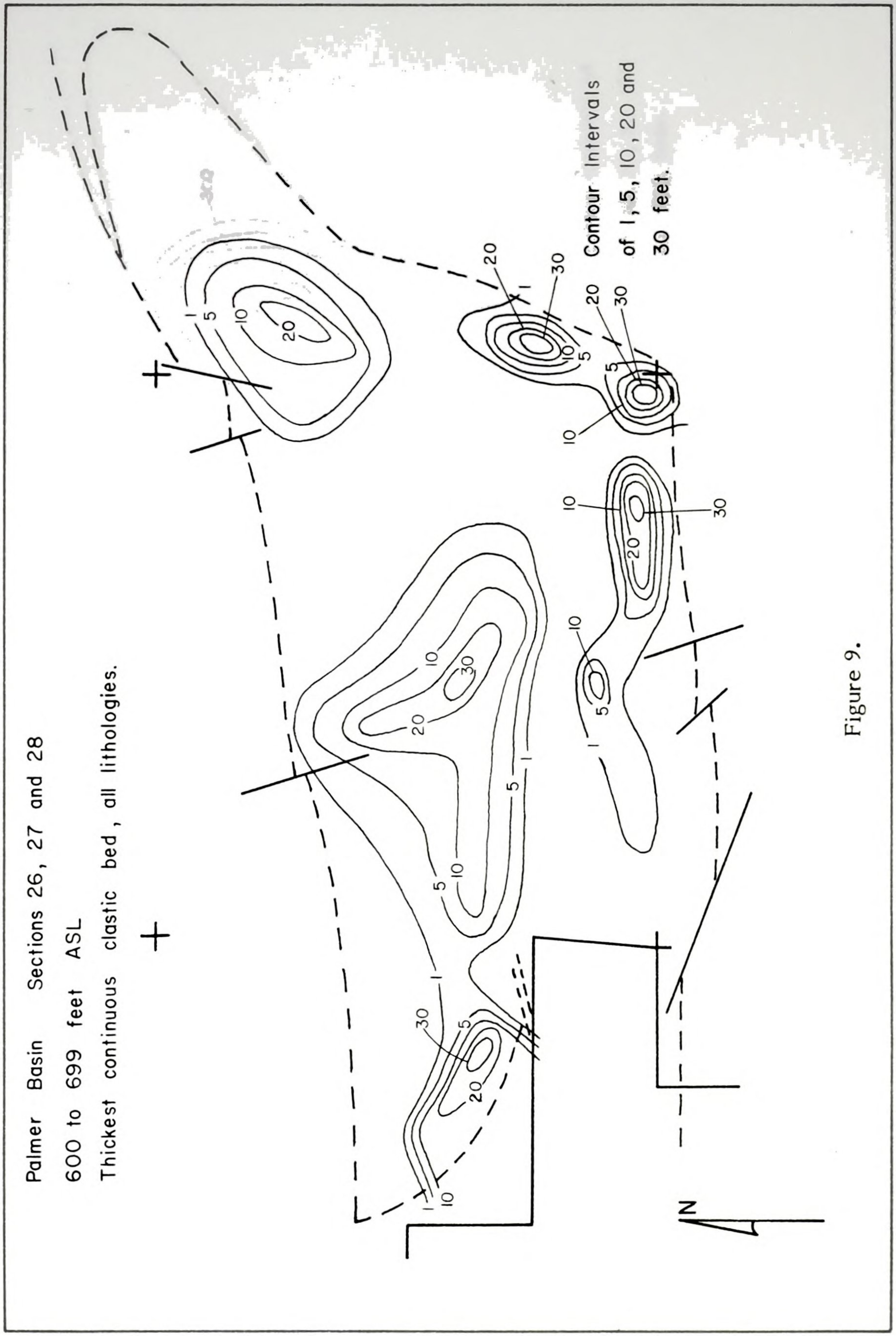
Palmer Basin Sections 26, 27 and 28
600 to 699 feet ASL
Thickest continuous clastic bed, all lithologies.
Contour Intervals of 1, 5, 10, 20 and 30 feet.
N

Figure 9.

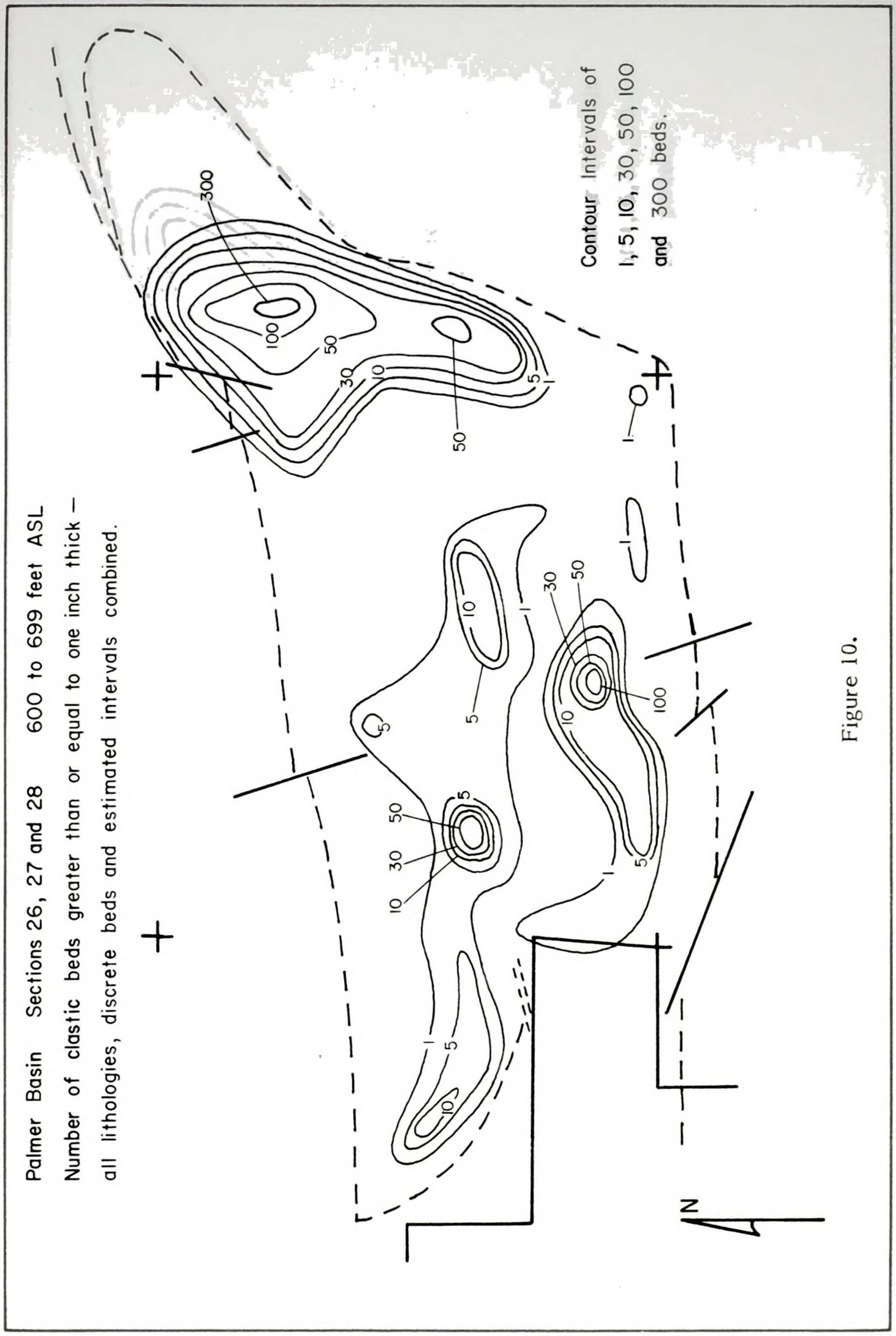
Palmer Basin Sections 26, 27 and 28 600 to 699 feet ASL
Number of clastic beds greater than or equal to one inch thick –
all lithologies, discrete beds and estimated intervals combined.
Contour Intervals of
1, 5, 10, 30, 50, 100
and 300 beds.
N

Figure 10.

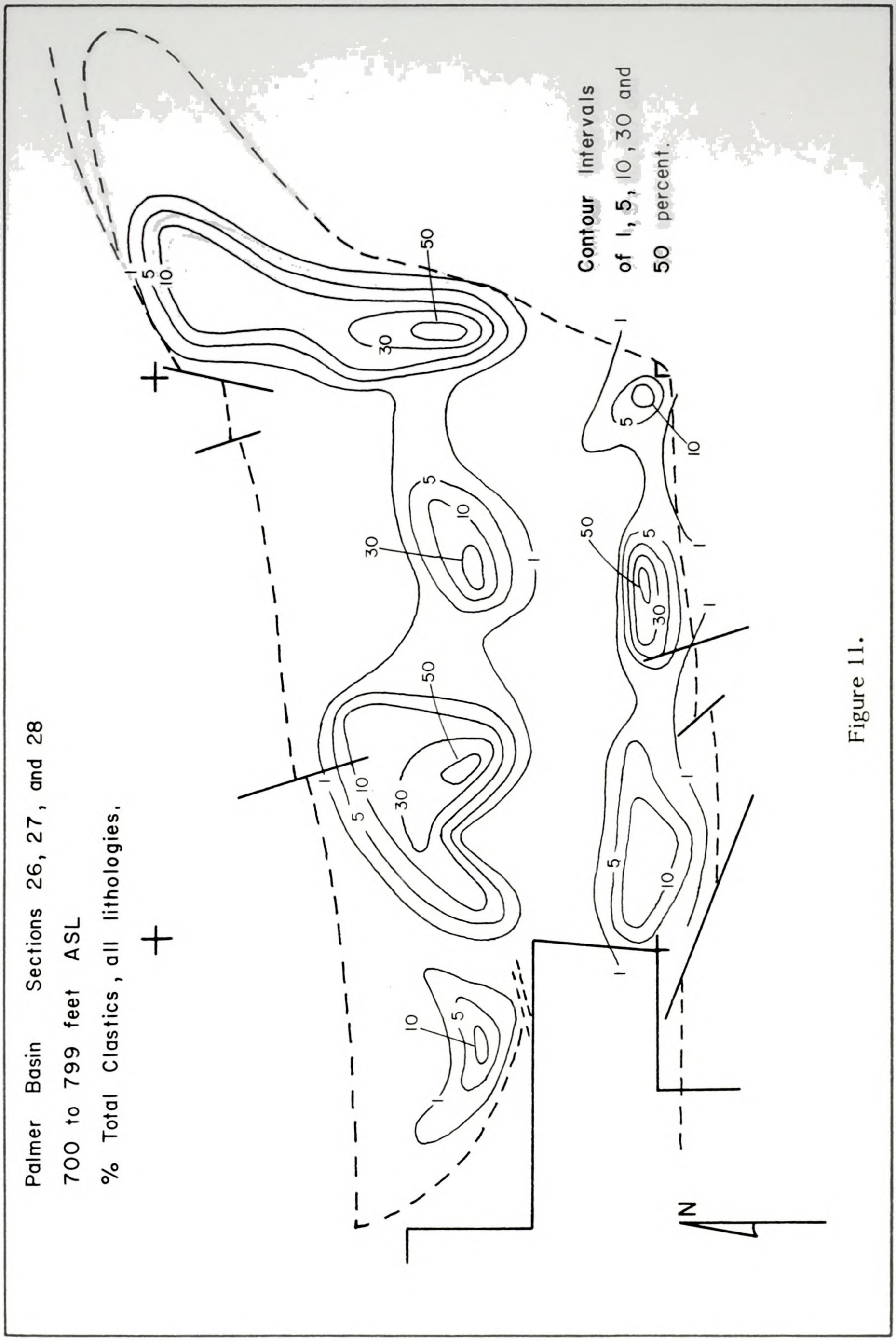
Palmer Basin Sections 26, 27, and 28
700 to 799 feet ASL
% Total Clastics, all lithologies,
Contour Intervals
of 1, 5, 10, 30 and
50 percent.
N

Figure 11.

Palmer Basin Sections 26, 27 and 28
700 to 799 feet ASL
Thickest continuous clastic bed, all lithologies.

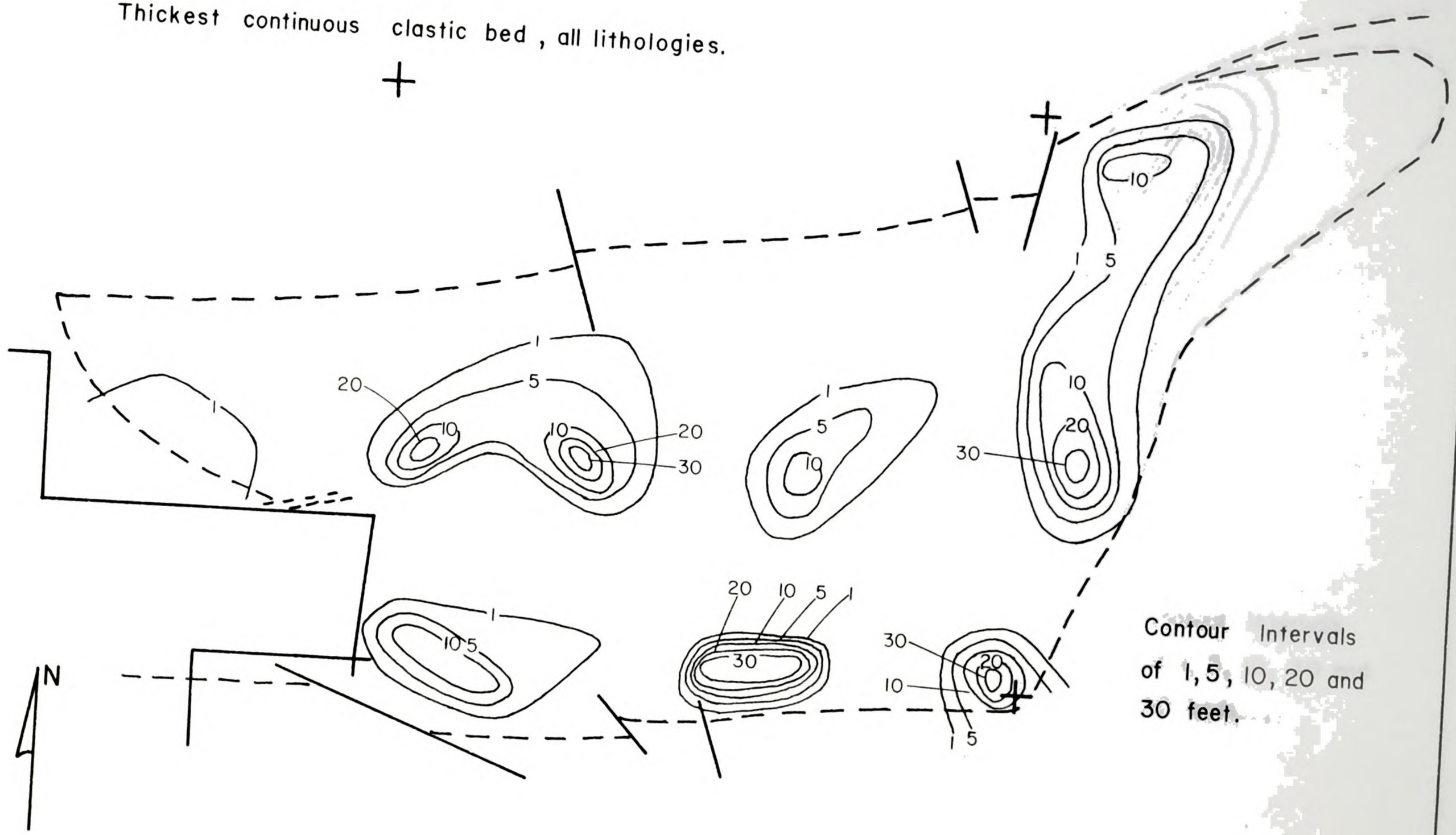

Figure 12.

Palmer Basin Sections 26, 27 and 28 700 to 799 feet ASL

Number of clastic beds greater than or equal to one inch thick— all lithologies, discrete beds and estimated intervals combined.

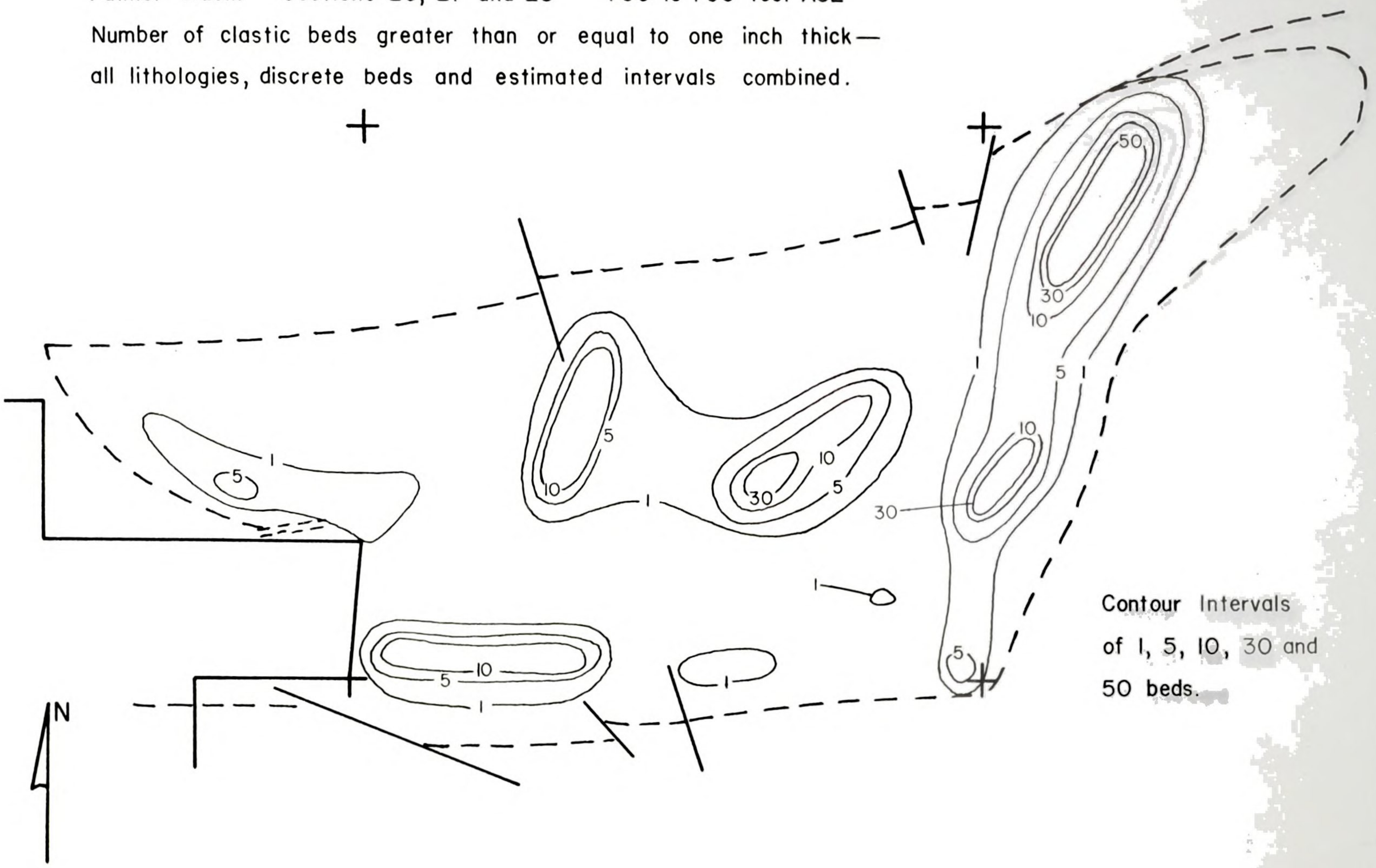

Figure 13.

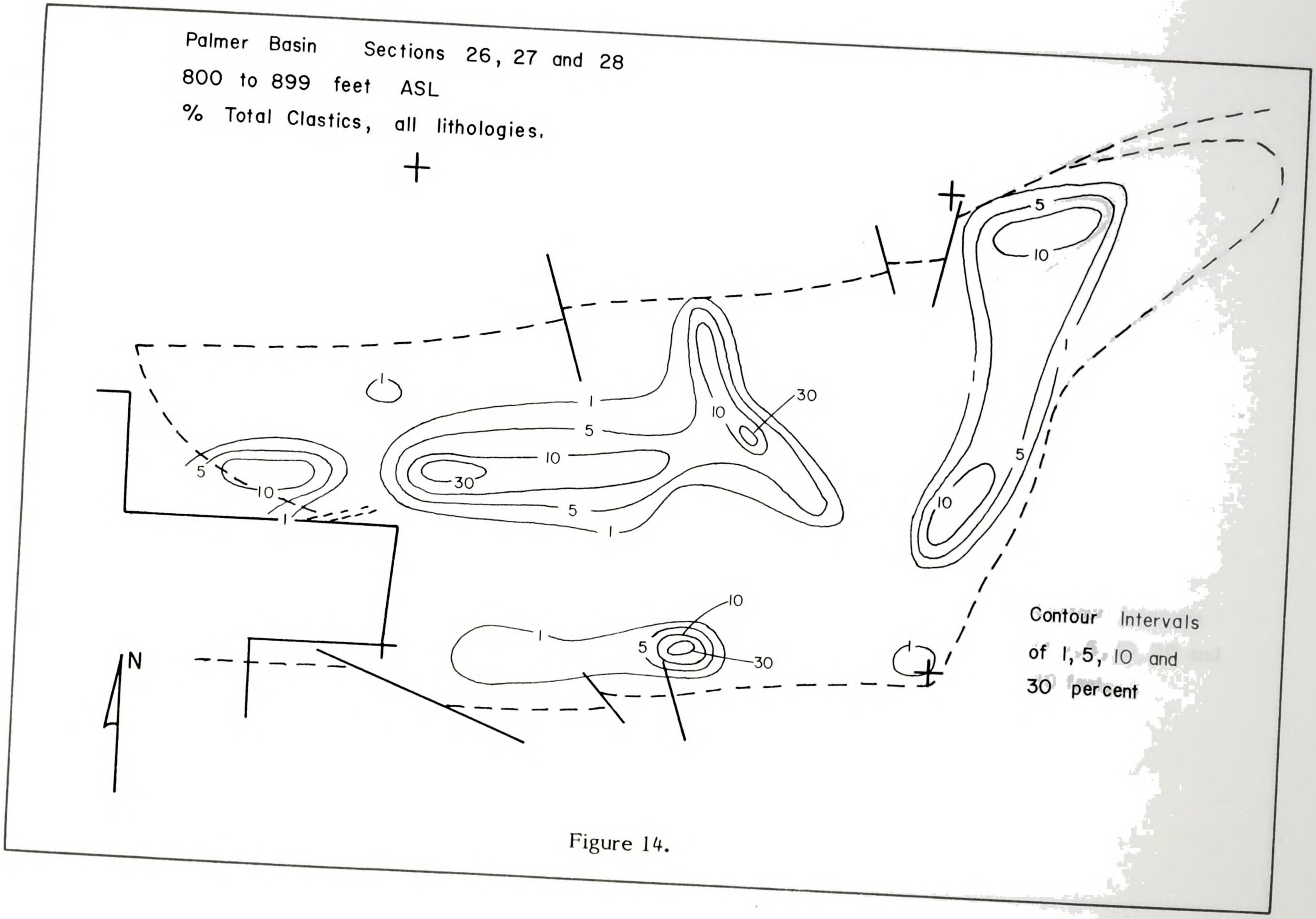
Palmer Basin Sections 26, 27 and 28
800 to 899 feet ASL
% Total Clastics, all lithologies.
1
5
10
30
N
Contour Intervals
of 1, 5, 10 and
30 percent

Figure 14.

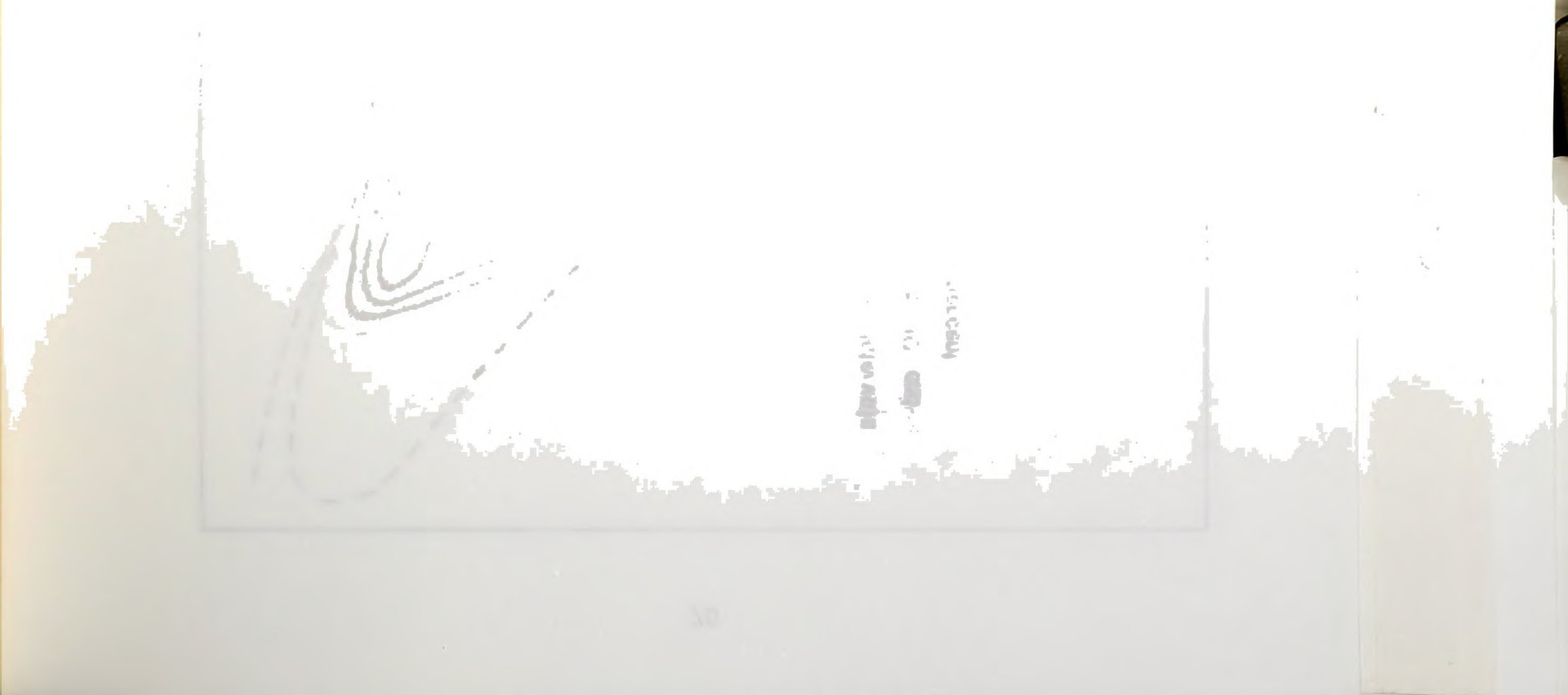

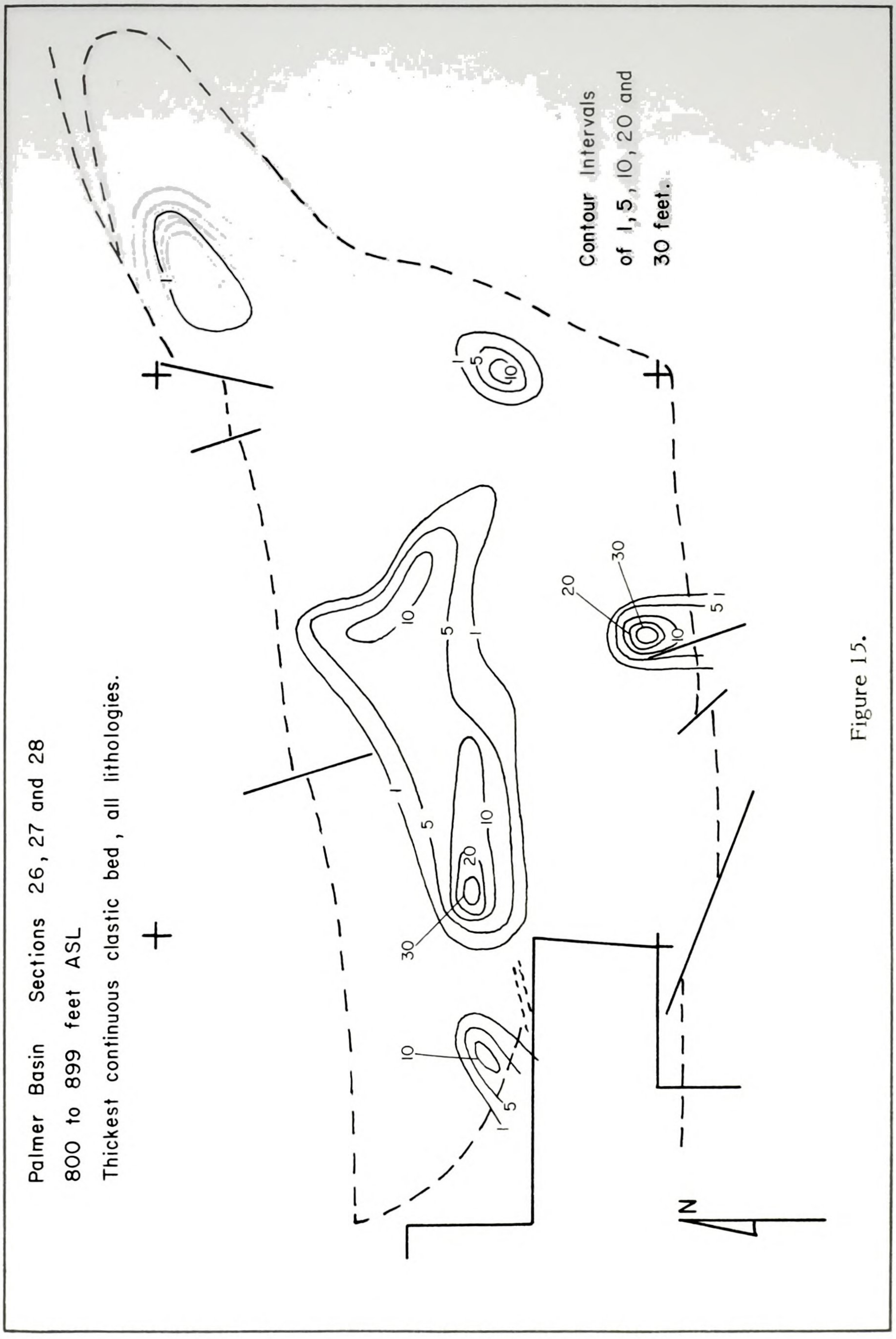
Palmer Basin Sections 26, 27 and 28
800 to 899 feet ASL
Thickest continuous clastic bed, all lithologies.
Contour Intervals
of 1, 5, 10, 20 and
30 feet.
N

Figure 15.

Palmer Basin Sections 26, 27 and 28 800 to 899 feet ASL

Number of clastic beds greater than or equal to one inch thick — all lithologies, discrete beds and estimated intervals combined.

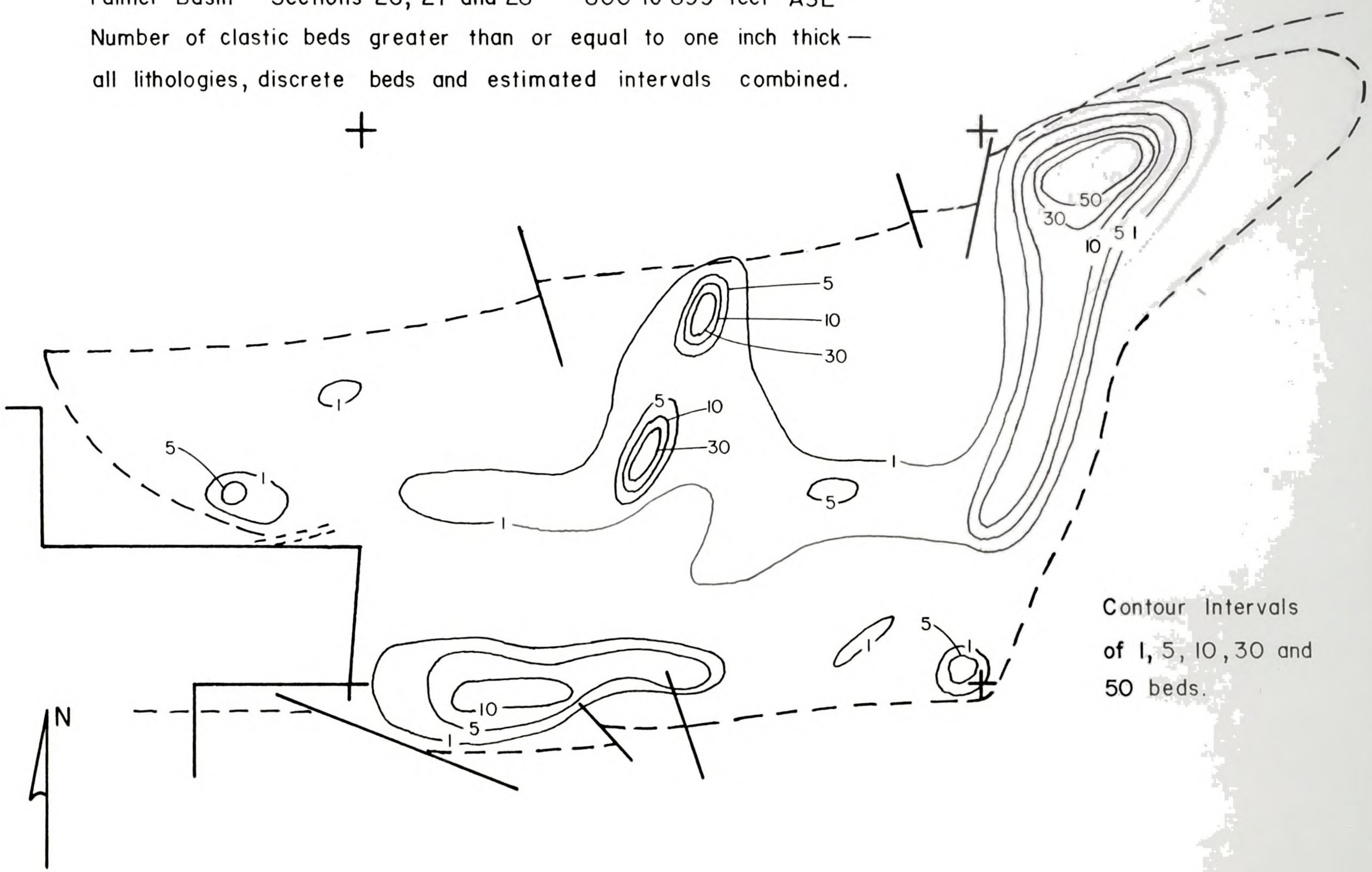

Contour Intervals of 1, 5, 10, 30 and 50 beds.

Figure 16.

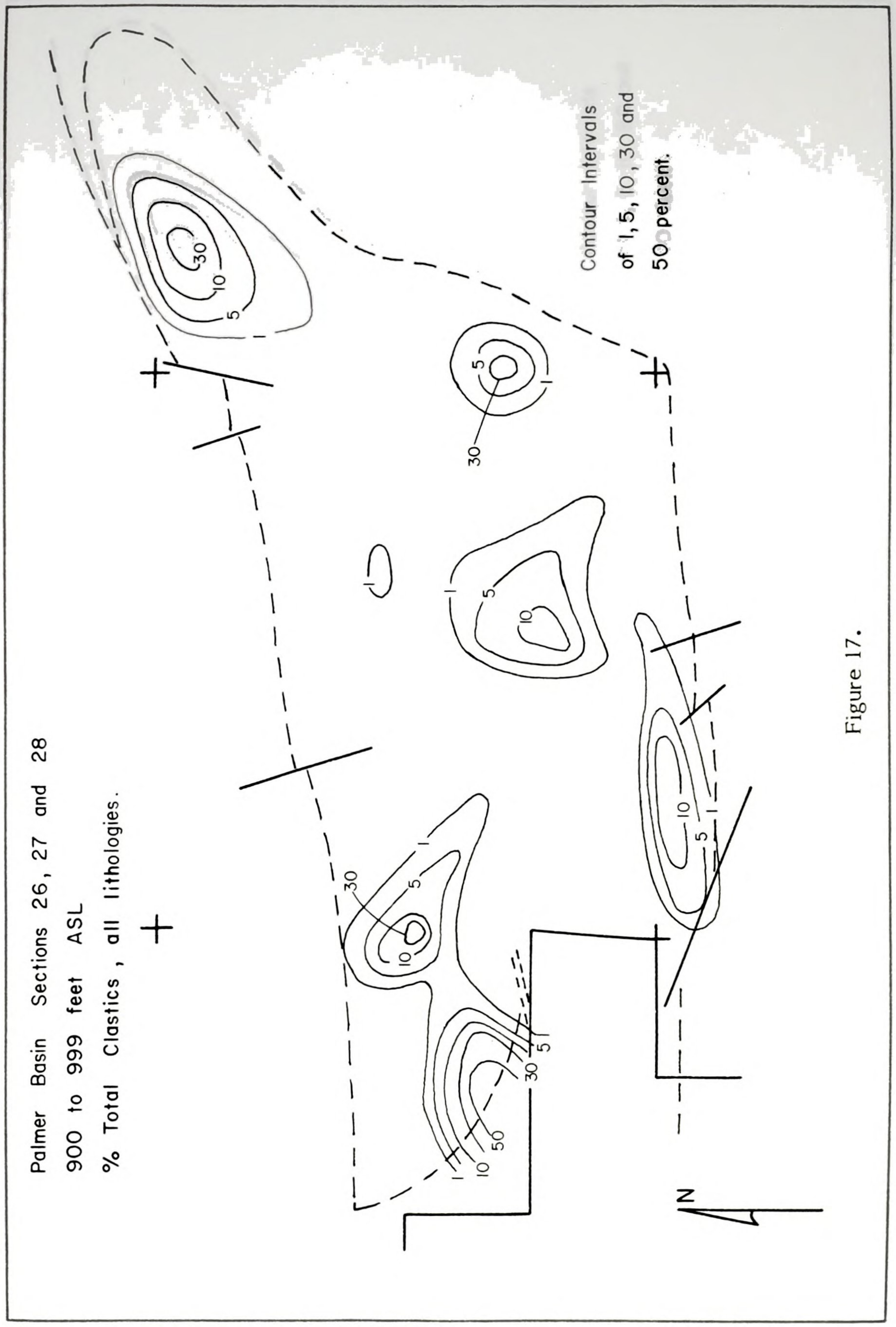
Palmer Basin Sections 26, 27 and 28
900 to 999 feet ASL
% Total Clastics, all lithologies.
Contour Intervals
of 1, 5, 10, 30 and
50 percent.
N

Figure 17.

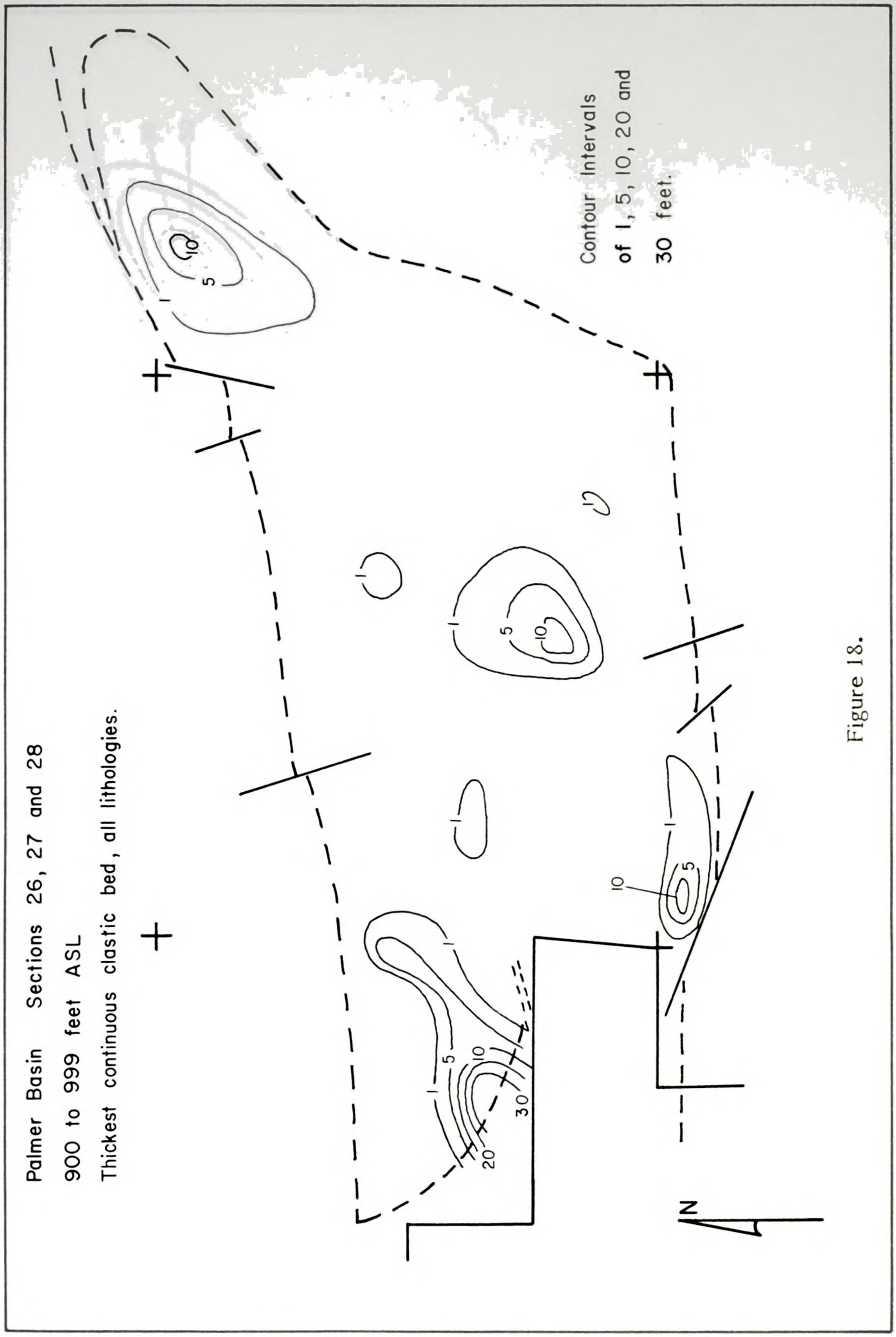
Palmer Basin Sections 26, 27 and 28
900 to 999 feet ASL
Thickest continuous clastic bed, all lithologies.
Contour Intervals
of 1, 5, 10, 20 and
30 feet.
N

Figure 18.

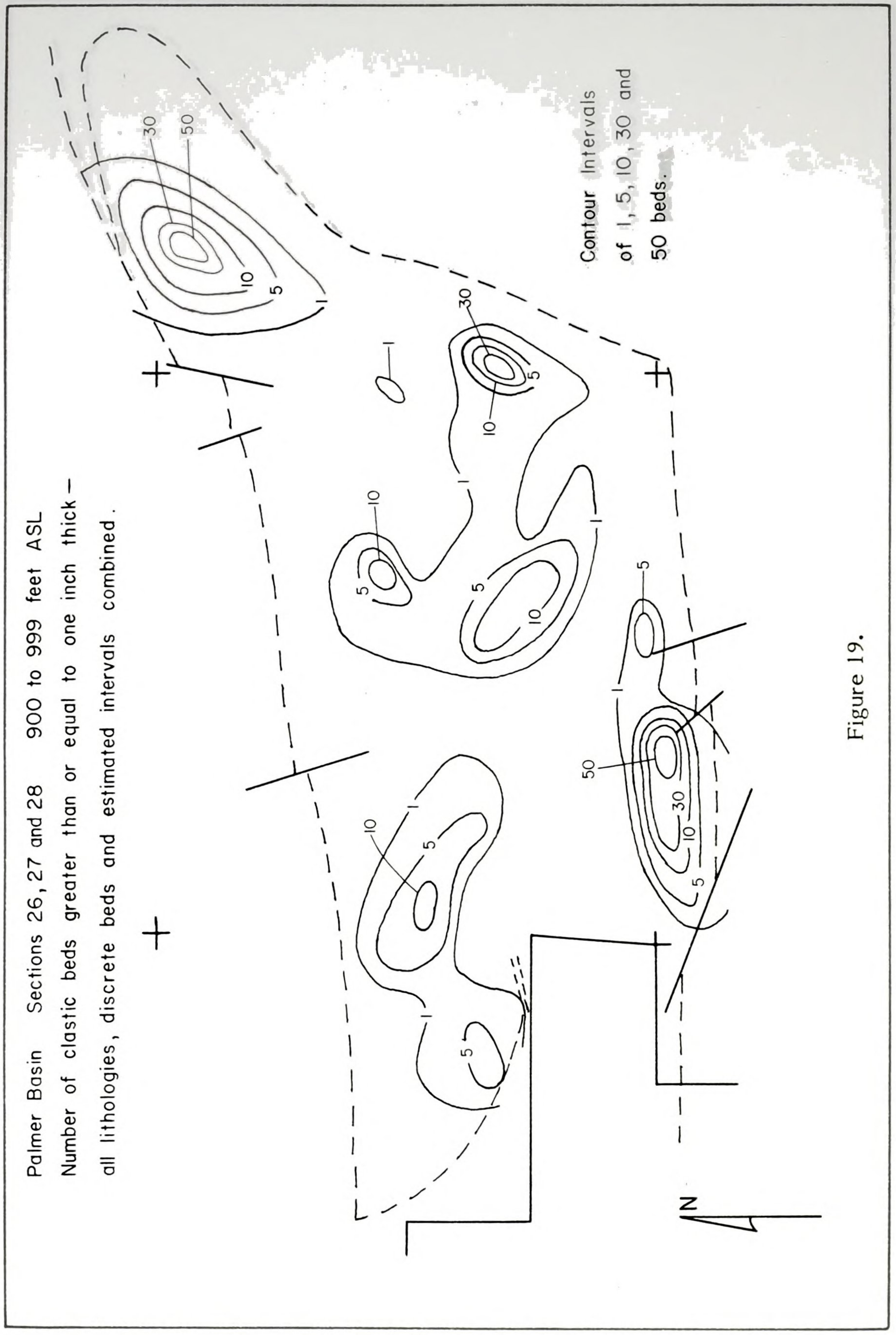

Palmer Basin Sections 26, 27 and 28 900 to 999 feet ASL
Number of clastic beds greater than or equal to one inch thick—
all lithologies, discrete beds and estimated intervals combined.

Figure 19.

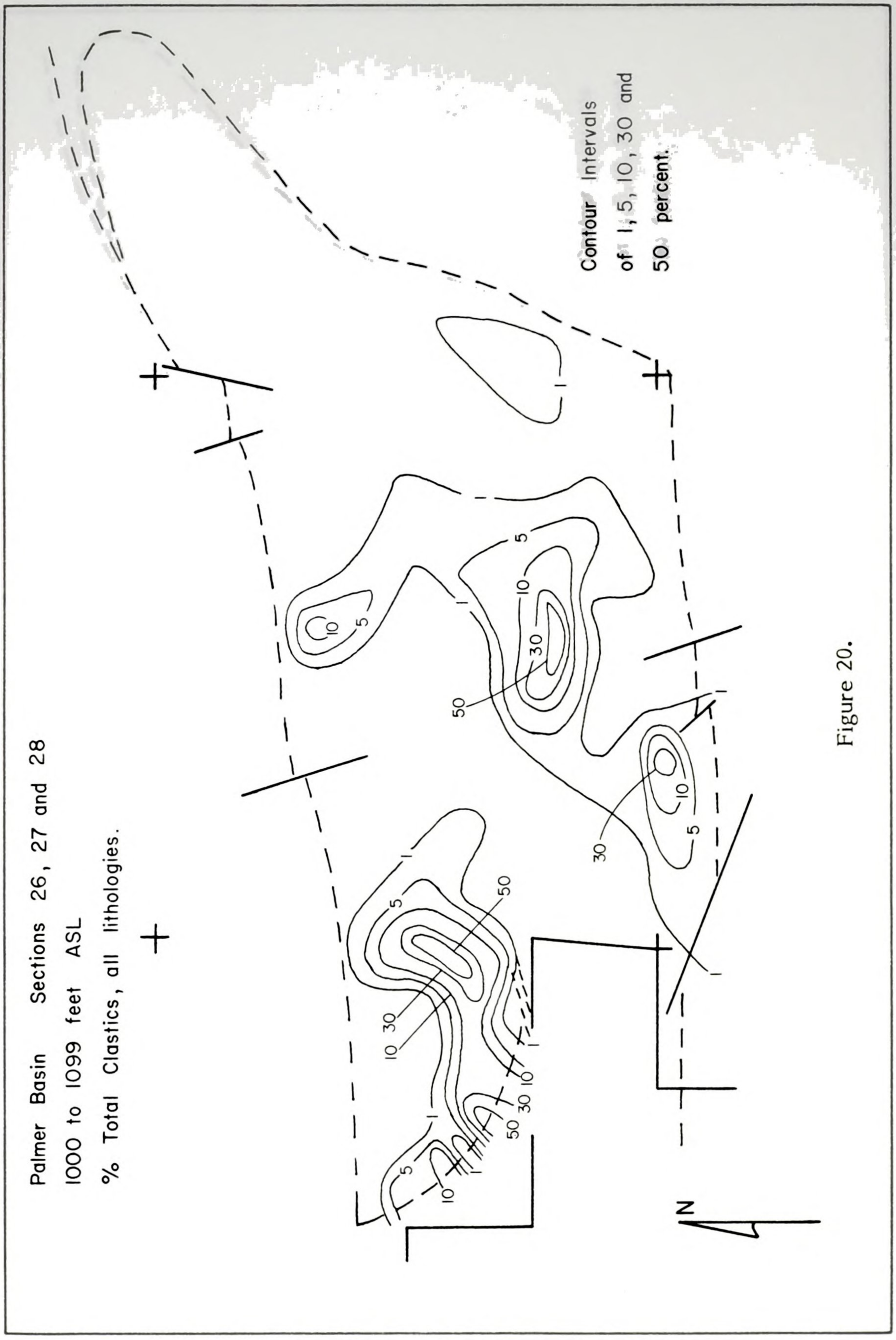
Contour Intervals
of 1, 5, 10, 30 and
50 percent.
Palmer Basin Sections 26, 27 and 28
1000 to 1099 feet ASL
% Total Clastics, all lithologies.
N

Figure 20.

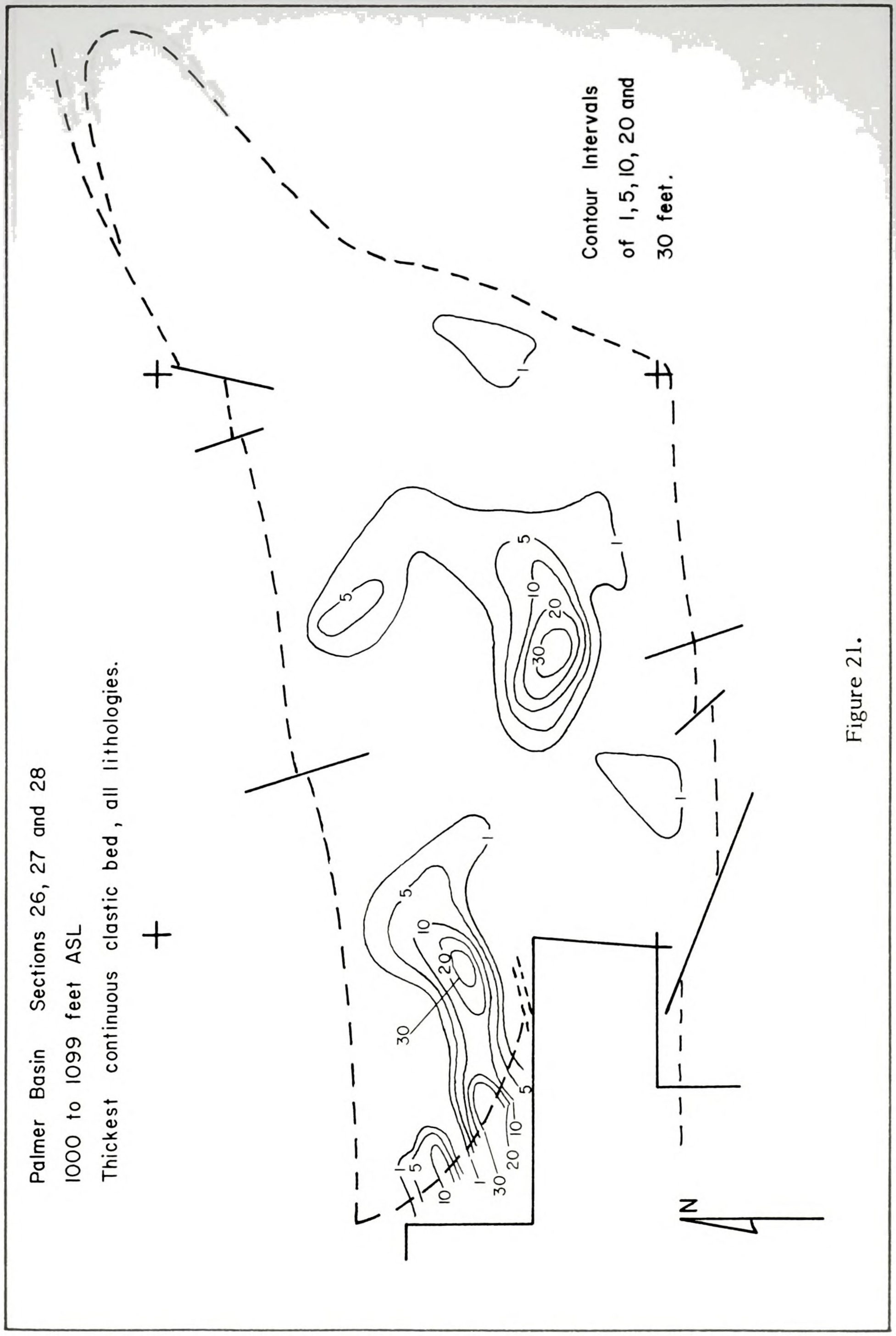

Palmer Basin Sections 26, 27 and 28
1000 to 1099 feet ASL
Thickest continuous clastic bed, all lithologies.

Figure 21.

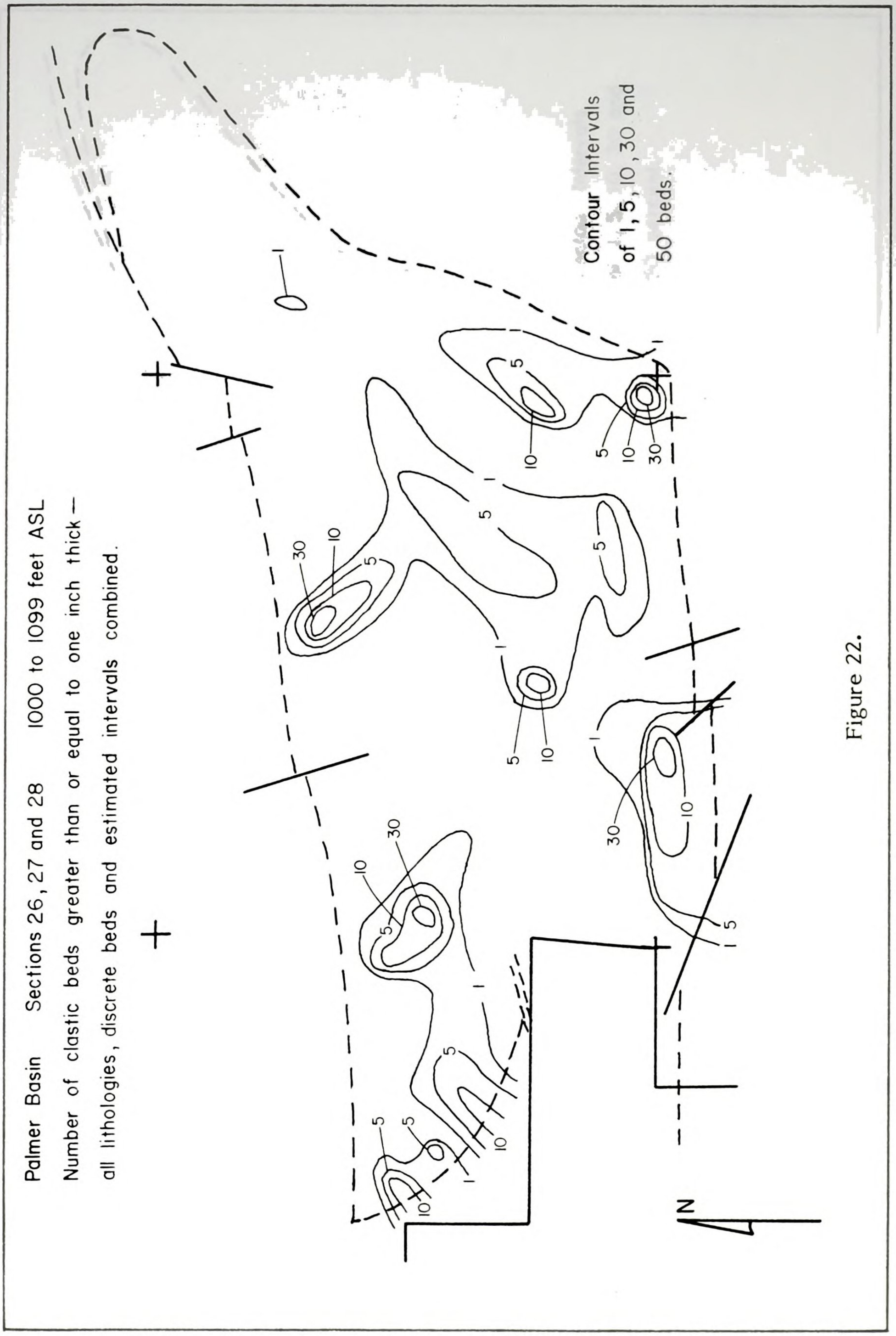

Palmer Basin Sections 26, 27 and 28 1000 to 1099 feet ASL
Number of clastic beds greater than or equal to one inch thick—
all lithologies, discrete beds and estimated intervals combined.

Figure 22.

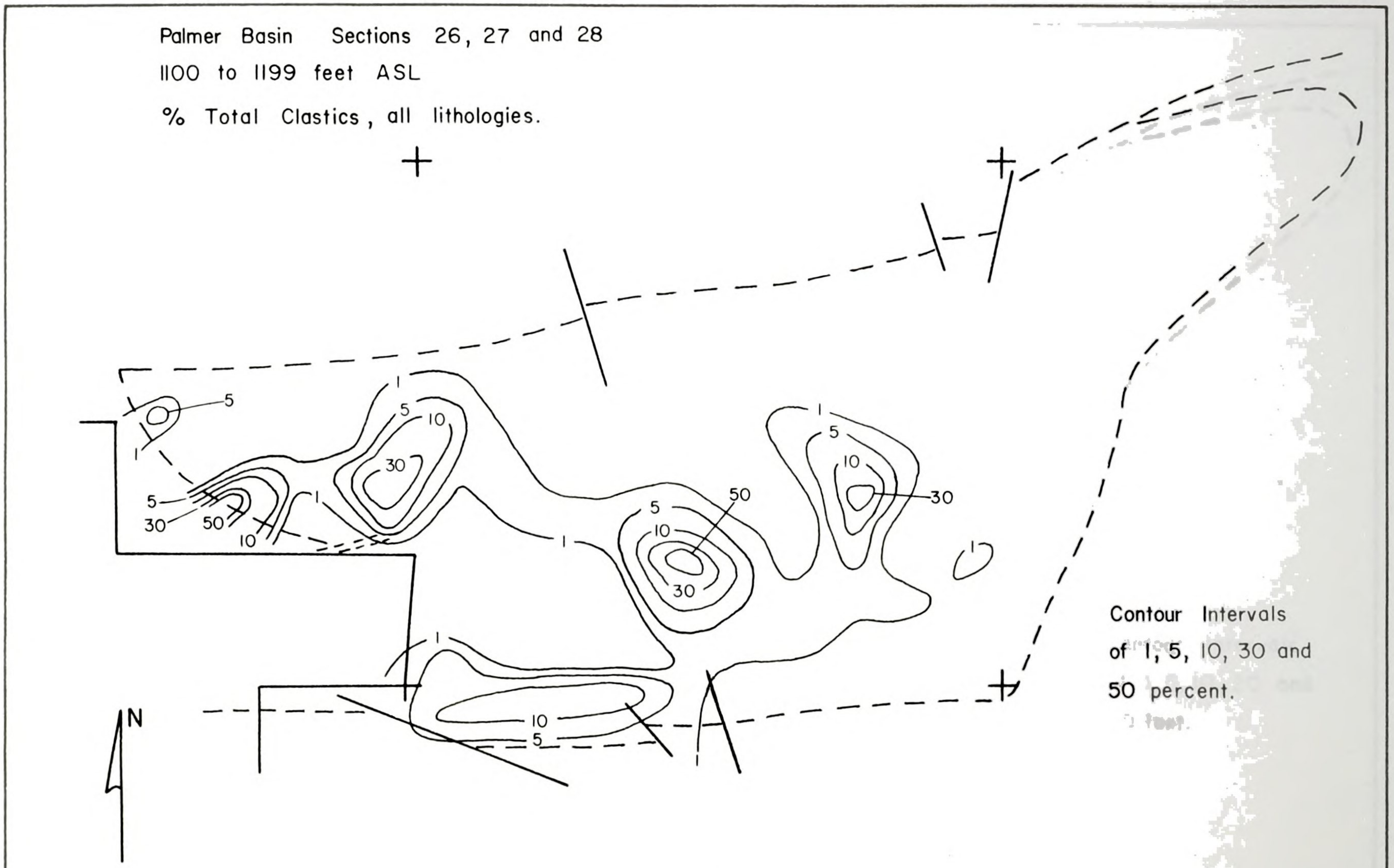
Palmer Basin Sections 26, 27 and 28
1100 to 1199 feet ASL
% Total Clastics, all lithologies.
1
5
10
30
50
N
Contour Intervals
of 1, 5, 10, 30 and
50 percent.

Figure 23.

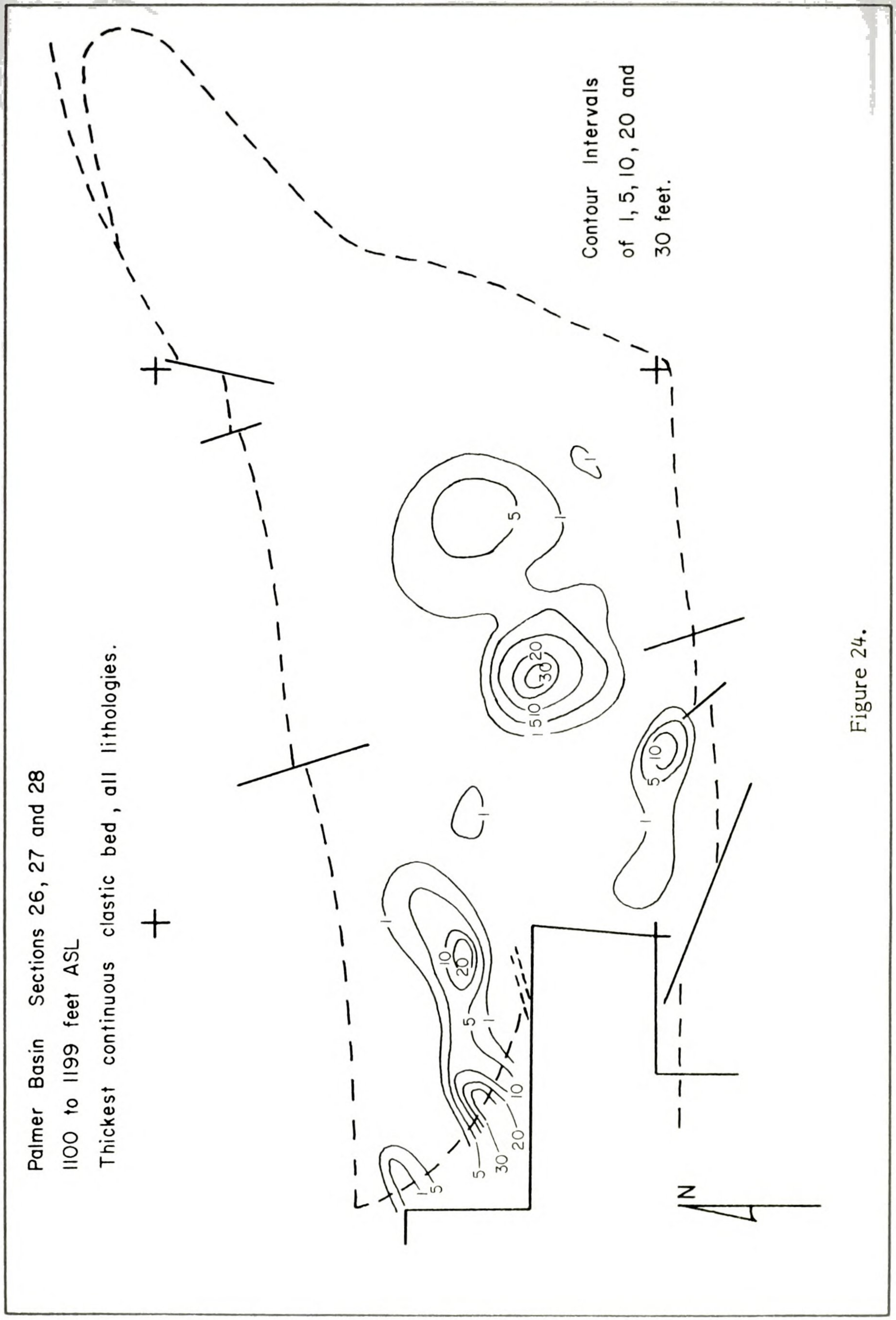
Palmer Basin Sections 26, 27 and 28
1100 to 1199 feet ASL
Thickest continuous clastic bed, all lithologies.
Contour Intervals
of 1, 5, 10, 20 and
30 feet.
N

Figure 24.

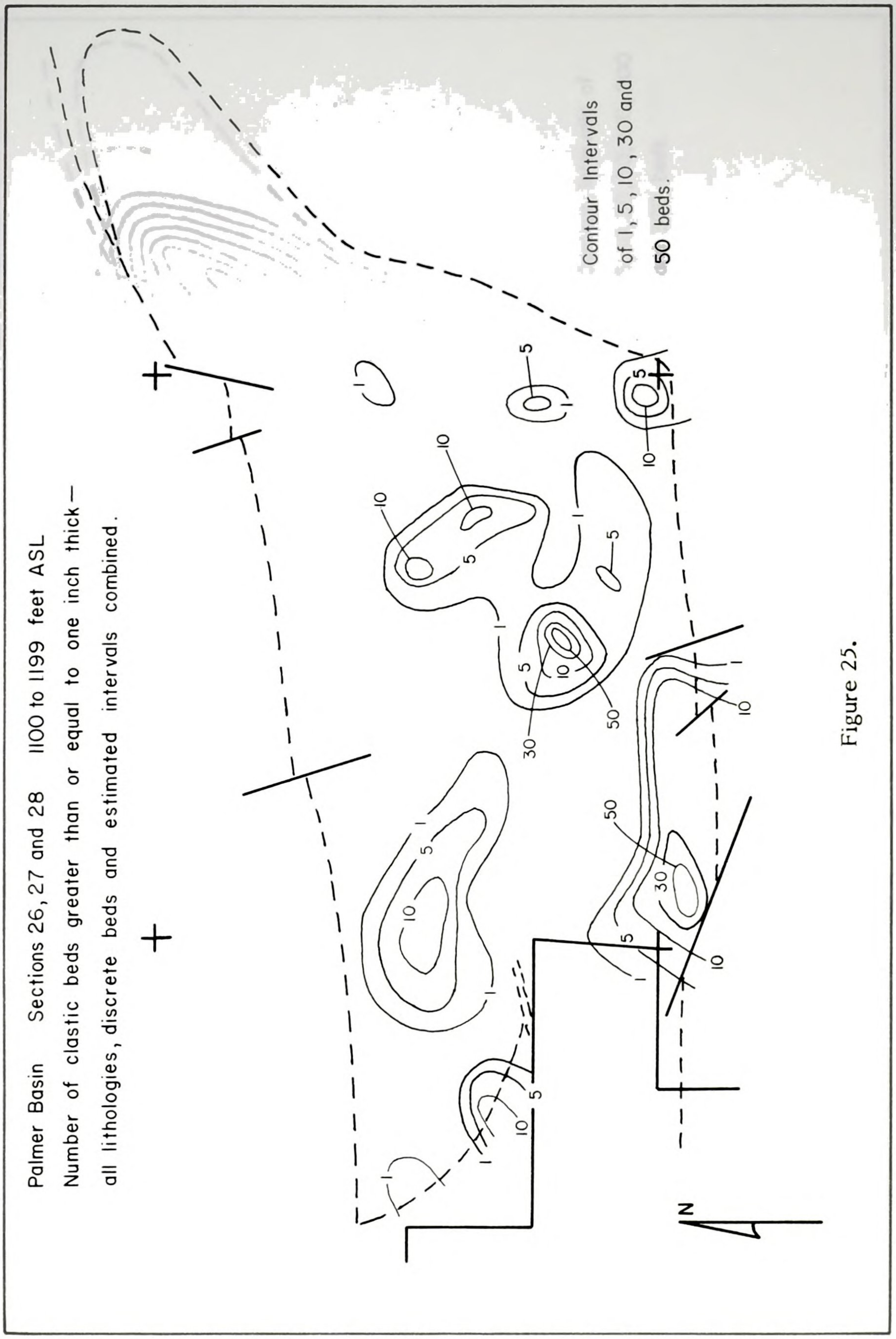
Palmer Basin Sections 26, 27 and 28 1100 to 1199 feet ASL
Number of clastic beds greater than or equal to one inch thick—
all lithologies, discrete beds and estimated intervals combined.
Contour Intervals
of 1, 5, 10, 30 and
50 beds.
N

Figure 25.

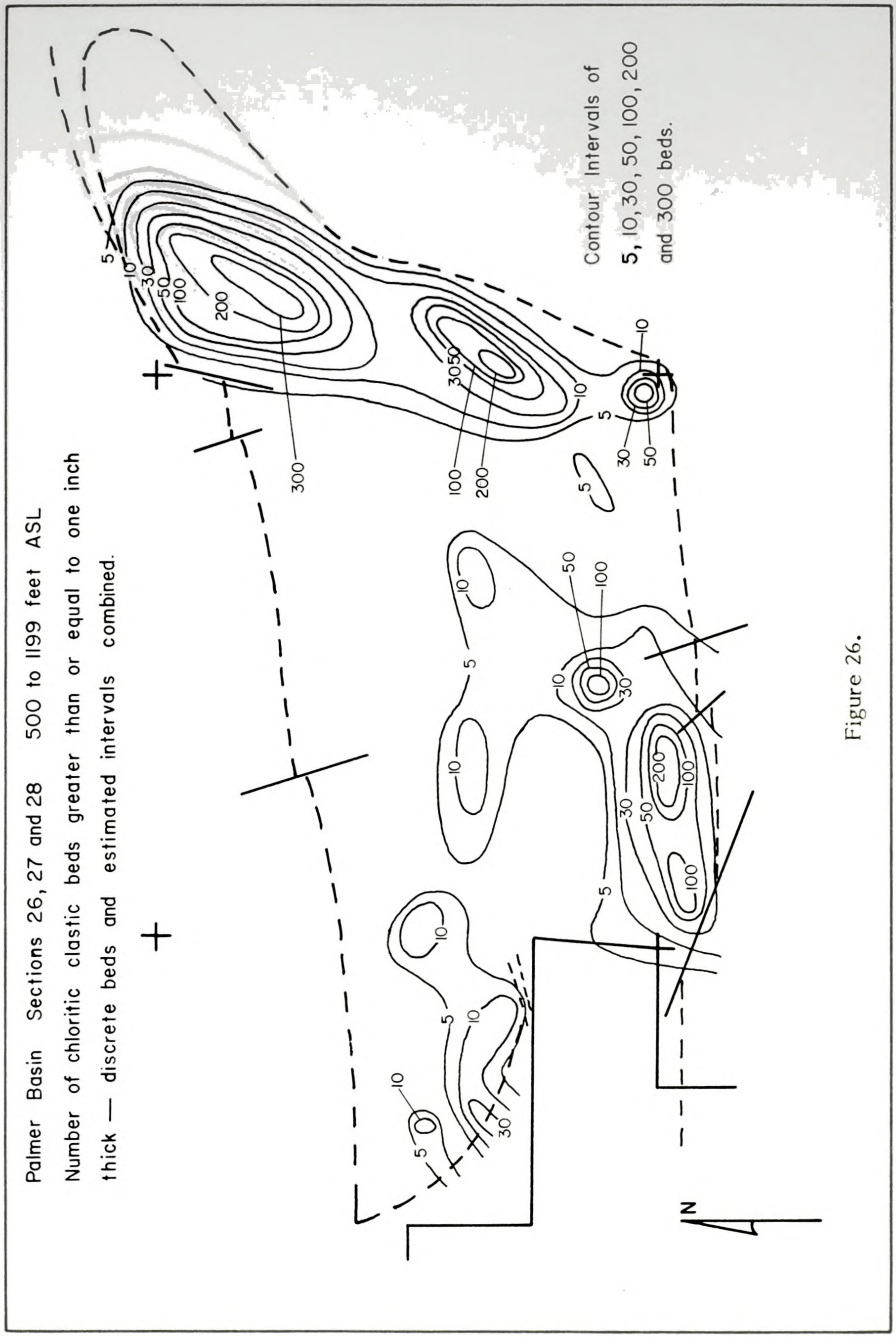
Palmer Basin Sections 26, 27 and 28 500 to 1199 feet ASL
Number of chloritic clastic beds greater than or equal to one inch thick — discrete beds and estimated intervals combined.
Contour Intervals of 5, 10, 30, 50, 100, 200 and 300 beds.
N

Figure 26.

Palmer Basin Sections 26, 27 and 28 500 to 1199 feet ASL

Number of clastic beds greater than or equal to one inch thick — all lithologies, discrete beds and estimated intervals combined.

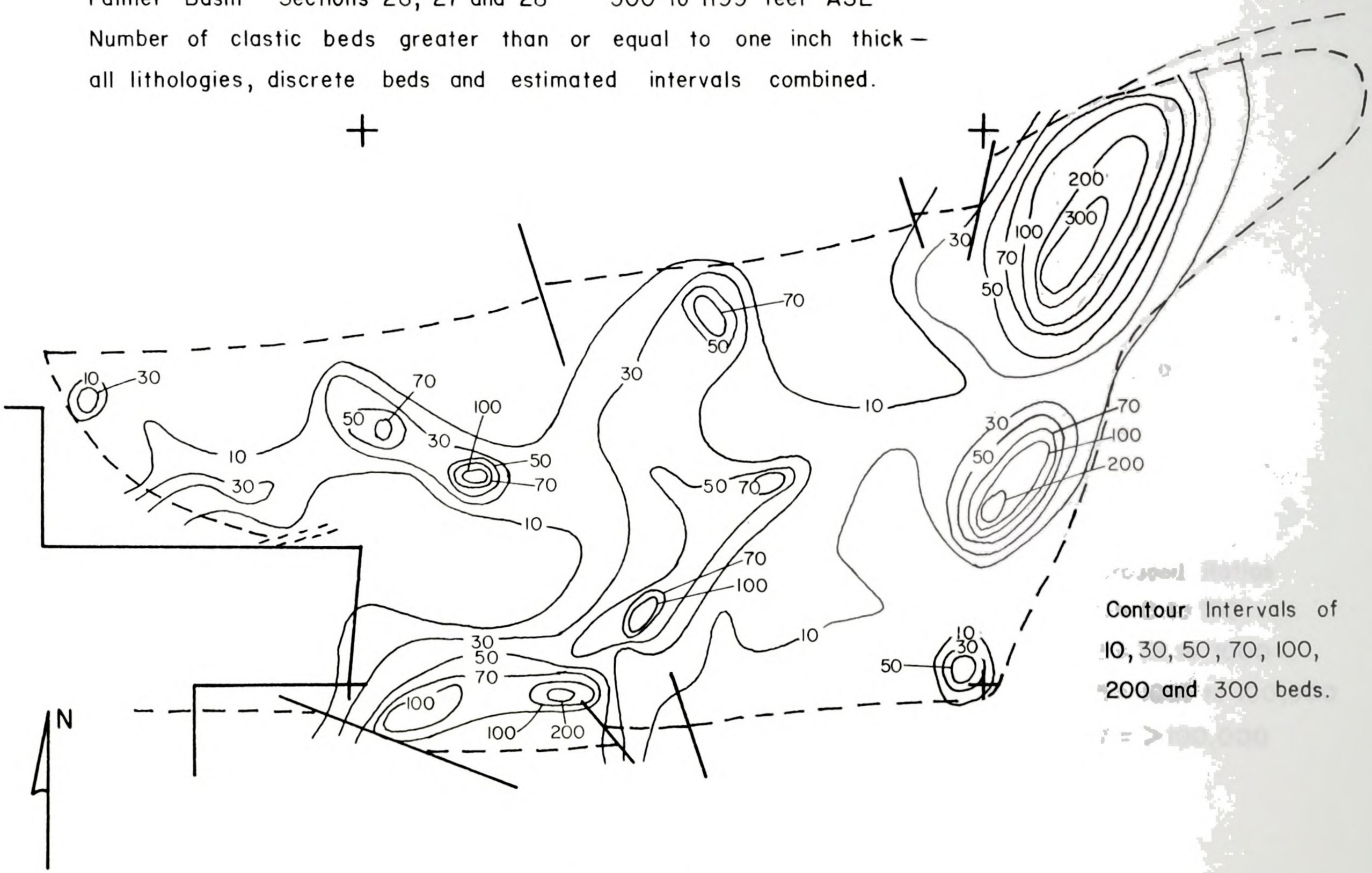

Contour Intervals of 10, 30, 50, 70, 100, 200 and 300 beds.

Figure 27.

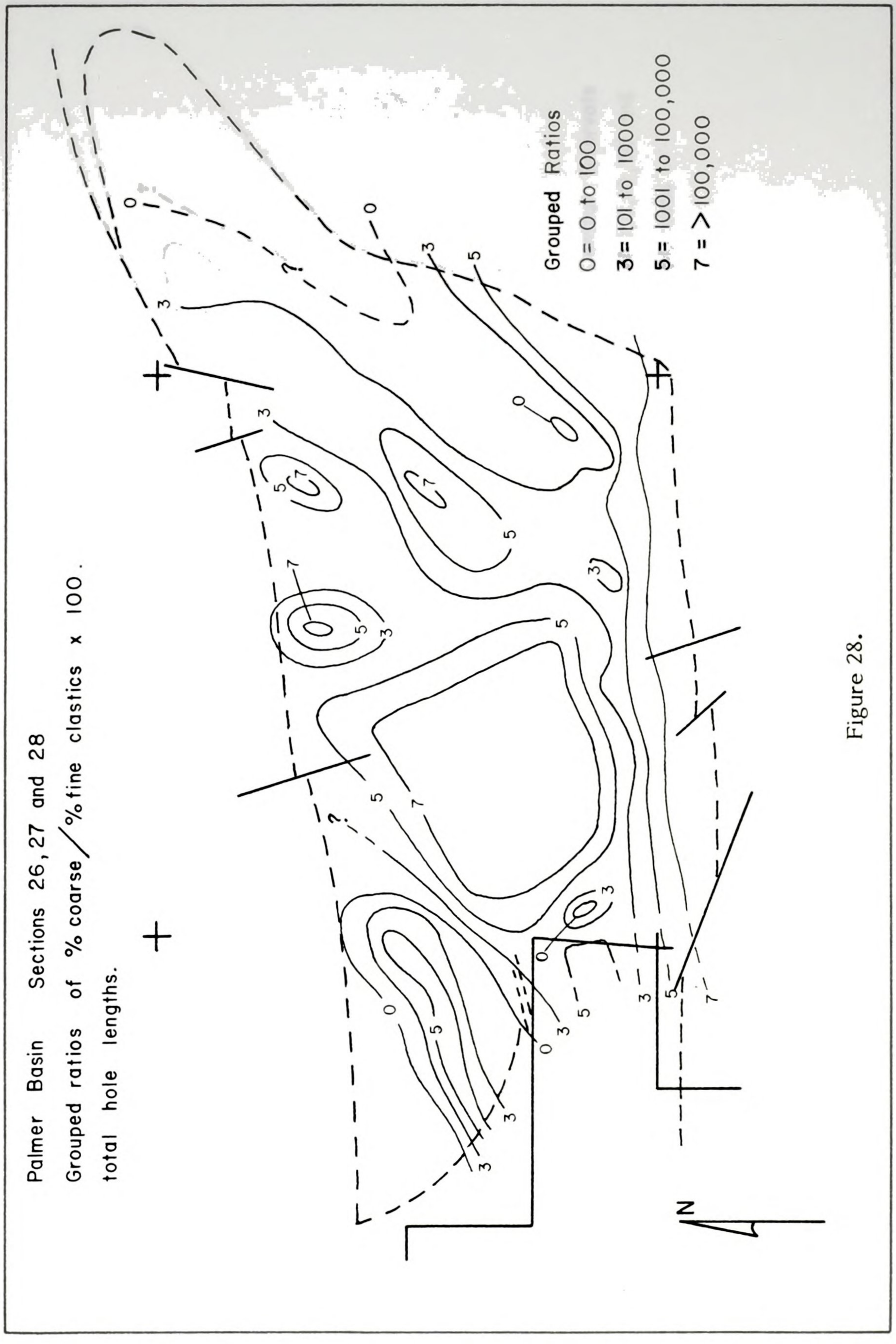

Figure 28.

Palmer Basin Sections 26, 27 and 28
Grouped ratios of % coarse / % fine clastics x 100.
total hole lengths.

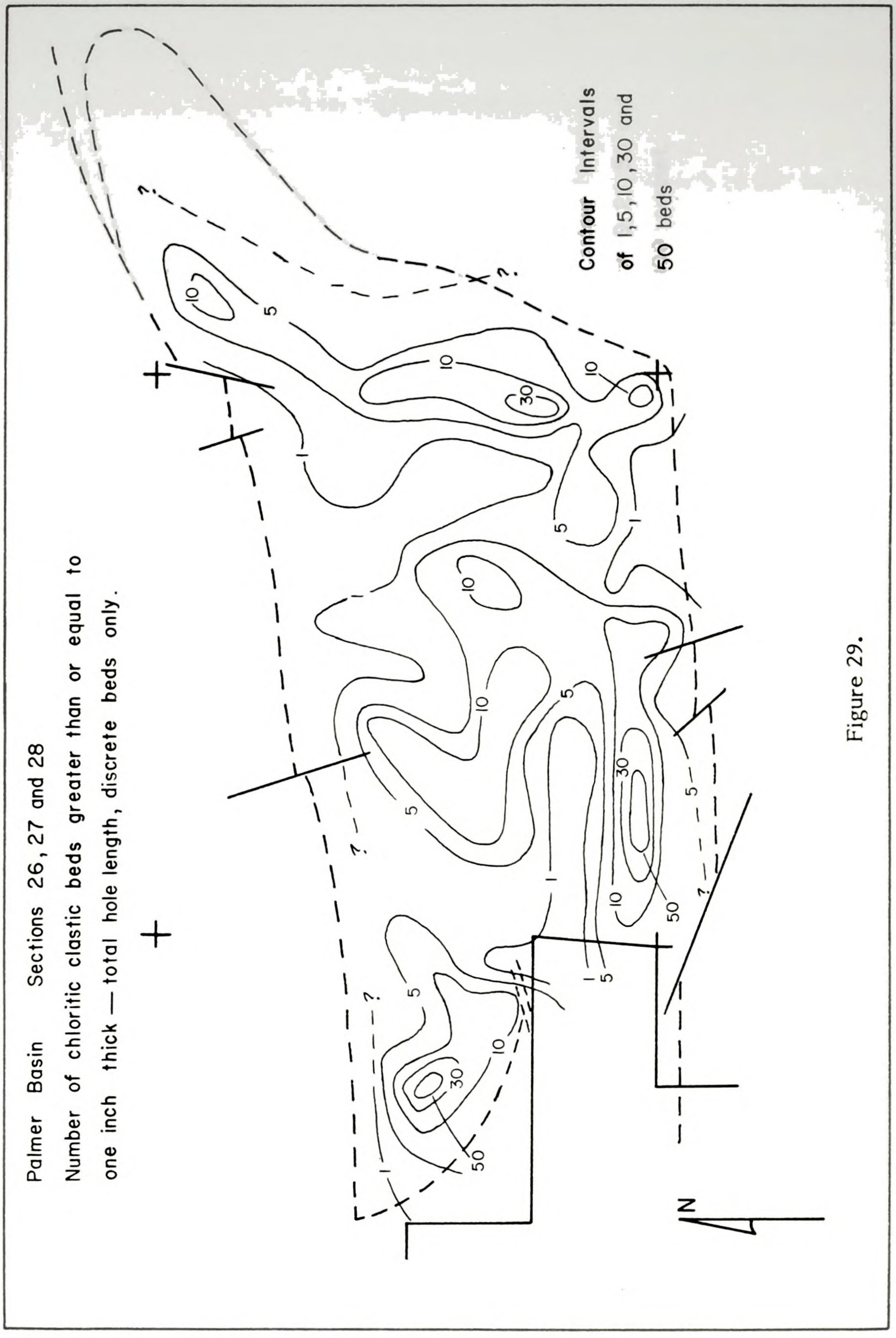
Palmer Basin Sections 26, 27 and 28
Number of chloritic clastic beds greater than or equal to one inch thick — total hole length, discrete beds only.
+
Contour Intervals of 1, 5, 10, 30 and 50 beds
?
1
5
10
30
50
N

Figure 29.

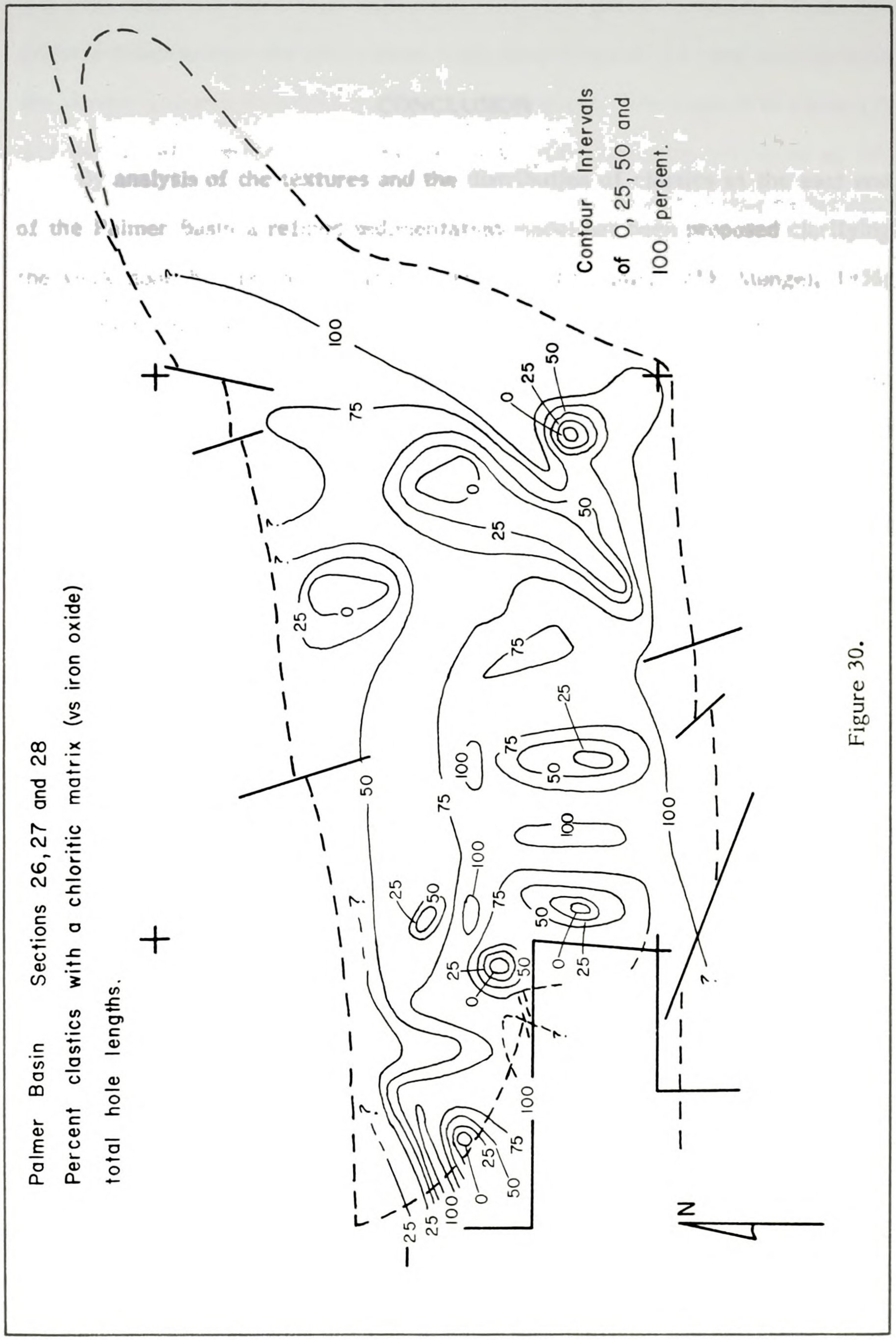
Palmer Basin Sections 26, 27 and 28
Percent clastics with a chloritic matrix (vs iron oxide)
total hole lengths.
Contour Intervals
of 0, 25, 50 and
100 percent.
N

Figure 30.

CONCLUSION

By analysis of the textures and the distribution of clastics at the east end of the Palmer Basin a refined sedimentation model has been proposed clarifying the work done by previous geologists (Davis, 1965; Gair, 1975; Mengel, 1956; Tyler and Twenhofel, 1952). The model proposed by this study is that of the mid-fan to outer-fan area of a submarine fan environment as described by Walker (1978) with a few minor changes to account more effectively for the observed textures (e.g., the fine grained nature of the quartz clastics along with the matrix support of the grains). Because the present-day observed lateral and vertical distribution of the clastics can be accounted for by the submarine fan environment, it is proposed that the Palmer Basin had attained roughly its present shape by Negaunee Iron Formation deposition time. That is, the observed textures and sedimentation patterns are not inconsistent with the idea that the Palmer Basin existed during Negaunee time. This is contrary to the models proposed by Cannon (1973), Morey (1978), and Sims (1976) whereby the Palmer Basin came into existence after deposition of the Negaunee Iron Formation by vertical faulting. This study also lends support to the rifting models proposed by Cambray (1977, 1978), Larue (1979, 1981), Larue and Sloss (1980), and Van Schmus (1976), by showing that the Palmer Basin did exist prior to the Penokean Orogeny. Their hypothesis that rifting, due to horizontal crustal movements, seems the most plausible to explain the creation of the Palmer Basin. Also, the existence of an eroding southern land mass lends support to the rifting models.

Because of the immature textures of the clastics and the lack of winnowing of fines, the sediments must have been deposited below wave base in the basin

and also could not have been transported for very great distances. These two criteria indicate that the paleo-slope must have dropped off very quickly from the southern source area into the Palmer Basin itself. The slope of this drop-off and the actual distance to the southern land mass cannot be estimated at this time. It can only be suggested that an extensive shelf area between source area and the depositional site must not have been present.

Gair (1975) suggested that the Palmer Basin was a shallow embayment off the main depositional trough for the Marquette Range Supergroup sediments and that the periodic influx of sediments was due to tectonic events (i.e., earthquakes). While the possibility of this embayment is plausible, the water depth necessary and the short transport distance suggests a deep trough which was continually subsiding during Negaunee deposition time. The idea that the influxes of clastic sediment were due to tectonic events is an attractive mechanism since the presence of faults along the south margin of the Palmer Basin very simply accounts for the rapid transition from eroding land mass to the deep-water environment. However, gravitational instabilities also could cause sediment to become mobile and flow downslope into the basin as proposed by Middleton and Hampton (1973) for other deposits. But, as noted above, the sharp transition from source area to deep-water deposition favors fault control.

Finally, slumping of the freshly deposited clastic sediment and banded iron formation layers, soon after deposition, can account for some of the complex folding patterns visible within the Palmer Basin. As noted by Helwig (1970) and Woodcock (1976) syn-sedimentary slumping may be indistinguishable from tectonic folds. Slumping can occur along the paleo-slope or in the suprafan lobes (Walker, 1978). Perhaps the seismic events which are inferred to have caused clastic influxes could also instigate slumping of previously deposited sediment. Measurement for randomness of fold axes could be used to distinguish between

slumping or tectonic folding (Hobbs et al., 1976). This is beyond the scope of this paper and can only be suggested for further work and better outcrop exposure through mine development.

Aalto, K. R. and Dott, R. H., Jr. 1970. Late
southwestern Oregon, and the problem of
Amer. [illegible]

REFERENCES

Aalto, K. R. and Dott, R. H., Jr., 1970. Late Mesozoic conglomeratic flysch in southwestern Oregon, and the problem of transport of coarse gravel in deep water. Geol. Assoc. Canada Spec. Paper 7, p. 53-65.

Bayley, R. W. and James, H. L., 1973. Precambrian iron formations of the United States. Econ. Geol., v. 68, p. 934-959.

Blatt, H., Middleton, G. and Murray, R., 1980. Origin of Sedimentary Rocks, second edition. Prentice-Hall, Inc., 782p.

Boyum, B. H., 1975. The Marquette mineral district of Michigan. Cleveland-Cliffs Iron Co., Ishpeming, Michigan, 59p.

Cambray, F. W., 1977. The geology of the Marquette District: a field guide. Michigan Basin Geol. Soc., May 14-15, 62p.

Cambray, F. W., 1978. Plate tectonics as a model for the environment of deposition and deformation of the early Proterozoic (Precambrian X) of northern Michigan. Geol. Soc. Amer. Abstr. w/Programs, v. 10, no. 7, p. 376.

Cannon, W. F., 1973. The Penokean Orogeny in nothern Michigan, in Huronian Stratigraphy and Sedimentation, G. M. Young (ed.). Geol. Assoc. Canada Spec. Paper 12, p. 251-271.

Cannon, W. F., 1976. Hard iron ore of the Marquette Range, Michigan. Econ. Geol., v. 71, p. 1012-1028.

Cannon, W. F. and Gair, J. E., 1970. A revision of stratigraphic nomenclature for middle Precambrian rocks in northern Michigan. Geol. Soc. Amer. Bull., v. 81, p. 2843-2846.

Cannon, W. F. and Klasner, J. S., 1975. Stratigraphic relationships within the Baraga Group of Precambrian age, central Upper Peninsula, Michigan. Jour. Res., U.S. Geol. Surv., v. 3, p. 47-51.

Cloud, P., 1973. Paleoecological significances of the Precambrian banded iron formations. Econ. Geol., v. 68, p. 1135-1143.

Condie, K. C., Macke, J. E. and Reimer, T. D., 1970. Petrology and geochemistry of early Precambrian greywackes from the Fig Tree Group, South Africa. Geol. Soc. Amer. Bull., v. 81, p. 2759-2776.

Davis, J. F., 1965. A petrologic examination of iron formation and associated greywackes and pyroclastic breccieas within the Negaunee Formation of the Palmer area, Marquette District, Michigan. Unpub. Ph.D. Dissertation, Univ. of Wisconsin, Madison, Wisconsin.

Dimroth, E., 1976. Aspects of the sedimentary petrology of cherty iron formation, in Handbook of Strata-bound and Strata-form Ore Deposits, K. H. Wolf (ed.), Elsevier Publishing, New York, v. 7, p. 203-254.

Drever, J. I., 1974. Geochemical model for the origin of Precambrian banded iron formations. Geol. Soc. Amer. Bull., v. 85, p. 1099-1106.

Eichler, J., 1976. Origin of the Precambrian banded iron formations, in Handbook of Strata-bound and Strata-form Ore Deposits, K. H. Wolf (ed.), Elsevier Publishing, New York, v. 7, p. 157-201.

Eriksson, K. A., 1980. Hydrodynamic and paleogeographic interpretation of turbidite deposits from the Archean Fig Tree Group of the Barberton Mountain Land, South Africa. Geol. Soc. Amer. Bull., Part I, v. 91, p. 21-26.

Eugster, H. P. and Chou, I-Ming, 1973. The depositional environments of Precambrian banded iron formations. Econ. Geol., v. 68, p. 1144-1168.

Friedman, G. M., 1958. Determination of sieve-size distribution from thin-section data for sedimentary petrological studies. Jour. Geol., v. 66, p. 394-416.

Friedman, G. M., 1962a. Comparison of moment measures for sieving and thin-section data in sedimentary petrological studies. Jour. Sed. Petrol., v. 32, p. 15-25.

Gair, J. E., 1975. Bedrock geology and ore deposits of the Palmer Quadrangle, Marquette County, Michigan. U.S. Geol. Surv. Prof. Paper 769, 159p.

Goldich, S. S., 1972. The Penokean Orogeny. 18th Ann. Inst. Lake Superior Geol., Tech. Sessions Abstr., Paper 25.

Goldring, R. and Bridges, P., 1973. Sublittoral sheet sandstones. Jour. Sed. Petrol., v. 43, p. 736-747.

Govett, G. J. S., 1966. Origin of banded iron formations. Geol. Soc. Amer. Bull., v. 77, p. 1191-1211.

Gross, G. A., 1972. Primary features in cherty iron formations. Sed. Geol., v. 7, p. 241-261.

Gross, G. A., 1980. A classification of iron formations based on depositional environments. Can. Mineral., v. 18, p. 215-222.

Grout, F. F., 1919. The nature and origin of the Biwabik iron-bearing formation of the Mesabi Range, Minnesota. Econ. Geol., v. 14, p. 452-464.

Gruner, J. W., 1937. Hydrothermal leaching of iron ores of the Lake Superior type - a modified theory. Econ. Geol., v. 32, p. 121-130.

Harms, J. C., Southard, J. B., Spearing, D. R. and Walker, R. G., 1975. Depositional environments as interpreted from primary sedimentary structures and stratification sequences. Soc. Econ. Paleo. Mineral., Short Course 2, Dallas, Texas, April, 1975, 161p.

Helwig, J., 1970. Slump folds and early structures, northeastern Newfoundland Appalachians. Jour. Geol., v. 78, p. 172-187.

Hobbs, B. E., Means, W. D. and Williams, P. F., 1976. An Outline of Structural Geology. John Wiley and Sons, Inc., New York, 571p.

Holland, H. D., 1973. The oceans: a possible source of iron in iron formations. Econ. Geol. v. 68, p. 1169-1172.

Hough, J. L., 1958. Fresh-water environment of deposition of Precambrian banded iron formations. Jour. Sed. Petrol., v. 28, p. 414-430.

Huber, N. K. and Garrels, R. M., 1953. Relation of pH and oxidation potential to sedimentary iron mineral formation. Econ. Geol., v. 48, p. 337-357.

James, H. L., 1954. Sedimentary facies of iron formations. Econ. Geol., v. 49, p. 235-285.

James, H. L., 1955. Zones of regional metamorphism in the Precambrian of Northern Michigan. Geol. Soc. Amer. Bull., v. 66, p. 1455-1488.

James, H. L., 1958. Stratigraphy of pre-Keweenawan rocks in parts of Northern Michigan. U.S. Geol. Surv. Prof. Paper 314-C, p. 27-44.

James, H. L., 1978. Subdivision of the Precambrian review. Precamb. Res., v. 7, p. 193-204.

James, N. P., 1979. Facies models 10: Shallowing upward sequences in carbonates, p. 109-119, in Facies Models, Geoscience Canada, Reprint Series 1, R. G. Walker (ed.). Geol. Assoc. Can., 211p.

Kellerhals, R., Shaw, J. and Arora, V. K., 1975. On grain size from thin sections. Jour. Geol., v. 83, p. 79-96.

Kimberly, M. M., 1978. Paleoenvironmental classification of iron formations. Econ. Geol., v. 73, p. 215-229.

Klasner, J. S., 1978. Penokean deformation and associated metamorphism in the western Marquette Range, northern Michigan. Geol. Soc. Amer. Bull., v. 89, p. 711-722.

Klasner, J. S. and Cannon, W. F., 1974. Geologic interpretation of gravity profiles in the western Marquette District, Northern Michigan. Geol. Soc. Amer. Bull., v. 85, p. 213-218.

Larue, D. K., 1979. Sedimentary history prior to chemical iron sedimentation of the Precambrian X Chocolay and Menominee Groups (Lake Superior Region). Unpub. Ph.D. Dissertation, Northwestern Univ., Evanston, Illinois, 173p.

Larue, D. K., 1981. The early Proterozoic pre-iron formation Menominee group siliciclastic sediments of the Southern Lake Superior Region: evidence for sedimentation in platform and basinal settings. Jour. Sed. Petrol., v. 51, p. 397-414.

Larue, D. K. and Sloss, L. L., 1980. Early Proterozoic sedimentary basins of the Lake Superior region. Geol. Soc. Amer. Bull., Part II, v. 91, p. 1836-1874.

Lepp, H. and Goldich, S. S., 1964. Origin of Precambrian iron formations. Econ. Geol., v. 59, p. 1025-1060.

Mancuso, J. J., 1966. Sequence of oxidation and related mineral changes, Negaunee Iron Formation, Eastern Marquette Range, Michigan. The Compass of Sigma Gamma Epsilon, v. 43, p. 227-236.

Mann, V. I., 1953. The relation of oxidation to the origin of soft iron ores of Michigan. Econ. Geol., v. 48, p. 251-281.

Mengel, J. T., Jr., 1956. The relationship of clastic sediments to iron formation in the vicinity of Palmer, Michigan. Unpub. M.S. Thesis, Univ. of Wisconsin, Madison, Wisconsin.

Meyn, H. D. and Palonen, P. A., 1980. Stratigraphy of an Archean submarine fan. Precamb. Res., v. 12, p. 257-285.

Middleton, G. V., 1962. Size and sphericity of quartz grains in two turbidite formations. Jour. Sed. Petrol., v. 32, p. 725-742.

Middleton, G. B. and Hampton, M. A., 1973. Sediment gravity flows: mechanics of flow and deposition, in Turbidites and Deep-water Sedimentation, G. B. Middleton and A. H. Bouma (eds.). Soc. Econ. Paleo. Mineral. Lect. Notes, p. 1-38.

Morey, G. B., 1978. Metamorphism in the Lake Superior region, U.S.A., and its relation to crustal evolution, p. 283-314, in Metamorphism in the Canadian Shield. Geol. Surv. Canada Paper 78-10, J. A. Fraser and W. W. Heywood (eds.), 367p.

Mutti, E. and Ricci Lucchi, F., 1978. Turbidites of the Northern Apennines, introduction to facies analysis. Inter. Geol. Rev., v. 20, p. 125-166.

Naylor, M. A., 1981. Debris flow (olistostromes) and slumping on a distal passive continental margin: the Palombini limestone-shale sequence of the Northern Apennines. Sedimentology, v. 28, p. 837-852.

Nelson, C. H. and Kulm, L. D., 1973. Submarine fans and deep-sea channels, in Turbidites and Deep-water Sedimentation. Soc. Econ. Paleo. Mineral. Short Course, May, 1973, Anaheim, California, 158p.

Normark, W. R., 1978. Fan valleys, channels and depositional lobes on modern submarine fans: characteristics for recognition of sandy turbidite environments. Amer. Assoc. Petrol. Geol. Bull., v. 62, p. 912-931.

Pettijohn, F. J., Potter, P. E. and Seiver, R., 1973. Sand and sandstone. Springer-Verlag, New York, 618p.

Pickering, K. T., 1981. Two types of outer fan lobe sequences, from the late Precambrian Kongsfjord formation submarine fan, Finnmark, North Norway. Jour. Sed. Petrol., v. 51, p. 1277-1286.

Ricci Lucchi, F. and Balmari, E., 1980. Basin-wide turbidites in a Miocene, over-supplied deep-sea plain: a geometrical analysis. Sedimentology, v. 27, p. 241-270.

Sims, P. K., 1976. Precambrian tectonics and mineral deposits, Lake Superior region. Econ. Geol. v. 71, p. 1092-1127.

Sims, P. K., Card, K. D., Morey, G. B. and Peterman, Z. E., 1980. The Great Lakes tectonic zone - a major crustal structure in central North America. Geol. Soc. Amer. Bull., Part I, v. 91, p. 690-698.

Snider, D. W., 1972. Mineralogic relationships within the gradational zone between the Siamo Slate and the Negaunee Iron Formation, sections 7 and 8, T47N-R26W, Marquette Co., Michigan. Unpub. M.S. Thesis, Bowling Green State Univ., Bowling Green, Ohio.

Stow, D. A. V. and Shanmugan, G., 1980. Sequence of structures in fine grained turbidites: comparison of recent deep-sea and ancient flysch sediments. Sed. Geol., v. 25, p. 23-42.

Turner, F. J., 1981. Metamorphic Petrology. McGraw-Hill Book Company, New York, 524p.

Tyler, S. A. and Twenhofel, W. H., 1952. Sedimentation and stratigraphy of the Huronian of Upper Michigan. Amer. Jour. Sci., v. 250, p. 1-27, 118-151.

Underwood, E. E., 1968. Particle-size distribution, in Quantitative Microscopy, R. T. DeHoff and F. N. Rhines (eds.). McGraw-Hill Book Company, 422p.

Van Hise, C. R., 1892. The iron ores of the Marquette district of Michigan. Amer. Jour. Sci., v. 43, p. 116-132.

Van Hise, C. R. and Bayley, W. S., 1897. The Marquette iron-bearing district of Michigan. U.S. Geol. Surv. Mon. 28, 608p.

Van Hise, C. R. and Leith, C. K., 1911. The geology of the Lake Superior region. U.S. Geol. Surv. Mon. 52, 641p.

Van Schmus, W. R., 1976. Early and middle Proterozoic history of the Great Lakes area, North America. Phil. Trans. R. Soc. Lond., v. 280, p. 605-628.

Walker, R. G., 1970. Review of the geometry and facies organization of turbidites and turbidite-bearing basins. Geol. Assoc. Can. Spec. Paper 7, p. 219-251.

Walker, R. G., 1975. Generalized facies model for resedimented conglomerates of turbidite association. Geol. Soc. Amer. Bull., v. 86, p. 737-748.

Walker, R. G., 1976. Facies models 2, turbidites and associated coarse clastic deposits. Geoscience Can., v. 3, p. 25-35.

Walker, R. G., 1978. Deep-water sandstone facies and ancient submarine fans: models for exploration for stratigraphic traps. Amer. Assoc. Petrol. Geol. Bull., v. 62, p. 932-966.

Walker, R. G., 1979. Facies model 8, turbidites and associated coarse clastic deposits, in Facies Models, R. G. Walker (ed.). Geoscience Can., Reprint Series 1, p. 91-103.

Walker, R. G. and Mutti, E., 1973. Turbidite facies and facies associations, in Turbidites and Deep-water Sedimentation. Soc. Econ. Paleo. Mineral. Short Course, May, 1973, Anaheim, California, p. 119-158.

Wicksell, S. D., 1925. The corpuscle problem. Biometrika, v. 17, p. 84-99.

Wicksell, S. D., 1926. The corpuscle problem, second memoir, case of ellipsoidal corpuscles. Biometrika, v. 18, p. 151-172.

Woodcock, N. H., 1976. Structural style in slump sheets: Ludlow Series, Powys, Wales. Jour. Geol. Soc. Lond., v. 132, p. 399-415.

APPENDIX I

GRAIN SIZE MEASUREMENT

The grain size distribution of the clastic lenses in the Negaunee Iron Formation were measured in the lab using quantitive methods. The goal of the exercise, besides fixing a relative grain size of the sediments, was to correlate the author's qualitative measurements of coarse, medium and fine grained with the standard phi size distribution (ϕ) and to perform statistical tests to quantify the qualitative measurements. Because the clastic sediments are highly lithified standard seiving methods could not be employed. A method, devised by Wicksell (1925, 1926) and applied toward turbudite formations by Middleton (1962), using thin sections was employed. The method uses the maximum and minimum axes of quartz grains in thin section. By use of a simple equation the ratio of the maximum and minimum axes are related to the standard sedimentological phi size distribution which would have been obtained by direct seiving of the sediments.

Many geologists, biologists and metallurgists have been concerned with the measurement of the size distribution of spheres and ellipses under the microscope (Wicksell, 1925, 1926; Friedman, 1958, 1962a; Middleton, 1962; Underwood, 1968; Kellerhals et al., 1975). The sample to be analyzed for its size distribution can be placed into two groups depending upon whether the sample consists of spheres (or ellipses) densely packed together so that edges are touching, or whether the sample consists of spheres (or ellipses) randomly dispersed in space with no individual grain contacts (Kellerhals et al., 1975). No solutions have been found for the former case (dense packing) while good statistical methods have been developed for the latter (randomly dispersed in

space). The success of the methods dealing with grains dispersed in space can be attributed to the fact that random dispersion can be modeled as a Poisson distribution and hence normal parametric statistics can be applied to obtain accurate solutions (Kellerhals et al., 1975). The problem of obtaining precise and accurate solutions with densely packed grains is related to theoretical problems of modeling the mathematical distribution of grain centers in space and thus applying statistical tests for accuracy (Kellerhals et al., 1975). The sediments used in this study are quartz-wackes with a high percent matrix (44% to 58%) and thus can be modeled as a Poisson distribution without sacrificing appreciable precision and accuracy. The case of densely packed spheres and ellipses will not be discussed further in this paper.

The equation Wicksell (1926) derived for ellipses which relates maximum and minimum axes to the phi size distribution in thin section is: $\phi = -\log_2 K \quad ab$, where a = maximum grain diameter, b = minimum grain diameter and K is a constant used to reduce the units seen on an objective to millimeters. Sixty one thin sections were randomly selected for the measurement of grain sizes. Traverses were made across each thin section under the microscope using an automatic point counter. Each time a quartz grain appeared under the occular cross-hairs its apparent long and short axes were measured as described by Middleton (1962). At least 100 grains were measured (usually 120) and care was taken to avoid counting the same grain twice thus avoiding violations of the rules of probability. An occular with calibrated cross-hairs was used and the microscope kept at 40 power (using this system, K = 0.025, one unit on the calibrated cross-hairs equals 0.025 millimeters). No grains with an apparent maximum axis smaller than 0.025 mm were measured since earlier work by James (1955) and Mancuso (1966) has determined that chemically precipitated cryptocrystalline quartz or chert in the Negaunee Iron Formation which has been

metamorphosed to the chlorite grade of the lower greenschist facies has a mean grain size of 0.03 mm. It is felt that the exclusion of grains with a maximum axis less than 0.025 mm would greatly reduce the chances of accidentally measuring chemically precipitated chert instead of true clastic quartz grains.

Figures 31 and 32 are plots of the results of the grain size measurement procedures as performed on 56 of the 61 thin sections (5 thin sections were cut parallel to bedding instead of the usual perpendicular to bedding to test the effect of any preferred orientation of quartz grains; this will be discussed later). The results are plotted as the mean grain size for each thin section versus the largest grain measured in each thin section. The 56 thin sections used in Figures 31 and 32 are divided into 3 groups based upon the grain size of the sample as recorded in the field as coarse, medium, and fine grained. The crosses are the means for each grain size as calculated from the measured thin sections in that group. Since the distribution of grain sizes in phi (ϕ) units is normally distributed (Blatt, Middleton, and Murray, 1980), normal parametric statistics can be applied to test whether the means for the coarse, medium, and fine grained groups are significantly different. The student's t-test was used to test this hypotheses.

Two methods were found to work equally well in computing the mean phi size of each thin section from the long and short axes measurement data. One involves using the equation from Wicksell (1926) on each pair of long and short axes measurements, then summing the resulting 100 plus phi sizes to get a mean and standard deviation (called the sum of phi method here). The second method involves summing all the long axes measurements and all the short axes measurements independently, finding a mean long axis value and a mean short axis value, then using the two mean values in the equation from Wicksell (1926) to get a mean phi size for the thin section (here called the long and short axes method).

Using the first method, the sum of phi, at the 95% confidence level ($\alpha = 0.05$ with d.f. = n-1), the mean coarse grain size is 1.38 ± 0.16 ϕ, the medium grain size is 2.03 ± 0.25 ϕ, and the fine grain size is 3.00 ± 0.49 ϕ. Thus at the 95% confidence level the field classification of grain sizes into coarse, medium and fine is significant. The same test was performed upon the values obtained for the largest grain visible in each thin section. Again at the 95% confidence level the mean grain size of the largest grain visible in the samples classified as coarse grained is -0.90 ± 0.28 ϕ, for medium grained 0.089 ± 0.46 ϕ, and for fine grained the value is 1.64 ± 0.68 ϕ. This indicates that in the three-fold classification of grain sizes used in this study, there are significant differences between each group based upon the largest grain visible in the thin section.

The second method, the mean long and short axes method, at the 95% confidence level results in a mean coarse grain size of 1.09 ± 0.17 ϕ, a mean medium grain size of 1.82 ± 0.27 ϕ, and a mean fine size of 2.87 ± 0.51 ϕ. Thus the mean long and short axes method resulted in an average reduction of mean grain sizes of 0.20 phi units with the fine grain sizes being reduced slightly less than the coarse.

Two linear regression programs were run using the sum of phi method data in one and the mean long and short axes method data in the other. Both were regressed against an x-axis of the largest grain visible in thin section, which is a constant here. Using 65 pairs of values in each run, the sum of phi method resulted in a r^2 value equal to 0.858 while the mean long and short axes method gave a r^2 value of 0.906. When just the means for coarse, medium, and fine are used (3 pairs of points for each) the sum of phi method gave a r^2 value of 0.99991 while the mean long and short axes method gave a r^2 value of 0.9442. Thus the

two methods result in approximately equal accuracy in correlating the largest grain visible in each thin section with the mean grain size for that thin section.

Because of this close correlation between the largest grain visible in thin section and the mean grain size for that thin section, it is possible to use the equation for the regression line generated from either Figure 31 or 32 to fine the mean grain size of thin sections not measured for this study using only the long and short axes of the largest grain visible in that thin section. While this would not be as an exact a method as counting 100 plus grains per thin section, the high r^2 coefficients for Figures 31 and 32 indicate that the resulting value would not deviate too far from the true value. The equation for the line generated by linear regression for the sum of phi method is: mean $\phi = 1.928 + 0.523x$, while the equation from the mean long and short axes method is: mean $\phi = 1.712 + 0.597x$ where x is the phi size taken from the largest grain visible in thin section (data used for Figures 31 and 32 and in regression are contained in Tables 1 and 2).

Middleton (1962) calculated the size of each grain from the measured long and short axes (sum of phi method used here). The benefit of using this method is that frequency graphs and values for the variance and standard deviation for each thin section can be obtained while these cannot be derived from the long and short axes method. Because the equation for obtaining phi values ($\phi = -\log_2 K$ ab) uses the product between the measured long and short axes, taking an average long and short measurement might possibly be a more accurate method, because the single derived ratio would be more representative of the thin section. The only way of testing which method might be more representative would be to sieve the clastic sediments and obtain a mean size which would be quite difficult considering the highly indurated nature of the clastics and the effect of authigenetic overgrowths upon biasing the sieve data

(authigenetic overgrowths can usually be seen in thin section and their effect discounted).

A X^2- distribution test (observed-expected) was run comparing the sum of phi method (expected) with the mean long and short axes method (observed) to see if there was a statistical difference between the two methods. At the 95% confidence level the X^2 test indicated no statistical difference between the two methods.

In order to assess the effects of operator error and possible preferred orientation of quartz grains, 4 thin sections were measured twice and 5 thin sections were cut parallel to bedding instead of the usual method of perpendicular to bedding. The results of these grain size measurements and the corresponding statistics are summarized in Table 3. All statistical tests were performed at the 95% confidence level. The t-test and F-test were used to compare the means and variances between long axes measurements and the sum of phi method of computing the phi size.

For the four thin sections measured twice, only slide number 73 (27-106-44.4') showed any statistical difference between the two measurements and this was only for comparison of means when the sum of phi method was employed. No statistical difference was noted between the variances and no statistical difference is evident for the comparison of long axes for slide number 73 for either the means or variances. Because there was only one rejection of the H_o hypothesis (no difference) for 16 statistical tests performed on the four thin sections measured twice, it is concluded that operator error is minimal and probably has no effect upon the phi sizes computed on the 61 other thin section.

Thin sections used in grain size measurement procedures were normally cut perpendicular to bedding. In order to test for possible preferred orientation of quartz grains in the clastic sediments studied five samples had thin sections

made both perpendicular and parallel to bedding (bedding usually determined by the contact with adjoining iron formation layers). Because of the small size of the core samples and their broken nature it was impossible to make the perpendicular and parallel thin sections from sides of the same cube of sediment. Instead the thin sections were made from closely spaced clastic samples, of which one sample would be stratigraphically higher than the other. While no graded bedding was visible in the thin sections cut perpendicular to bedding the possibility exists for a gradation in grain size between the two thin sections cut from one sample location. Table 3 contains the statistics for comparison of means and variances at the 95% confidence level for the t-test and F-test which were used to test the H_o hypothesis of no difference between the samples. Of the 20 statistical tests performed, only 9 had the H_o hypothesis accepted. This indicates that there are significant differences, in most samples, between the thin sections cut perpendicular and parallel to bedding (numbers 73 and 68 showed minor differences). Many workers on graywackes and turbiditic type sediments have noted imbrication or a preferred orientation of the clastic grains in these type of sediments (Walker and Mutti, 1973; Harms et al., 1975; Walker, 1975; Mutti and Lucchi, 1976; Normark, 1978; Walker, 1978; Walker, 1979; Eriksson, 1980; Meyn and Palonen, 1980). It is postulated that the differences observed between thin sections cut perpendicular and parallel to bedding might be due to imbrication of quartz grains in these clastic sediments. However, the possibilities exist for the differences to be the result of either a gradation in grain size between the two thin sections cut from one sample location as described previously or strain as a result of the Penokean orogeny.

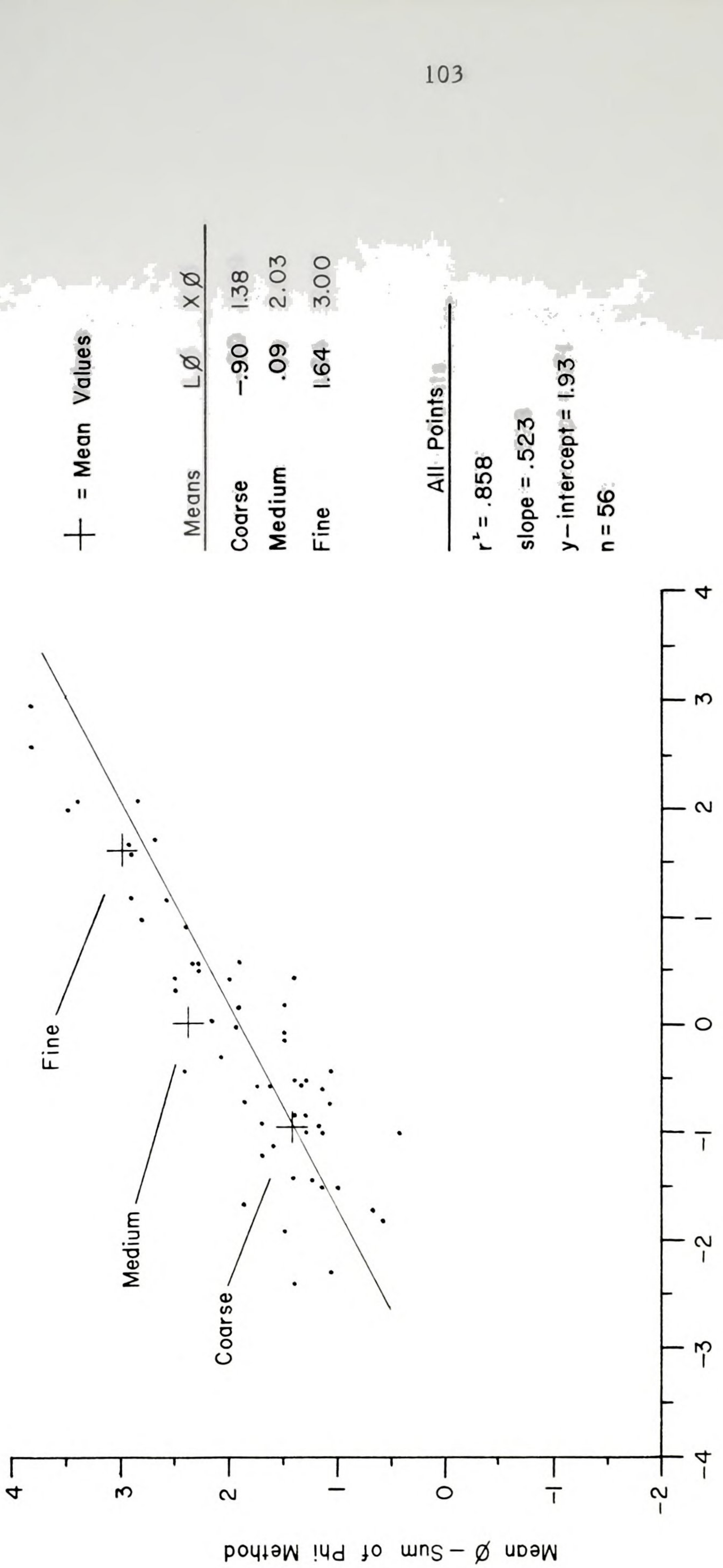

Figure 31. Thin section grain size data. Largest grain size versus mean grain size by sum of phi method. Note linear trend. See text for discussion.

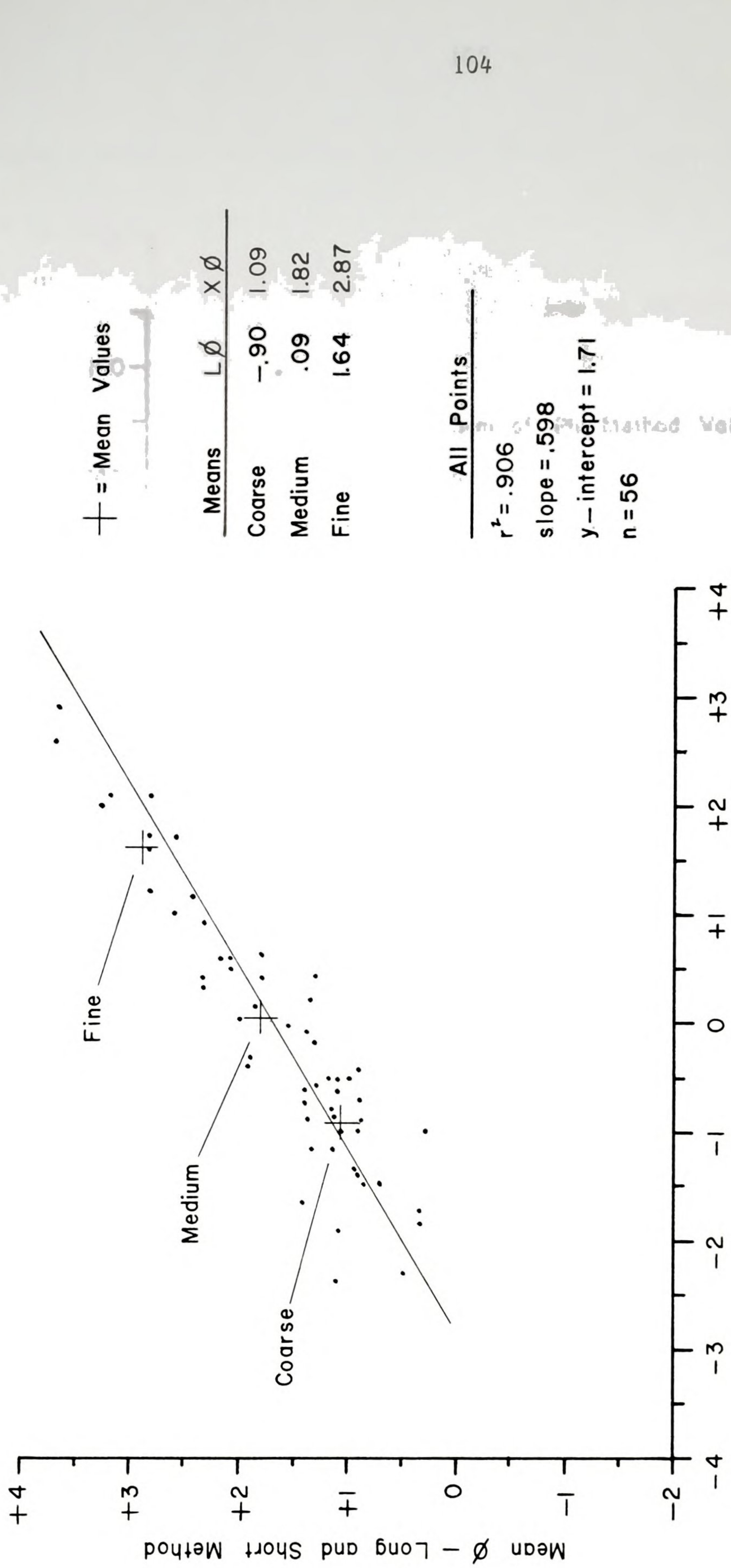

Figure 32. Thin section grain size versus mean grain size by long and short axes method. Note linear trend. See text for discussion.

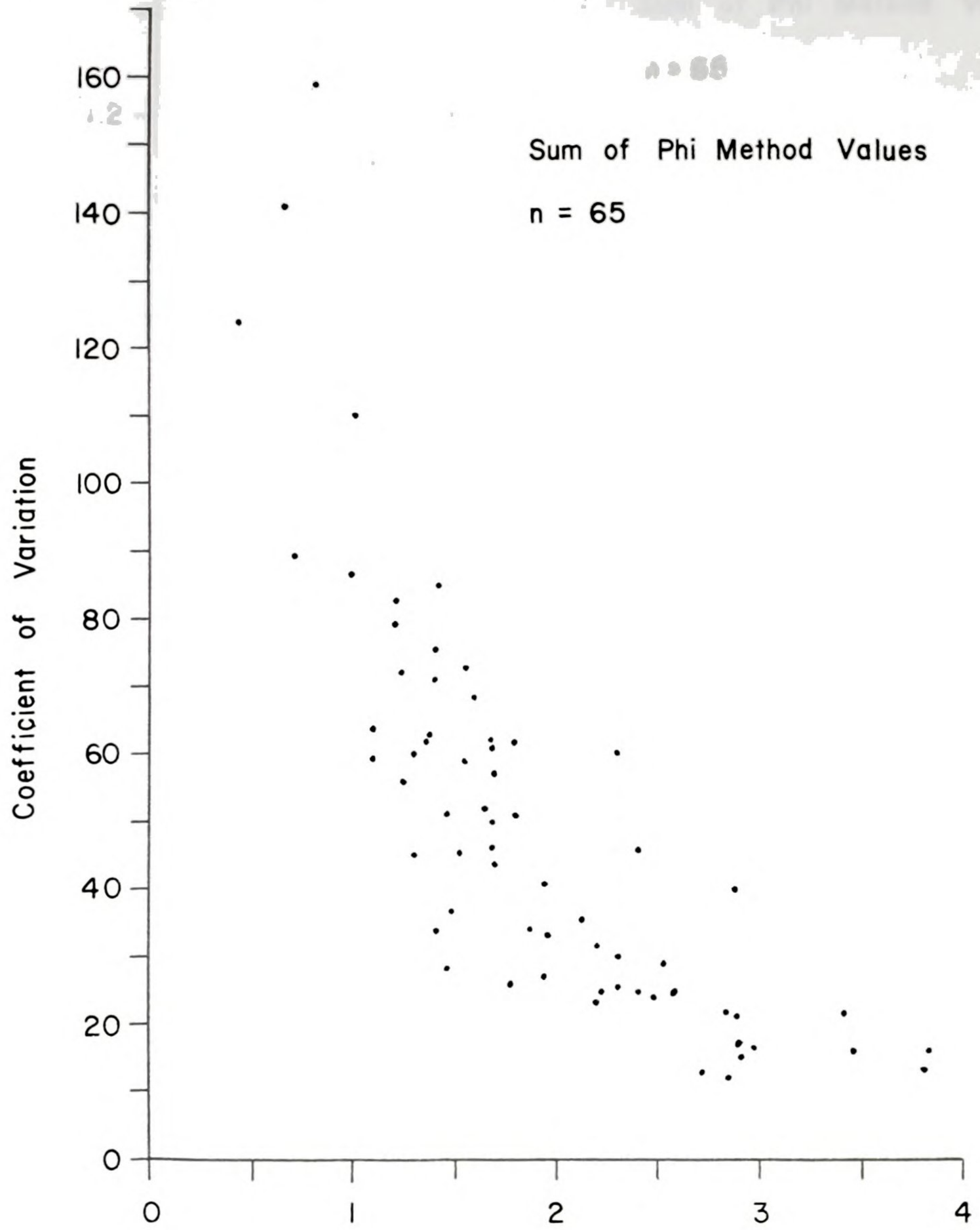

$$\text{coefficient of variation} = \frac{\text{standard deviation}}{\text{mean}} \times 100$$

Figure 33. Plot of mean phi values versus coefficient of variation of thin section grain size data. Note increasing variation with increasing coarseness.

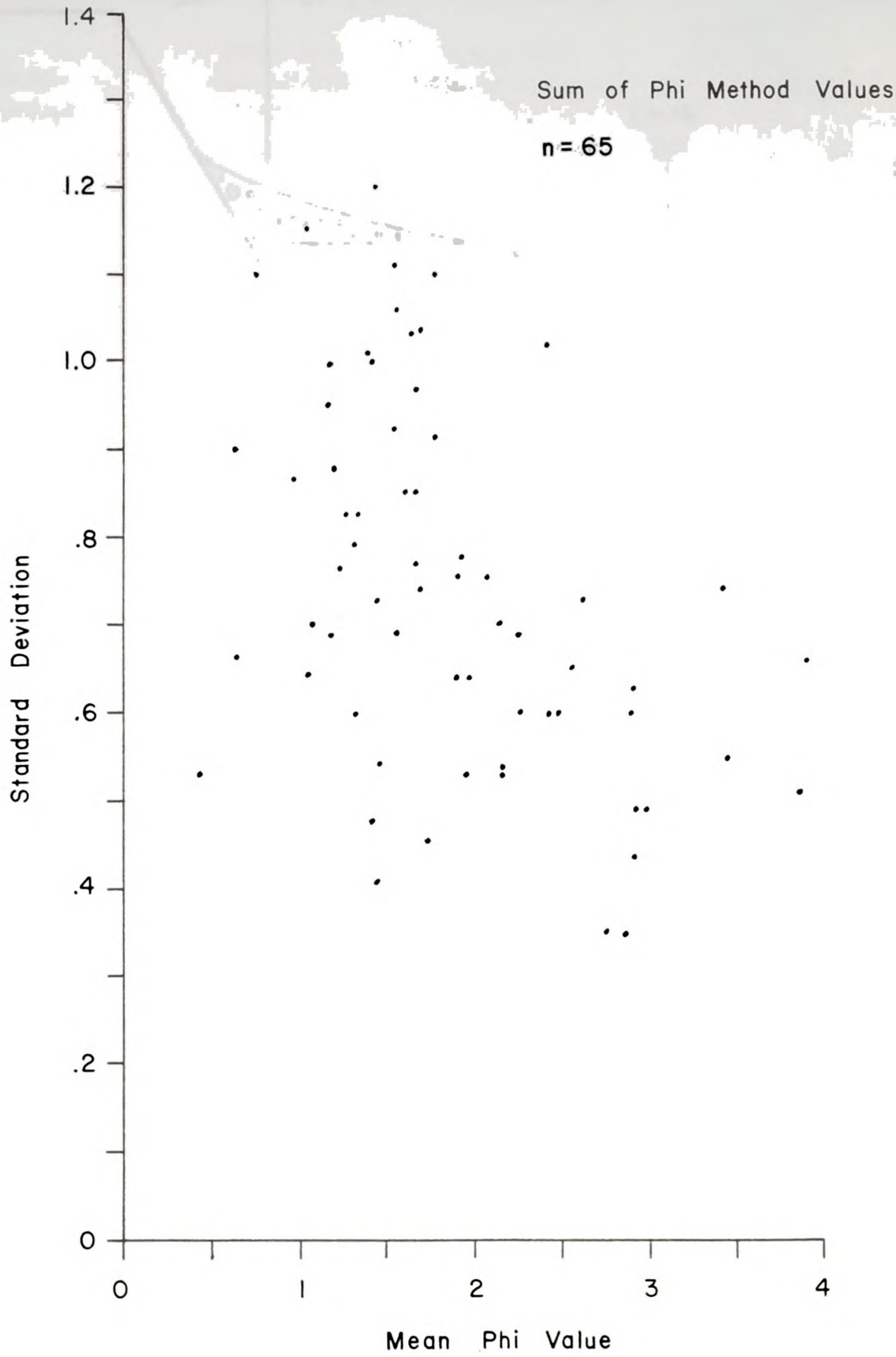

Figure 34. Plot of mean phi values versus standard deviation of thin section grain size data. Note increase of standard deviation with increasing coarseness.

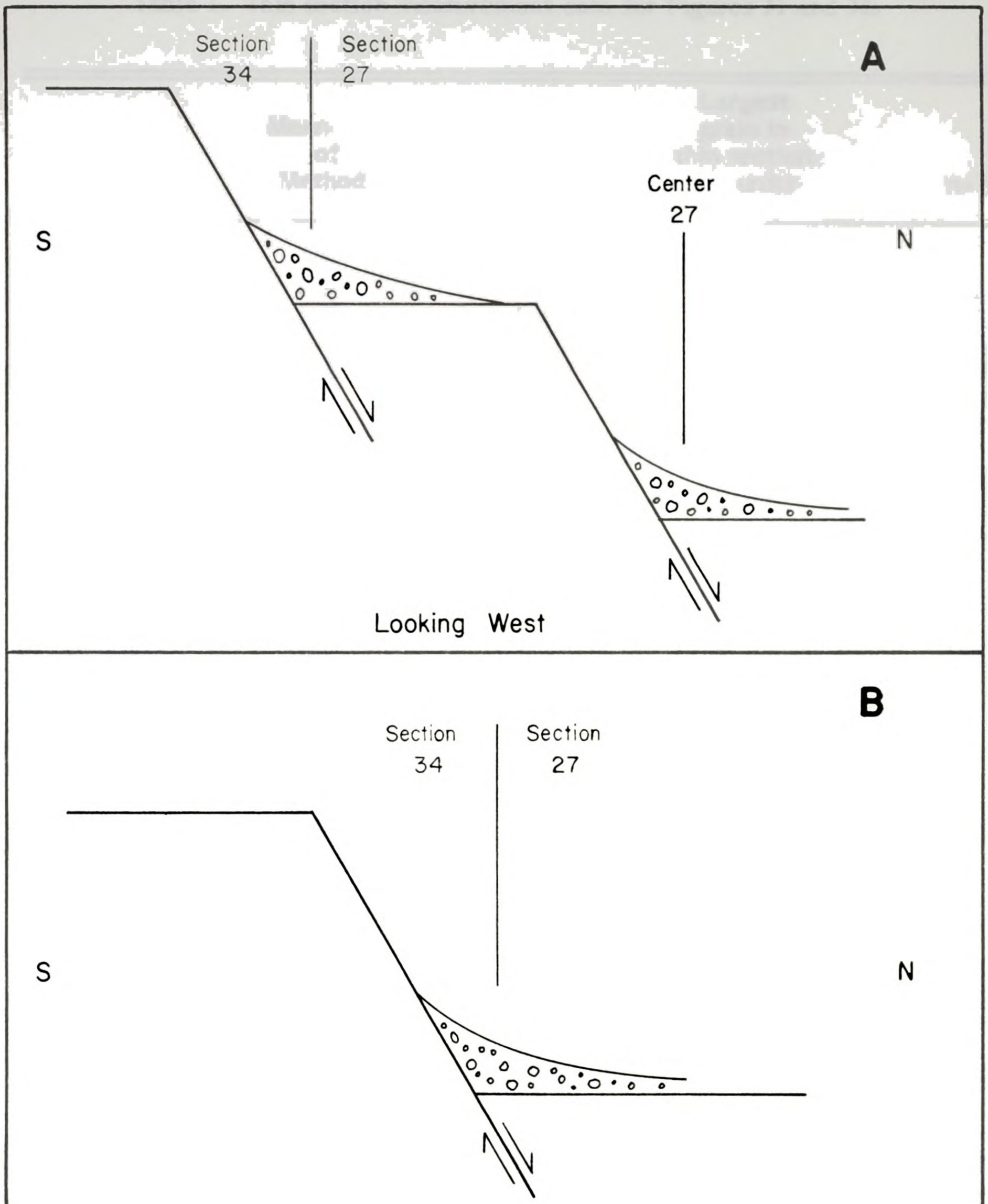

Figure 35. Two possible fault models to explain observed sedimentation patterns in the Eastern Palmer Basin. See text for details.

Table 1. Thin section measurement data for Figures 31 and 32.

Hole Number	Mean Phi Sum of Phi Method	Mean Phi Long and Short Axes Method	Largest grain in thin section Phi units	n=?
Chloritic Coarse				
27-92-605.5	1.8	1.4	-1.7	140
96-858	1.7	1.3	-0.6	140
92-719P	.68	0.5	-0.7	100
92-719	2.3	2.1	0.5	100
91-593	0.6	0.3	-1.8	127
93-7	1.1	0.9	-0.4	120
93-32P	1.7	1.4	-0.9	120
93-32	1.9	1.6	-.004	100
93-14	0.7	0.3	-1.7	140
98-590	1.2	0.8	-1.5	100
28-27-425	1.3	1.1	-1.0	140
27-360P	1.7	1.4	-1.6	140
27-360	0.99	0.7	-1.5	120
39-202	1.1	0.5	-2.3	157
15-350	1.4	0.9	-1.4	132
34-6-29.5	1.3	1.2	-0.8	130
5-44.2	1.6	1.2	-1.2	130
Chloritic Medium				
26-7-265	2.1	1.9	-0.3	100
27-91-80	1.4	1.0	-0.5	150
90-189.9	2.8	2.6	1.0	80
90-208.5	1.3	1.1	-0.5	120
28-28-52P	2.95	2.9	1.9	100
28-52	2.7	2.6	1.7	100
28-340	2.4	2.3	0.9	100
21-715	2.2	2.0	0.006	100
11-1356	2.4	1.9	-0.4	100
39-251	1.7	1.4	-0.6	120
11-1425A	2.3	2.2	0.6	100
11-1425B	2.2	2.1	0.8	100
Chloritic Fine				
26-6-315.5	3.8	3.7	2.6	100
5-657	1.5	1.3	-0.2	120
27-106-360	3.8	3.7	2.9	84
106-443.3	2.8	2.8	2.1	100
28-20-618.5	2.9	2.8	1.7	100
20-571.8	2.9	2.8	1.2	60
21-355	3.5	3.3	2.0	100

Table 1 (continued).

Hole Number	Mean Phi Sum of Phi Method	Mean Phi Long and Short Axes Method	Largest grain in thin section Phi units	n=?
Iron Coarse				
27-89-40	1.7	1.3	-1.2	135
89-127	1.2	0.9	-0.9	145
98-51.5	2.0	1.8	0.4	60
90-579.7	0.4	0.3	-1.0	100
98-281	1.7	1.4	-0.9	146
99-209.6	1.5	1.4	0.2	100
97-270	1.3	0.9	-1.4	120
99-126	1.4	1.3	0.4	100
99-150A	1.8	1.4	-0.7	100
99-150B	1.7	1.4	-0.8	100
99-107	1.2	1.1	-0.6	130
100-21	1.3	1.1	-0.5	135
98-352.5	1.4	1.2	-0.8	120
28-39-106.8	1.2	0.9	-1.0	100
30-39.4A	1.6	1.2	-1.3	100
30-39.4B	1.5	1.1	-1.9	100
Iron Medium				
27-90-32.8	1.9	1.7	0.2	100
98-285	2.5	2.3	0.3	100
94-222	2.3	2.1	0.6	100
106-44.4P	1.9	1.7	0.6	100
106-44.4A	1.9	1.8	0.6	100
106-44.4B	1.8	1.7	0.8	100
89-73.6	1.4	1.1	-2.4	120
111-819.5	1.1	0.9	-0.7	120
28-39-80.5	2.6	2.4	1.2	50
19-259	1.5	1.4	-0.1	120
Iron Fine				
28-21-318	2.5	2.3	0.4	100
30-229	3.4	3.2	2.1	50
27-215.5	2.9	2.8	1.6	100

Table 2. Thin section measurement data for Figures 33 and 34.

Hole Number	Mean Phi Sum of Phi Method	Mean Phi Long and Short Axes Method	Largest grain in thin section Phi units	n=?
Chloritic Coarse				
27-92-605.5	1.8	0.91	51	140
96-858	1.7	0.97	57	140
92-719P	0.68	0.67	99	100
92-719	2.3	0.60	26	100
91-593	0.6	0.90	141	127
93-7	1.1	0.70	64	120
93-32P	1.7	0.74	44	120
93-32	1.9	0.75	40	100
93-14	0.7	1.11	159	140
98-590	1.2	0.99	83	100
28-27-425	1.3	0.76	60	140
27-360P	1.7	0.77	46	140
27-360	0.99	0.86	87	120
39-202	1.1	1.15	110	157
15-350	1.4	1.20	85	132
34-6-29.5	1.3	0.58	45	130
5-44.2	1.6	0.92	59	130
Chloritic Medium				
26-7-265	2.1	0.76	36	100
27-91-80	1.4	1.04	75	150
90-189.9	2.8	0.63	22	80
90-208.5	1.3	0.83	62	120
28-28-52P	2.95	0.49	17	100
28-52	2.7	0.35	13	100
28-340	2.4	0.60	25	100
21-715	2.2	0.70	32	100
11-1356	2.4	1.11	46	100
39-251	1.7	0.84	50	120
11-1425A	2.3	0.53	23	100
11-1425B	2.2	0.52	24	100
Chloritic Fine				
26-6-315.5	3.8	0.51	13	100
5-657	1.5	0.69	46	120
27-106-360	3.8	0.66	17	84
106-443.3	2.8	0.35	12	100
28-20-618.5	2.9	0.43	15	100
20-571.8	2.9	0.49	17	60
21-355	3.5	0.55	16	100

Table 2 (continued).

Hole Number	Mean Phi Sum of Phi Method	Mean Phi Long and Short Axes Method	Largest grain in thin section Phi units	n=?
Iron Coarse				
27-89-40	1.7	1.03	61	135
89-127	1.2	0.95	79	145
98-51.5	2.0	0.64	33	60
90-579.7	0.4	0.53	123	100
98-281	1.7	0.85	52	146
99-209.6	1.5	0.54	37	100
97-270	1.3	0.79	60	120
99-126	1.4	0.48	34	100
99-150A	1.8	1.10	62	100
99-150B	1.7	1.03	62	100
99-107	1.2	0.69	56	130
100-21	1.3	0.83	62	135
98-352.5	1.4	0.73	51	120
28-39-106.8	1.2	0.88	72	100
30-39.4A	1.6	1.06	67	100
30-39.4B	1.5	1.11	73	100
Iron Medium				
27-90-32.8	1.9	0.78	41	100
98-285	2.5	0.73	29	100
94-222	2.3	0.69	30	100
106-44.4P	1.9	0.63	34	100
106-44.4A	1.9	0.52	27	100
106-44.4B	1.8	0.46	26	100
89-73.6	1.4	1.00	71	120
111-819.5	1.1	0.64	59	120
28-39-80.5	2.6	0.65	25	50
19-259	1.5	0.41	28	120
Iron Fine				
28-21-318	2.5	0.60	24	100
30-229	3.4	0.74	22	50
27-215.5	2.9	0.60	21	100

TABLE 3 SUMMARY STATISTICS

DIFFERENCES EXIST ? 95 % C.I.

SAME THIN SECTION MEASURED TWICE

	LONG AXES		SUM OF PHI	
NUMBER	MEANS	VARIANCES	MEANS	VARIANCES
18A — 18B	NO	NO	NO	NO
42A — 42B	NO	NO	NO	NO
52A — 52B	NO	NO	NO	NO
73A — 73B	NO	NO	YES	NO

THIN SECTIONS CUT PERPENDICULAR TO EACH OTHER

	LONG AXES		SUM OF PHI	
NUMBER	MEANS	VARIANCES	MEANS	VARIANCES
68 — 68P	NO	YES	NO	NO
71 — 71P	YES	YES	YES	NO
73 — 73P	NO	NO	NO	YES
77 — 77P	YES	NO	YES	YES
79 — 79P	YES	YES	YES	NO

MEANS BY t-test VARIANCES BY F-test